ANNALS OF THE NEW YORK ACADEMY OF SCIENCES
Volume 53, Art. 5. Pages 995–1118

Editor
Roy Waldo Miner

Associate Editor
B. J. Henegan

SPECIFIC METHODS OF ANALYSIS

BY

J. B. Bateman, D. L. Clegg, L. C. Craig, J. D. H. Donnay, E. C. Dunlop, G. D. Gregory, R. E. Grim, M. W. Harris, I. M. Kolthoff, T. S. Lee, H. A. Liebhafsky, R. H. Muller, and A. Rothen

Consulting Editor
Samuel E. Q. Ashley

NEW YORK
PUBLISHED BY THE ACADEMY
July 20, 1951

THE NEW YORK ACADEMY OF SCIENCES

(Founded in 1817)

OFFICERS, 1951

President
WILLIS A. GIBBONS

Vice-Presidents
JOHN RAY DUNNING WALTER S. ROOT

Recording Secretary
HARRY A. CHARIPPER

Corresponding Secretary
JAMES B. ALLISON

Treasurer
DONALD M. BENJAMIN

Editor
ROY WALDO MINER

Elected Councilors

1949–1951
EDITH QUIMBY JOHN TEE VAN W. G. BYWATER

1950–1952
E. H. NORTHEY JOHN A. AESCHLIMANN ERICH M. SCHLAIKJER

1951–1953
EDWIN J. deBEER DAVID B. STEINMAN OSKAR P. WINTERSTEINER

Finance Committee
ROBERT F. LIGHT, *Chairman* GORDON Y. BILLARD HARDEN F. TAYLOR

Executive Director
EUNICE THOMAS MINER

SECTION OF GEOLOGY AND MINERALOGY
SIDNEY PAIGE, *Chairman* M. HALL TAYLOR, JR., *Secretary*

SECTION OF BIOLOGY
ELI D. GOLDSMITH, *Chairman* CHARLES W. MUSHETT, *Secretary*

DIVISION OF MYCOLOGY
BENJAMIN M. DUGGAR, *Chairman* WILLIAM J. ROBBINS, *Secretary*

SECTION OF PSYCHOLOGY
THOMAS N. JENKINS, *Chairman* N. L. HOOPINGARNER, *Secretary*

SECTION OF ANTHROPOLOGY
PAUL FEJOS, *Chairman* JANE BELO, *Secretary*

SECTION OF PHYSICS AND CHEMISTRY
CHARLES O. BECKMANN, *Chairman* FRANK BRESCIA, *Secretary*

SECTION OF OCEANOGRAPHY AND METEOROLOGY
WILLIAM L. DONN, *Chairman* RICHARD J. ROMMER, *Secretary*

SECTION OF MATHEMATICS AND ENGINEERING
ABRAHAM SLAVIN, *Chairman* SEBASTAIN B. LITTAUER, *Secretary*

These Sections and the Division hold meetings regularly, one evening each month, during the academic year, October to May, inclusive.
Two-day conferences also are held at irregular intervals. All meetings are held at the building of The New York Academy of Sciences, 2 East Sixty-third Street, New York 21, New York.

ANNALS OF THE NEW YORK ACADEMY OF SCIENCES
VOLUME 53, ARTICLE 5. Pages 995–1118
July 20, 1951

Editor
ROY WALDO MINER

Associate Editor
B. J. HENEGAN

SPECIFIC METHODS OF ANALYSIS

Consulting Editor and Conference Chairman
SAMUEL E. Q. ASHLEY

CONTENTS

PAGE
X-Ray Absorptions in Chemical Analysis and Control. *By* H. A. Liebhafsky 997
The Analytical Specificity of Countercurrent Distribution. *By* J. D. Gregory and L. C. Craig 1015
Method and Application of Differential Thermal Analysis. *By* R. E. Grim 1031
Optical Properties of Surface Films. *By* A. Rothen 1054
Measurement of Properties of Thin Films on Chromium by the Reflection of Polarized Light. *By* J. B. Bateman and M. W. Harris .. 1064
Goniometric Analysis of Crystals. *By* J. D. H. Donnay 1082
Quantitative Analysis by Means of Catalytic Hydrogenation Reactions. *By* E. C. Dunlop 1087
Analysis of Mixtures Based on Rates of Reaction. *By* T. S. Lee and I. M. Kolthoff 1093
Automatic Paper Chromatography. *By* R. H. Müller and D. L. Clegg 1108

This series of papers is the result of a conference on *Specific Methods of Analysis*, held by the Section of Physics and Chemistry of The New York Academy of Sciences on May 25 and 26, 1949.

Copyright, 1951, by The New York Academy of Sciences

X-RAY ABSORPTION IN CHEMICAL ANALYSIS AND CONTROL

By Herman A. Liebhafsky
Research Laboratory, General Electric Company, Schenectady, New York

Three X-ray processes are potentially useful in analytical chemistry: the diffraction of X rays by crystals, the emission of characteristic spectra, and the absorption of X rays by matter. The first process can establish structure and composition. The others establish composition only. In the past, the analytical chemist has used each process to a very limited extent, because there was no convenient way to measure the intensity of an X-ray beam with sufficient speed and precision. Of the three, he has logically found that X-ray diffraction is the most useful for the following reasons: first, he had many ways of determining composition, but few of establishing structure; second, it is often possible by X-ray methods to establish structure, but usually it is impossible to do quantitative analysis without making a precise intensity measurement. As a consequence, the unique contribution that X-ray absorption methods can make to chemical analysis and control, though long known to physicists, has not been generally appreciated.

Owing to marked and relatively recent progress in measuring the intensity of X-ray beams, this situation is now changing. There are available today three X-ray detectors that convert X-ray beams into electric currents proportional in magnitude under the simplest conditions to the intensities of the beams. These devices are the ionization chamber, the Geiger counter, and the photoelectric X-ray detector. The ionization chamber, the oldest of the three, has found little or no recent application in chemical analysis or control, nor, in view of the generally greater suitability of the other two devices, is it likely to do so. The analytical chemist can proceed on the basis that the Geiger counter or the photoelectric detector, both of which will be discussed subsequently, are capable of meeting any reasonable requirements that he is likely to impose. He is thus in a position to realize the advantages of X-ray absorptometry, some of which accrue from the facts that it can be accomplished without noticeably altering the sample, and that a single measurement can often be made in a matter of seconds once the sample is in the beam.

The advantages and limitations of X-ray absorptometry are in general deducible from the known characteristics of X rays. The reader is referred to several excellent books[1–4] for a thorough discussion of these. This brief review, being largely qualitative, will present only the necessary minimum of fundamental information about X rays, and it cannot discuss all the advantages or limitations of X-ray absorptometry. (For a more complete treatment, see bibliographical reference 5 and others listed in the bibliography therein.)

X-Ray Absorption Described. The outstanding characteristic of X rays, from which certain others derive, is their high energy, or small wavelength (near 1 Å.). Because of this characteristic, the absorption of X rays usually involves only electrons near the atomic nucleus. The absorption of ultraviolet, visible, or infrared rays, on the other hand, affects the electrons that determine the chemical properties of the elements. X-ray absorption is thus essentially an atomic process and virtually independent, therefore, of the chemical or physical state. In relation to chemical analysis, for example, an oxygen atom will show the same X-ray absorption in oxygen gas, in ice, water, or steam, or in sand.

The energies of X rays are high enough to make their spectra relatively simple. The established "absorbancy index" for X rays is the mass absorption coefficient, μ_m, which equation 5 defines in measurable terms. This coefficient contains the information of interest to the analytical chemist who wishes to use X-ray absorptometry in chemical analysis or control.

FIGURE 1, a "log-log" plot, shows how μ_m varies with wavelength for three common metals and illustrates the fact that all X-ray absorbancy curves are essentially simple. They consist of large regions in which X-ray absorption is continuous, but these regions are separated by sharp discontinuities ("absorption edges") where the absorbancy suddenly decreases at a "critical" wavelength. These wavelengths are the maximum capable of ejecting a certain kind of electron from the atom. It will be noted that the critical wavelengths for both the K and L electrons of lead fall within the range of FIGURE 1, but that this range includes only the K wavelength for copper. Aluminum shows continuous absorption throughout. Each critical wavelength is characteristic of an element, so that the positions of absorption discontinuities can be used to identify the elements in a sample (qualitative analysis). Generally, however, not all critical wavelengths will be equally suited to the identification of a given element.

The contrast between the discontinuous absorption of radiant energy thousands of Ångstroms in wavelength, and that of X rays, will be clear from the foregoing paragraph. The contrast between continuous absorption in the two cases is no less marked. The mass absorption coefficients in regions of continuous absorption can be expressed as the following approximate function of wavelength λ and of atomic number Z:

$$\mu_m = (Z^4\lambda^3)NC/A. \tag{1}$$

In this equation, N is Avogadro's number, A is the atomic weight, and C is assumed to be constant in the range between adjacent critical absorption wavelengths. The scattering of X rays by electrons gives rise to an additive term, usually unimportant except at low Z and λ, that has been omitted from equation 1.

Because X-ray absorption is an atomic process, the mass absorption coefficient of a sample usually stands in a simple additive relationship to those of the elements present. If, for example, sample S contains elements A, B, and C in the proportions by weight x, y, and $(1 - x - y)$, respectively, then

$$\mu_m^S = x\mu_m^A + y\mu_m^B + (1 - x - y)\mu_m^C \tag{2}$$

without restriction in relation to the chemical or physical state of S, A, B, or C. For the purposes of chemical analysis or control, the mass absorption coefficient of a sample depends only on its ultimate composition, and on the wavelength of the X-ray beam, if the beam is monochromatic. With polychromatic beams, there may occasionally be departures from equation 2 ("deviations from additivity"), which are not discussed in this review (bibliographical reference 6, Figure 4).

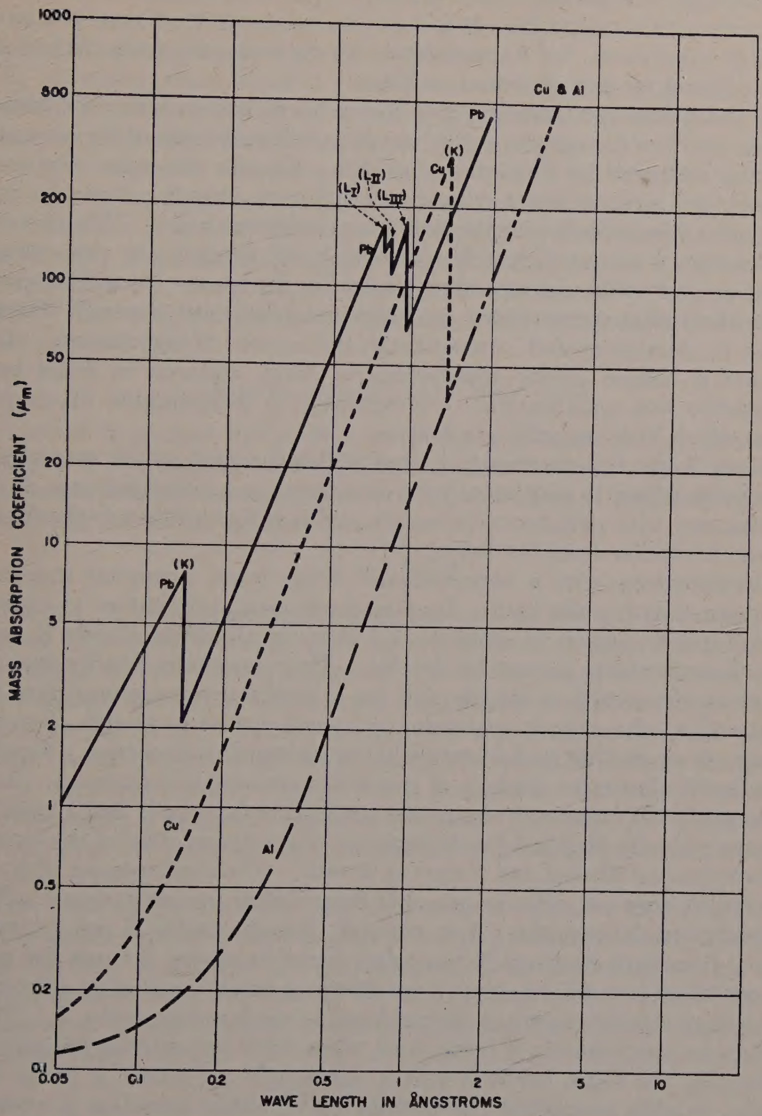

FIGURE 1. Log-log plot showing mass absorption coefficient as a function of wavelength for three common metals. Note the characteristic discontinuities separated by the uncharacteristic continuous regions.

Types of X-Ray Absorptometry. X-ray absorptometry may be subdivided into absorption spectrometry, absorptometry with filtered beams, and absorptometry with polychromatic beams, the order being that of decreasing restrictions on wavelength. It will not be necessary to discuss the intermediate subdivision, for its usefulness can be estimated from that of the limiting cases for any particular problem.

In absorption spectrometry, the X-ray beam becomes monochromatic before it strikes the sample, or the wavelength distribution of the emergent beam is measured by diffraction methods. Because this type of absorptometry can serve to locate critical absorption wavelengths, it can be used for qualitative analysis with the limitations indicated below. The decrease in absorbancy at such a critical wavelength will naturally be proportional to the amount of the corresponding element in the beam. As will be shown later, absorption spectrometry can often establish very precisely this decrease in absorbancy and, consequently, the amount of the element. This method is unique among absorptometric X-ray methods in being both qualitative and quantitative. Consequently, it is applicable to samples about which little or nothing is known.

When X-ray absorptometry is done without regard to the presence of absorption edges, it may usually be considered as a simplified case of absorptometry with polychromatic beams, and it is then subject to the fundamental limitation described below.

Absorptometry with a polychromatic X-ray beam somewhat resembles colorimetry with white light. Its most fundamental limitation as an analytical tool is implicit in equation 1. Because all atoms absorb X rays, such measurements cannot be specific. They cannot ordinarily identify unknown elements in a sample, and (as a corollary) they cannot give the composition of a sample containing unknown elements, though they can usually show whether such a sample has an assumed composition. Figure 1 abundantly illustrates the lack of specificity inherent in equation 1. Note particularly that the mass absorption coefficients for copper and aluminum become virtually identical just beyond the K absorption edge of the former.

Experimental Method and Nature of Results. The measurement of X-ray absorption does not differ in principle from similar measurements common in analytical laboratories. For example, polychromatic X rays from a source (usually a standard X-ray tube) might be passed through the sample contained in a cell, whereupon the emergent beam would enter a detector to yield an electric current, i, proportional to the beam intensity, I. When absorption spectrometry is being done, there must be provision for suitably diffracting the beam before it strikes the sample (to render it monochromatic) or after emergence (to analyze it). Neither operation is possible without radically reducing the intensity (say, by several powers of 10) below that of the corresponding polychromatic beam.

Under the simplest conditions, the decreases in beam intensity and in output current that measure X-ray absorption by a sample in a cell follow the usual exponential law, which may be written:

$$\log[I_0/I] = \log[i_0/i] = km. \tag{3}$$

In this equation, I_0 and i_0 refer to the empty cell, k is a proportionality constant that contains the information of chemical interest, and m is the mass of the sample. The effect of certain departures from "simplest conditions" ("deviations from linearity") is discussed below. (For other, less important departures, see the original literature.[6–8])

By "deviation from linearity" is meant a curvature in a plot of i on a logarithmic ordinate against m (or thickness), in other words, a variation in k, the slope of such a plot, and a departure from equation 3. Such a deviation will occur even with a monochromatic beam if the detection and amplification system becomes nonlinear, so that i no longer varies directly as I. One remedy is to restrict the range of operation until satisfactory linearity is achieved. For example, when the range of sample masses is chosen large enough from the viewpoints of convenience and precision, i_0 may equal 1000 i. For samples of masses m_1 and m_2, however, equation 2 takes the more practical form

$$\log[I_1/I_2] = \log[i_1/i_2] = k[m_2 - m_1]. \qquad (4)$$

Another important deviation from linearity peculiar to polychromatic beams is a consequence of the fundamental nature of X-ray absorption. The proportionality constant, k, is related as follows to the mass absorption coefficient of the sample

$$\mu_m = 2.303ak, \qquad (5)$$

in which a is the cross-sectional area (sq. cm.) of the cell containing the sample. For most elements, μ_m is known to increase approximately with the cube of the wavelength (equation 1) between adjacent critical absorption wavelengths. (The fact that the lines in FIGURE 1 have a slope near 3 illustrates this point.) Consequently, when a polychromatic beam passes through a sample, the longer wavelengths are the more strongly absorbed, so that the beam becomes "harder" as it progresses. It follows that k will decrease as m, the mass of sample, increases. This behavior is extremely important to the analytical chemist who plans to use polychromatic beams for precise work.

The effect of the deviation just discussed can often be estimated if the change in the "effective wavelength" of the polychromatic beam is known. (The effective wavelength of a polychromatic beam is defined as that of a monochromatic beam absorbed to the same extent under the experimental conditions.) FIGURE 2 illustrates the points discussed (see bibliographical reference 7, pp. 862–3).

X-Ray Absorption Spectrometry

It has been mentioned that absorption measurements near a critical wavelength can yield both qualitative and quantitative information. Glocker and Frohnmayer,[9] using photographic methods, did the classical work in this field twenty-five years ago with results that were excellent for the times.

Their method will be illustrated by applying it to determining the proportion of total bromine (free or combined) x in a sample weighing m grams.

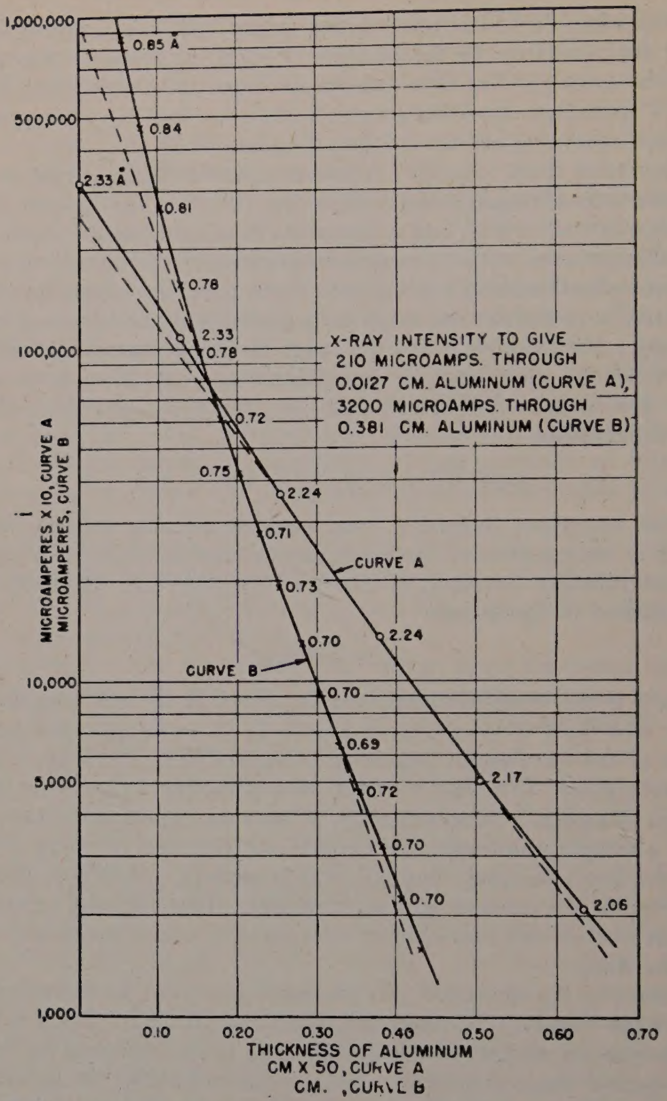

FIGURE 2. X-ray absorbancy curves for aluminum over two ranges of thickness. Decrease in effective wavelength with increasing thickness of sample is principally responsible for curvature shown, which grows more pronounced as wavelength increases.

The experimental data will be the results of absorbancy measurements at wavelengths just above and just below (λ and λ′, respectively) the critical absorption wavelength, 0.918 Å. On the basis of equations 2, 3, and 5,

$$\log I_0/I = k_{\mathrm{Br}}mx + km(1 - x) \quad (\lambda > 0.918 \text{ Å.}) \tag{6}$$

$$\log I_0'/I' = k_{\mathrm{Br}}'mx + k_{\mathrm{S}}'m(1 - x) \quad (\lambda' < 0.918 \text{ Å.}) \tag{7}$$

where

$$k_{\mathrm{Br}}' > k_{\mathrm{Br}} \text{ (see FIGURE 4).} \tag{8}$$

In these equations, S refers to the sample less the bromine, and the I_0's usually apply to the empty cell. Now, the more nearly identical are λ and λ', the more nearly (in the simplest case)

$$I_0 = I_0' \text{ and } k_S = k_S'. \tag{9}$$

If equation 9 is valid, then by substitution, and by subtracting equation 7 from equation 6, one obtains

$$\log I'/I = (k_{Br} - k_{Br}')mx = -cmx. \tag{10}$$

The constant c, which is characteristic for each element and for each absorption discontinuity, can be determined empirically or calculated from known mass absorption coefficients by equation 5. When either part of equation 9 does not hold, the effect is to introduce into equation 10 factors that can be determined by making additional measurements.

Glocker and Frohnmayer determined the characteristic constant c for nine elements (bibliographical reference 9, Table 4) ranging in atomic numbers from 42 (molybdenum) to 90 (thorium). They proved that identical results could be obtained with the sample in the primary (polychromatic) or in the diffracted (monochromatic) beam. The method was applied with good results to the determination of barium in glass, of antimony in a silicate, of hafnium in the mineral alvite, and of molybdenum, antimony, barium, and lanthanum in a solution of their salts.

Andrews[10] used an ionization chamber as detector to determine iron (0.44 per cent) in beryllium according to a procedure resembling that just described. Engström succeeded in applying the method to microscopic sections of tissue and claimed that "in analyses of calcium and phosphorus in biological material, quantities of 10^{-10} to 10^{-11} gram have been determined by the method with an error of 10 per cent."[11] These amounts seem very small indeed.

Limitations. The element to be determined may be present in an amount so small that the absorbancy of the rest of the sample near the critical wavelength is great enough to make the method insensitive (see equations 6, 7, and 10), or the characteristic constant c may not be large enough to permit attainment of the precision desired. Measurements at certain critical absorption wavelengths, *e.g.*, the K series for the light elements, are difficult to make, because X rays of long wavelength are strongly absorbed by air and by window materials. There may be interference owing to the nearness of critical wavelengths characteristic of other elements in the sample, *e.g.*, the K wavelengths of lead and thallium differ by only 0.004 Å. The seriousness of these limitations can sometimes be reduced by selecting a more favorable critical absorption wavelength. More important, however, is the promise of progress in this direction that is held out by recent improvements in the equipment available for such work.

Dow Spectrometer. An outstanding example of such equipment is the Dow automatic X-ray absorption spectrometer being developed by Frevel and North,[12,13] who are now preparing to publish an account of their work. The front of the instrument is shown in FIGURE 3. The spectrometer itself is housed in the case that supports control and recording apparatus and extends a considerable distance beyond the right edge of the photograph.

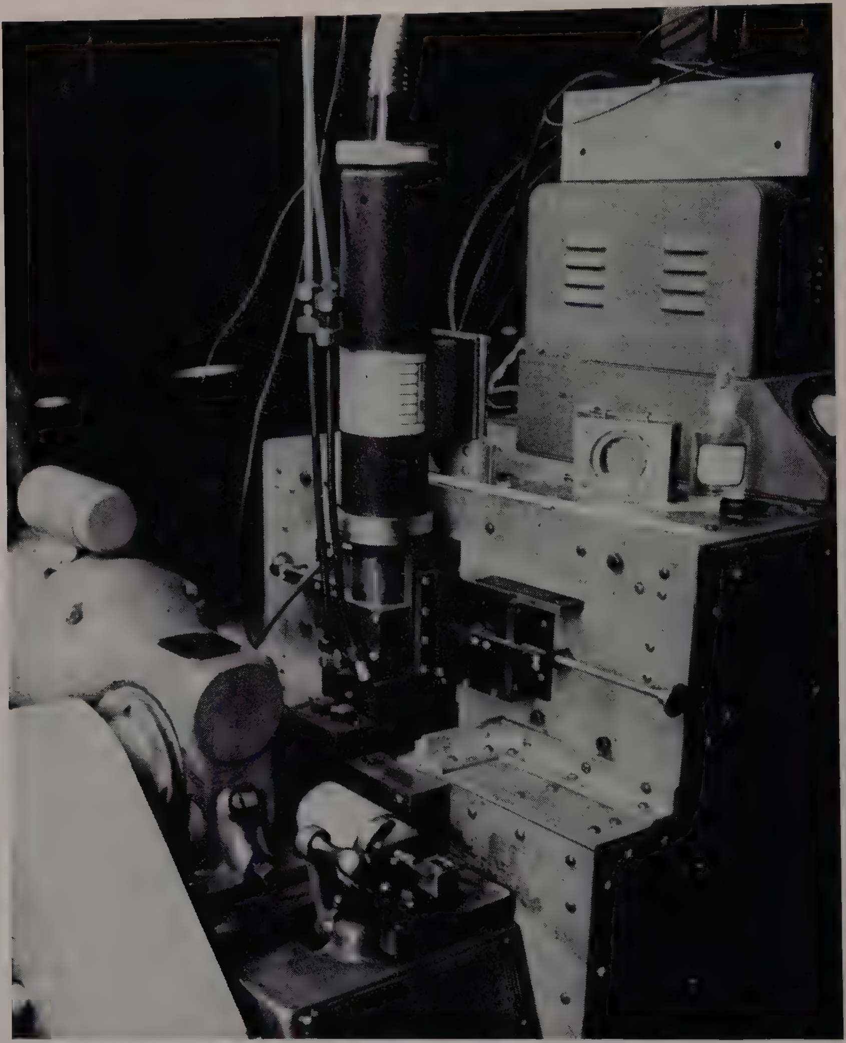

FIGURE 3. Dow automatic X-ray recording spectrometer, front view. Note cell on spectrometer case, which extends off photograph to right. Driving mechanism (left front) and vertical X-ray tube (center) are shown. (Courtesy Dow Chemical Company.)

A cone of polychromatic X rays (generated by the tube mounted vertically in front of the spectrometer case) passes through the cell containing the sample and into the case, where the unabsorbed radiant energy strikes a multiple-crystal "lens," comprised of four sodium chloride crystals, whose monochromatic beams are focused on a Geiger counter so that the sum of their intensities can be automatically recorded as an output current. Variation of wavelength is accomplished by a lathe lead screw (see the front of FIGURE 3) which moves the lens and the detector (at twice the lens speed) along the optical axis. "Voltage is stable to within 0.05 per cent during measurement. . . . The probable error of the mean of a single intensity measurement is 0.5 per cent for all measurements made for a period of approximately five minutes at rates of 10,000 counts per minute and higher. Repeated measurements give agreement within one per cent. The time for an I/I_0 measurement is 10 to 15 minutes."[12]

It seems safe to predict from these data that the Dow spectrometer will make possible greater accuracy than was achieved by Glocker and Frohnmayer, who found, for example, 5.45 per cent barium in a glass that gave 5.8 per cent upon chemical analysis. The increased convenience in measurement arising out of the use of modern instrumentation, however, will often outweigh any such gain in accuracy. In the barium determination just mentioned, Glocker and Frohnmayer used a 90-minute exposure, after which the film had to be painstakingly developed and microphotometered. On the Dow instrument, output currents proportional to intensities are simply taken from a chart (bibliographical reference 5, Figure 3).

FIGURE 4 shows how experimental data for the determination of bromine (*cf.* the first part of this section) on the Dow spectrometer are extrapolated to give the decrease in absorbancy at the critical wavelength.

As regards precision, time required, and range of determinable elements (now down to atomic number 22), Frevel and North have improved the method of Glocker and Frohnmayer to the point where it deserves serious consideration by analytical chemists. Analyses for the lighter elements can of course be carried out on the Dow instrument by making measurements at various wavelengths in regions of continuous absorption.

X-Ray Absorptometry with Polychromatic Beams

The use of monochromatic X-ray beams is desirable in chemical analysis because it simplifies the interpretation of results, but there are many applications in which the concomitant reduction in beam intensity cannot (or need not) be tolerated. Outstanding among these are control operations, two of which will be described below.

Absorptometry with polychromatic beams received a powerful impetus from the invention of the multiplier phototube[14, 15] and its subsequent conversion into a photoelectric X-ray detector by the addition of a suitable phosphor (see FIGURE 5). Morgan,[16] who had been investigating photoelectric cells for the control of roentgenographic exposures in medical work, was apparently the first to make this conversion. Independently and somewhat later, Smith[17] and Moriarty[18] constructed such a detector in solving a war problem that was fundamentally identical with many problems in chemical control.

Control Problems. If a hand-grenade fuse contains too little powder, the grenade explodes prematurely and may endanger the man who is trying to use it. An infallible, non-destructive, rapid test is obviously required, and none was available until Smith and Moriarty provided the one described below.

Fuses to be tested were mounted upright on a belt that carried them through a polychromatic X-ray beam. The absorbance of a fuse containing the proper amount of powder was great enough so that the intensity of the transmitted beam, as measured by a photoelectric X-ray detector, was too low to trip the detector circuit. With a defective fuse in the beam, however, the increased output current from the multiplier phototube set into operation four means of identifying the defective fuse. The equipment inspected fuses at a rate of approximately 4,000 an hour, and this rate was not limited by the detecting or recording apparatus.

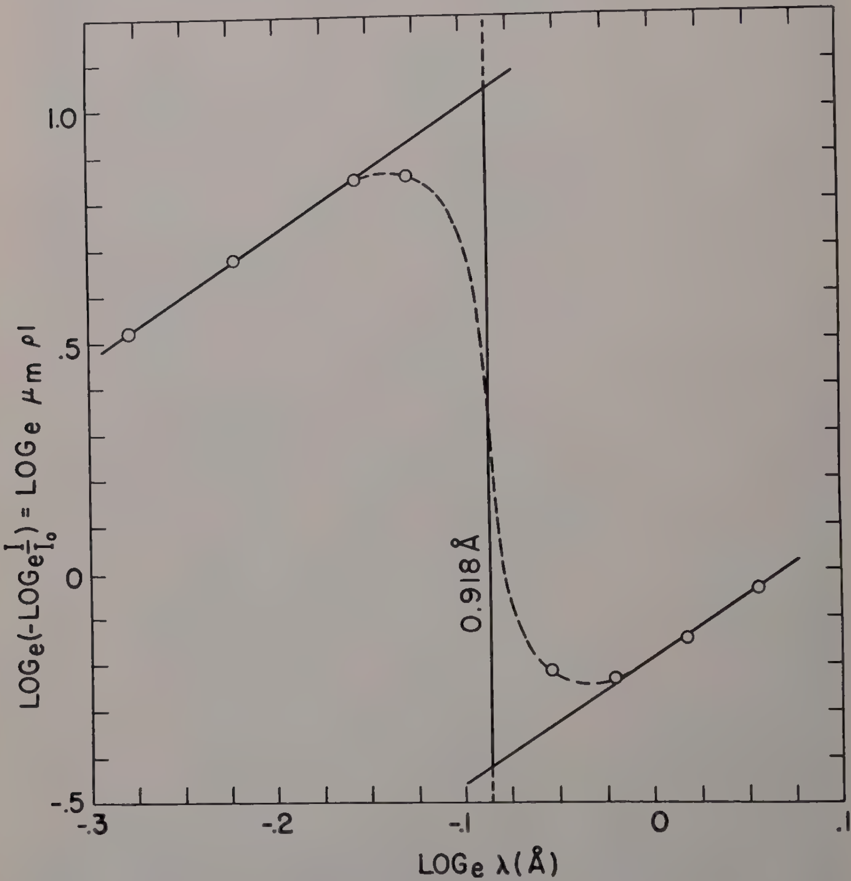

FIGURE 4. Extrapolation of experimental data in region near absorption edge to give bromine content of sample. A log-log plot permits linear extrapolation (*cf.* FIGURE 1). (Courtesy Dow Chemical Company.)

Clapp and Pohl[19] solved another important control problem by using a polychromatic X-ray beam to measure the thickness of steel strip. During the measurement, the strip is hot (1400° to 1700°F.), moving (2000 feet per minute horizontally with possible vertical vibrations up to several inches in amplitude), and subjected to a spray of cooling water. As is being done to an increasing extent in instrumental analysis, the measurement is accomplished by means of a servo system, which is adequately described in bibliographical reference 19.

It seems reasonable to hope that X-ray absorptometry with polychromatic beams can be used to solve various other production problems, such as assessing roughly the quality of crushed minerals on a conveyer belt, or controlling the addition of a material, *e.g.*, tetraethyl lead to gasoline, to a moving "base stock."

Chemical Analysis. The use of polychromatic X-ray beams in chemical analysis is not new. Fuller[20] used photographic means to compare the absorbancies of alloys for the purpose of establishing their composition. Aborn and Brown,[21] acting upon a suggestion of Calingaert, applied absorptometry of this type to the determination of tetraethyl lead in gasoline and used an ionization chamber as detector. Recently, Sullivan and Friedman[22] employed a Geiger counter for the same purpose.

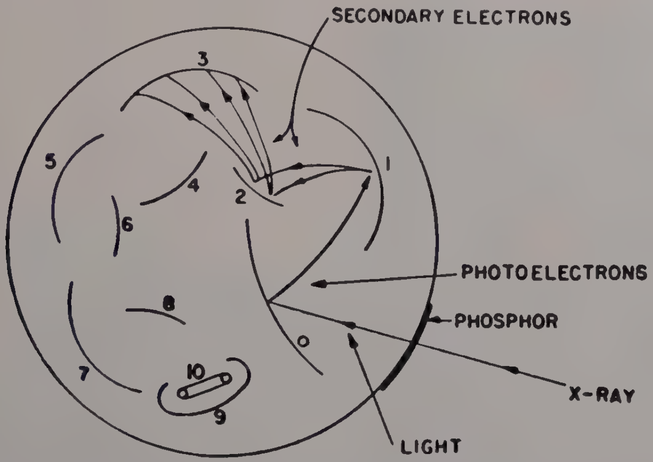

FIGURE 5. Schematic diagram of photoelectric X-ray detector. Phosphor converts X-rays into light that liberates electrons from photocathode O. These are guided electrically to the successive dynodes 1 to 9, where multiplication to give secondary electrons occurs. The greatly (10^5 to 10^6 times) amplified beam is finally gathered by anode 10 for subsequent external amplification (over 10^4 times in photometer of FIGURE 6), if desired.

The successful solution of the fuse-testing problem led to an investigation of the photoelectric X-ray detector as a tool for chemical analysis.[23] The laboratory photometer incorporating this detector is shown in FIGURE 6. Early work on solids, liquids, and gases was done by the direct method.[7] The intensity of the polychromatic X-ray beam was adjusted to a standard initial value by varying the X-ray tube voltage until the desired output current was obtained with a standard thickness of aluminum in the beam, the voltage across the detector and the amplifier setting being fixed. Output currents obtained with known weights of sample in the beam were then used to give information about the composition of the sample. In general, these output currents are plotted as in FIGURE 2, and the slopes of the curves (or straight lines, equation 4) are interpreted according to equations 5 and 2.

To illustrate such an interpretation, a common analytical problem, the determination of chlorine in a chlorinated hydrocarbon polymer, will be briefly discussed.[7] In such a polymer, chlorine may be thought of as replacing hydrogen. Because the former element has by far the greater mass absorption coefficient, this replacement will increase k, and this increase will be proportional to the extent of the replacement. Consequently, a plot of k against chlorine content for a family of such polymers should show an intercept on the k axis that represents k for the unchlorinated hydrocarbon. The other k values should fall upon a straight line whose slope depends upon the difference between the mass absorption coefficient

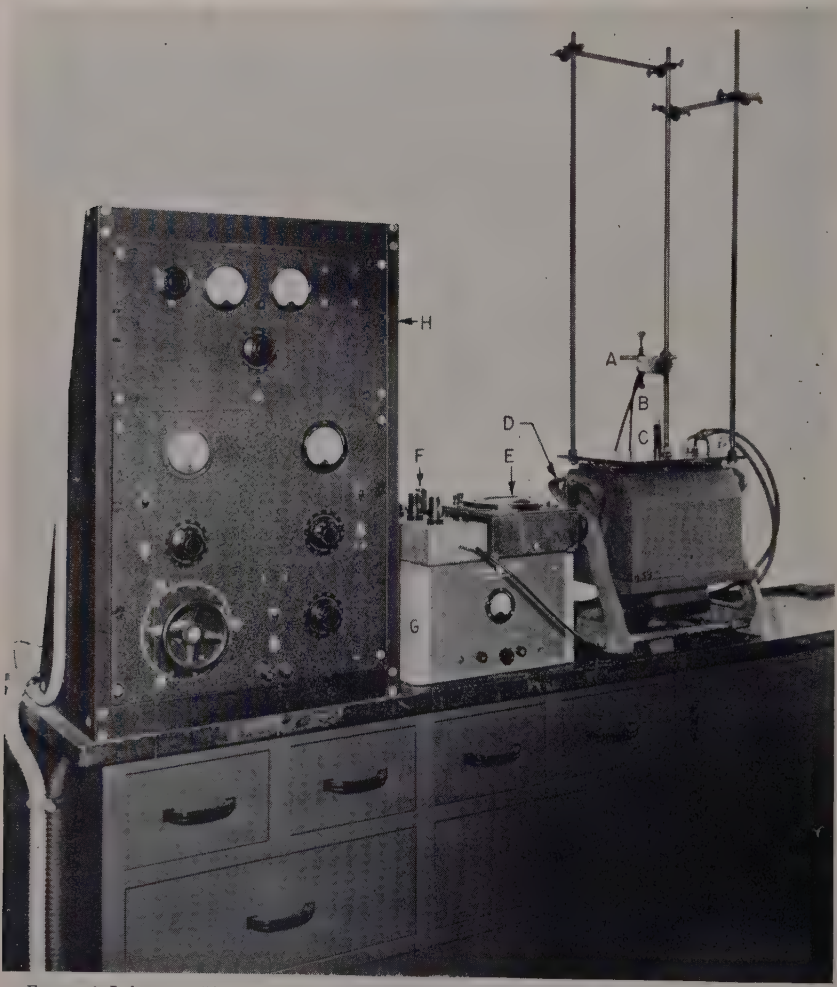

FIGURE 6. Laboratory X-ray photometer. A. Photoelectric X-ray detector. B. Sample cell. C. Sample. D. CA-5 X-ray tube and housing. E. Milliammeter. F. Amplifier and rectifier vacuum tubes. G. Regulated power supply for amplifier tubes and phototube anode voltage. H. Control panel.

for chlorine and that for hydrogen. FIGURE 7 shows that these expectations are realized.

The abscissas in FIGURE 7 are the results of chlorine determinations by a conventional method. The solid line shows that X-ray and conventional results are in good agreement. It is obvious that these data could be used as an empirical calibration curve, with the help of which chlorine determinations could be carried out on unknowns of this type about as satisfactorily as by the conventional method, and in one tenth the time. The circles and the dotted line in FIGURE 7 are calculated results based upon

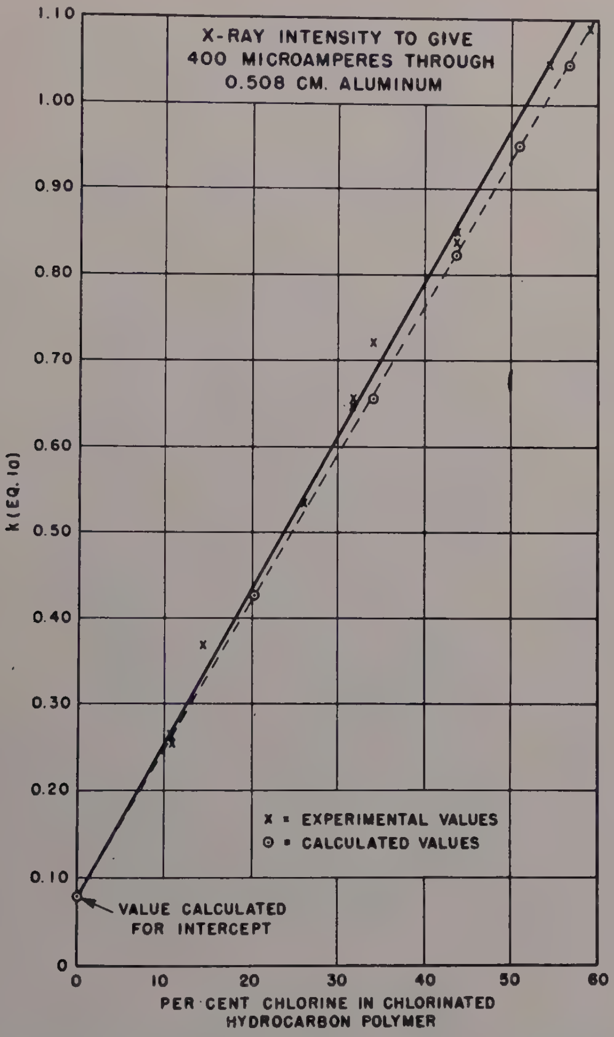

FIGURE 7. Chlorine contents of chlorinated hydrocarbon polymers. A comparison of results by the direct method with those from conventional analyses.

known mass absorption coefficients (bibliographical reference 7). The slope-intercept relationship of FIGURE 7 is common to many other problems, such as the determination of sulfur or of additives (such as tetraethyl lead) in petroleum products.

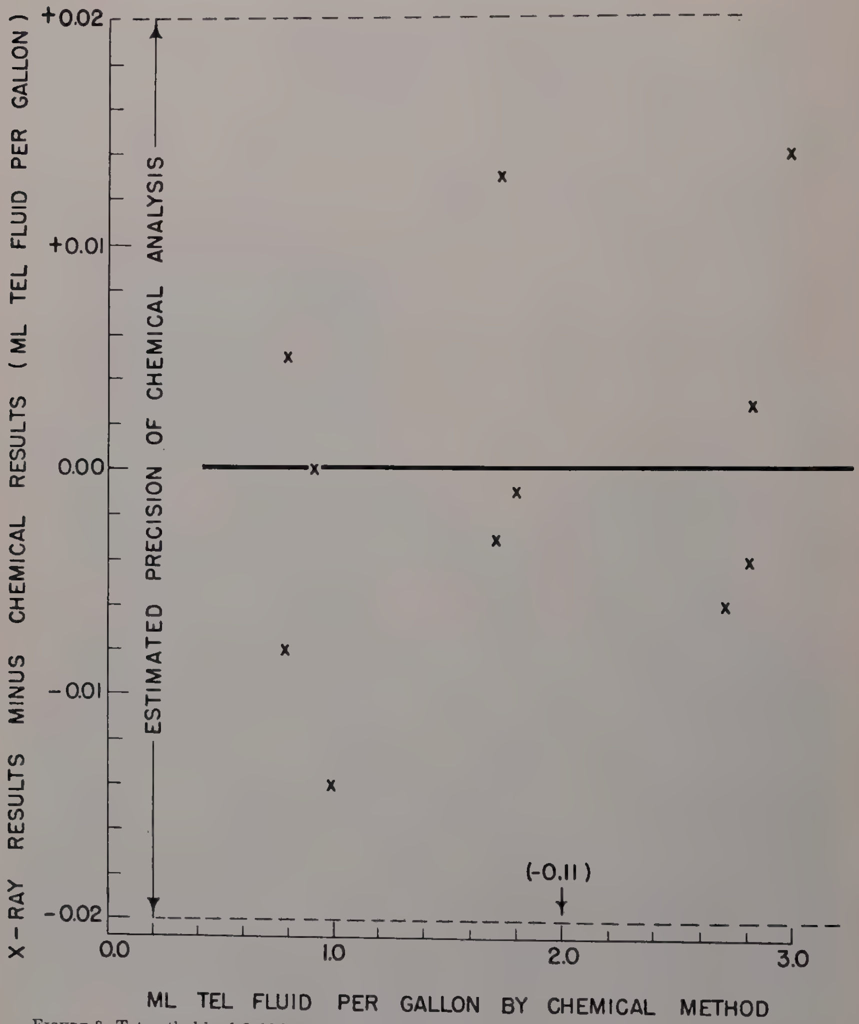

FIGURE 8. Tetraethyl lead fluid in gasoline. A comparison of results by the comparative method (variation in base stock allowed for) with those from conventional analyses.

The direct method has been used in this laboratory in point-to-point explorations of impregnated materials to test their uniformity. For this work, the diameter of the X-ray beam was reduced (in some cases to 0.15 cm.), and considerably over ten thousand output-current readings were taken. Each reading gave information in a matter of seconds that would have required several hours to obtain by conventional methods. Had conventional methods been used, moreover, analytical and performance data could not have been obtained on the same specimen, an overriding consideration in this case.

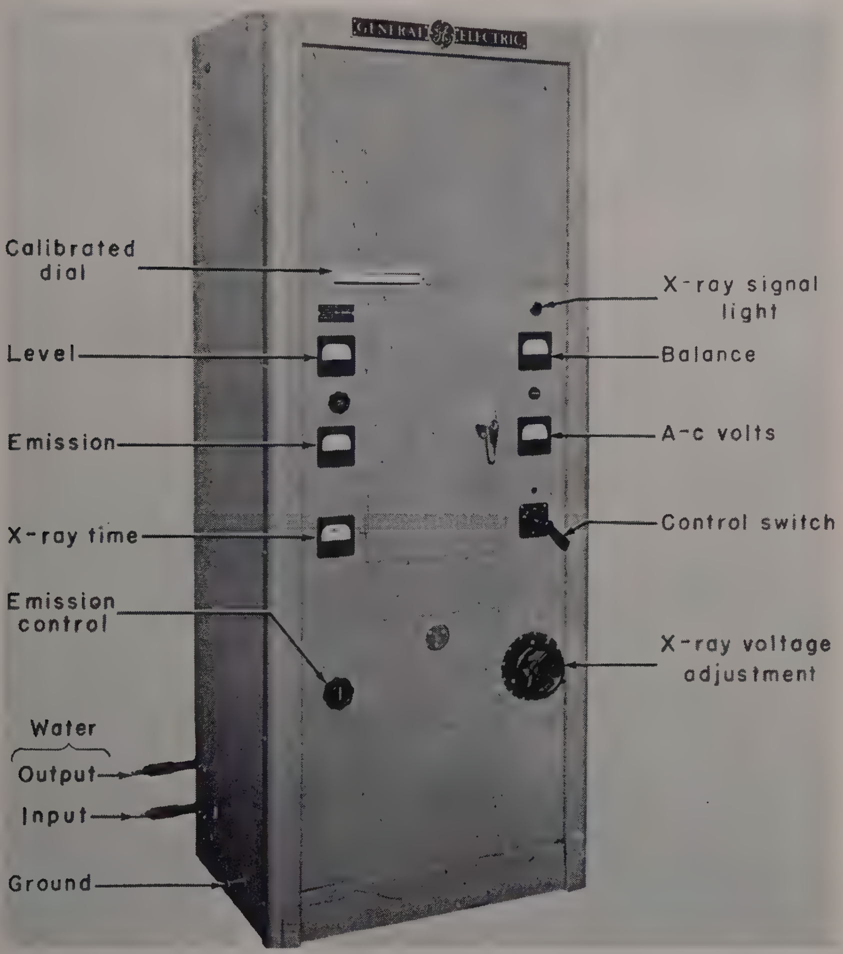

FIGURE 9. General Electric X-ray photometer. Front view, oblique from left, with parts named.

Though the direct method is well suited to exploratory work and yields results precise enough for many purposes, it is subject to uncertainties arising from voltage fluctuations and from changes in the effective wavelength of the polychromatic beam.[6] For an unfiltered beam of this kind, the variation of output current with primary voltage is much more pronounced than for a monochromatic beam, because the change in the total X-ray output affects the current readings in the former case. Rapid commutation in the beam between the unknown and a suitable standard can

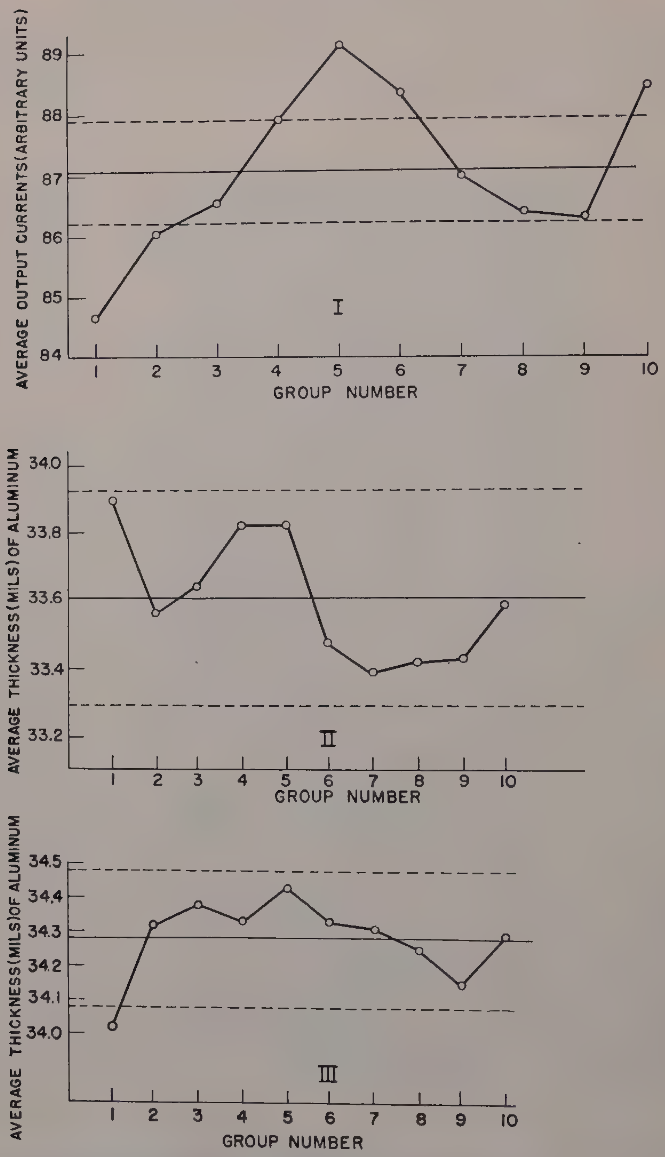

FIGURE 10. Control charts to illustrate voltage fluctuation problem. Ten readings constitute each group. I. Output currents on laboratory photometer (FIGURE 6). II. Thicknesses of aluminum required to balance 250 mils of aluminum against 280 mils (both approximate) on the G. E. X-ray photometer. Regulated voltage source. III. Experiments of Chart II with 110-volt line as voltage source.

reduce the uncertainties due to both causes, and the comparative method of X-ray absorptometry uses this procedure. Readings of output currents are taken alternately for standard and unknown. From these readings, the amount of standard equivalent in absorbancy to the unknown can be calculated. As a consequence, the interpretation of the results does not directly involve output currents, and this is the great advantage of the comparative method. In many cases, aluminum is a satisfactory standard.

The laboratory photometer was used in carrying out the following three types of determinations by the comparative method[6]: identifications of certain new compounds, determination of tetraethyl lead fluid in gasoline, and determination of sulfur in crude oil. The results were generally satisfactory, and the expected improvement over the direct method was realized. FIGURE 8 shows a set of such results for one of a number of similar problems in the petroleum industry. The measurements were made on unknown samples kindly sent us by the Ethyl Corporation; details of the work have recently appeared.[6]

General Electric X-Ray Photometer. When the direct method is being used with polychromatic beams, an extremely constant voltage source is necessary if the results are to be precise. This point is illustrated for the laboratory photometer (FIGURE 6) by the upper control chart[24] in FIGURE 10. Although the voltage source was a synchronous motor-generator set, the output of which was further regulated by two Sola transformers in series, it is clear that the output current readings in this chart show an "assignable cause of variation," which must have been the inconstancy of the voltage source. The introduction of the split-beam technique and the comparative method should improve this situation. Michel and Rich,[25] in developing the G. E. X-ray photometer, decided to use a "chopper" on a single beam in order to accomplish this purpose, but other methods are conceivable.

In the G. E. X-ray photometer (FIGURE 9), the rate of synchronous commutation between standard and sample is so high (30 times per second) that the ordinary 110-volt alternating current usually requires no regulation to be satisfactory as a power source. This point is illustrated by the two lower control charts in FIGURE 10. The regulated voltage source of the middle chart was that used for the laboratory photometer. The two lower charts show systems much more nearly "in control" than that of the upper chart, and they indicate that our 110-volt line is a satisfactory power source for the General Electric X-ray photometer.

The dotted lines in FIGURE 10 are the conventional 3 $\bar{\sigma}$ limits (bibliographical reference 24, p. 53, ¶ 14) from which the precision may be estimated when the system is in control. In the middle chart, for example, the total thickness of aluminum in the beam (*ca.* 280 mils) should be established to within approximately 0.3 mil by the average of virtually each group of ten readings.

Conclusion

The Geiger counters and photoelectric X-ray detectors now available have increased the usefulness of X-ray absorptometry. To a large extent, these devices are complementary. At present, Geiger counters are favored in X-ray spectrometry, although the photoelectric detector may eventually enter this field.[26] Absorptometry with polychromatic beams, especially in control applications and point-to-point explorations, where speed is vital, is best done with the photoelectric detector, because it is virtually instantaneous.

Geiger counters are incorporated in the improved diffraction equipment (Norelco, G. E. XRD-3) now available, which makes this equipment readily adaptable to X-ray absorptometry. In fact, it would be logical for absorption methods to be tested in research laboratories on such equipment before they are applied in the plant on commercial instruments such as the G. E. X-ray photometer. Recently, Kehl and Hart[27] have determined sulfur in hydrocarbons by X-ray absorptometry on just such a diffraction apparatus, and Vollmar, Petterson, and Petruzzelli[28] presented work of the second kind at the San Francisco meeting of the American Chemical Society.

Bibliography

1. Clark, G. L. 1940. Applied X-Rays 3rd ed. McGraw-Hill. New York.
2. Compton, A. H. & S. K. Allison. 1943. X-Rays in Theory and Experiment. 2nd ed. Van Nostrand. New York.
3. Hirst, H. 1943. X-Rays in Research and Industry. Chemical Publishing Co. Brooklyn, N. Y.
4. Sproull, W. T. 1946. X-Rays in Practice. McGraw-Hill. New York.
5. Liebhafsky, H. A. 1949. Anal. Chem. **21:** 17.
6. Zemany, P. D., E. H. Winslow, G. S. Poellmitz, & H. A. Liebhafsky. 1949. Anal. Chem. **21:** 493.
7. Liebhafsky, H. A., H. M. Smith, H. E. Tanis, & E. H. Winslow. 1947. *Ibid.* **19:** 861.
8. Winslow, E. H., H. M. Smith, H. E. Tanis, & H. A. Liebhafsky. 1947. Anal. Chem. **19:** 866.
9. Glocker, R. & W. Frohnmayer. 1925. Ann. Physik **76:** 369.
10. Andrews, C. L. 1938. Phys. Rev. **54:** 994.
11. Engström, A. 1946. Nature **158:** 664.
12. Frevel, L. K. 1948. Dow Chemical Co. Midland, Mich. Personal communication. Oct. 18.
13. Frevel, L. K. 1948. *Ibid.* Nov. 5.
14. Rajchman, J. A. & R. L. Snyder. 1940. Electronics **13** (12): 20 (December).
15. Zworykin, V. A. & J. A. Rajchman. 1939. Proc. I.R.E. **27:** 558.
16. Morgan, R. H. 1942. Am. J. Roentgenol. Radium Therapy **48:** 220.
17. Smith, H. M. 1945. Gen. Elec. Rev. **48** (3): 13 (March).
18. Moriarty, C. D. 1945. Elec. Eng. **64** (12): 433 (December); 1947. Gen. Elec. Rev. **50** (2): 39.
19. Clapp, C. W. & R. V. Pohl. 1948. Elec. Eng. **67** (5): 441 (May).
20. Fuller, T. S. 1922. Gen. Elec. Rev. **25:** 746.
21. Aborn, R. H. & R. H. Brown. 1929. Ind. Eng. Chem., Anal. Ed. **1:** 26.
22. Sullivan, M. V. & H. Friedman. 1946. Ind. Eng. Chem., Anal. Ed. **18:** 304.
23. Liebhafsky, H. A. & E. H. Winslow. 1945. Gen. Elec. Rev. **48** (4): 36 (April).
24. American Society for Testing Materials. 1940. Manual on Presentation of Data. Third printing.
25. Michel, T. C. & T. A. Rich. 1947. Gen. Elec. Rev. **50** (2): 45 (February).
26. Coltman, J. W. & Fitz-Hugh Marshall. 1947. Nucleonics **1** (3): 58 (November).
27. Kehl, W. L. & J. C. Hart. 1948. Symposium on Rapid Methods of Analysis Used in the Petroleum Industry. Twenty-eighth Annual Meeting, American Petroleum Institute, Chicago, Ill., Nov. 8 (Preprint).
28. Vollmar, R. C., E. E. Petterson, & P. A. Petruzzelli. 1949. Chem. Eng. News **27:** 610.

THE ANALYTICAL SPECIFICITY OF COUNTERCURRENT DISTRIBUTION

By J. Delafield Gregory and Lyman C. Craig
The Rockefeller Institute for Medical Research, New York, N. Y.

The rapid development of modern biochemistry has brought the realization that classical techniques of isolation and purification are frequently inadequate to cope with the types of compounds encountered. Instability, high molecular weight, and annoying physical properties, such as failure to crystallize, are often handicaps, together with the likelihood that, in a biological environment, closely related analogs and isomers may be found occurring together to aggravate the problems of separation. The need for analytical methods, which can be applied as generally as possible in such cases, has led to the development of countercurrent distribution in this laboratory. Since it is essential to have techniques which are sensitive and specific, but which operate under the mildest experimental conditions, the method has been designed to utilize the advantages of working with dilute solutions.

In this procedure, a compound or mixture is partitioned between series of immiscible phases in a simple countercurrent order in separate contacting cells, every individual partition attaining essentially complete equilibrium. Only the case of partition between two liquid or solvent phases will be considered here, although the principles apply regardless of the nature of the phases.[1]

Before considering the potentialities of the method as an analytical tool, it will be necessary to outline briefly the actual procedure and some of the simple mathematics which furnish its basis and validity. Then, the apparatus currently in use and the type of results which can be obtained will be described.

When a single pure solute is dissolved in either one of a pair of immiscible phases and the phases are shaken together, the solute will partition itself between the two in a characteristic proportion at equilibrium.[2] The ratio of the fraction in the upper phase to that in the lower (assuming equal volumes) is called the partition ratio or distribution coefficient, K. The following development deals only with sufficiently dilute solutions, so that the partition ratio is not significantly affected by the total concentration, and so that, in case of a mixed solute, every individual species behaves independently of the others and has its own reproducible K. This ratio, it should be emphasized, is not directly related to the relative solubilities in the two phases, since solubility implies saturated solutions where conditions are very different from those in the dilute solutions considered here.

The case of a pure solute which partitions equally between the two phases is taken for illustration in FIGURE 1, assuming equal volumes of the phases throughout. After the first equilibration, each phase contains half the material. They are separated and the upper transferred to the adjacent cell, which contains fresh lower phase; fresh upper is added to cell 0. After equilibration of both cells, the uppers are each moved one cell to the right and the equilibration repeated. Every time the whole series of upper phases is moved one stage, one *transfer* has been made. At any given stage, the numbers in FIGURE 1 represent the fraction of the original starting solute now found in each phase. The overall effect of progressive transfers is to cause a series of upper phase portions to pass over a series of lower phases. For the sake of consistency, it will be considered that the upper phases always move to the right. The two series "flow," although discontinuously, countercurrent to each other.

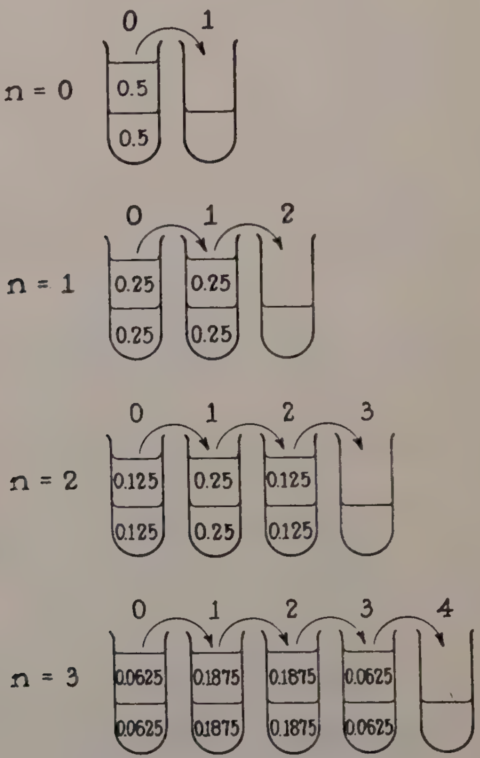

FIGURE 1. Schematic diagram of countercurrent distribution of a substance with partition ratio of unity.

When a similar analysis is carried through, using a general expression for the fractions in the upper and lower phases, instead of this specific case, it is found that for any number of transfers, n, the contents of each of the $n + 1$ cells at the end of the distribution is given by the terms of the expansion of the binomial[3]

$$\left(\frac{1}{K+1} + \frac{K}{K+1}\right)^n. \qquad (1)$$

For a given number of transfers, when the terms of the expansion are plotted as ordinates against their position in the series of cells, a curve such as one of those in FIGURE 2 results. The shape and position of the curve depend on the partition ratio of the solute, since the upper phase, moving to the right, carries it along further the higher its K, that is, the more it favors the upper phase. The curve of a substance with K greater than unity is a mirror image of the curve for the reciprocal K, but at the other end of the series.

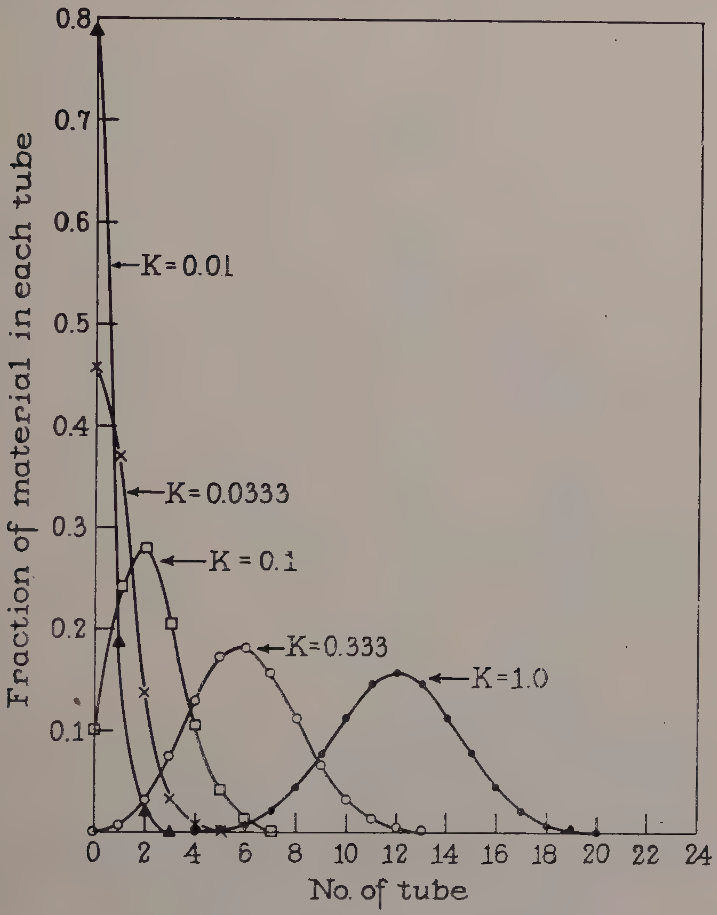

FIGURE 2. Theoretical curves for twenty-four transfer distribution.

When the starting material contains more than one species, each will form its own particular distribution, and the curve found at the end of the process by the determination of the material in each tube will be the sum of the individual binomial curves.

If a particular K is considered (equal to unity for illustration), and the other variable, the number of applied transfers, is changed, the effect can be seen in FIGURE 3. With more transfers, the curve becomes lower and broader, but its width does not increase as fast as the total number of tubes, as shown in the table in FIGURE 3. The ability to apply larger numbers of transfers allows more complex mixtures to be fractionated, since there is room in the distribution pattern for more discrete curves to appear.

For a given K, the curve always maintains the same position relative to the total number of tubes (the center when $K = 1$). This follows from the relationship of N, the number of the tube containing the maximum, to n, the number of transfers[4] (the total number of tubes is $n + 1$).

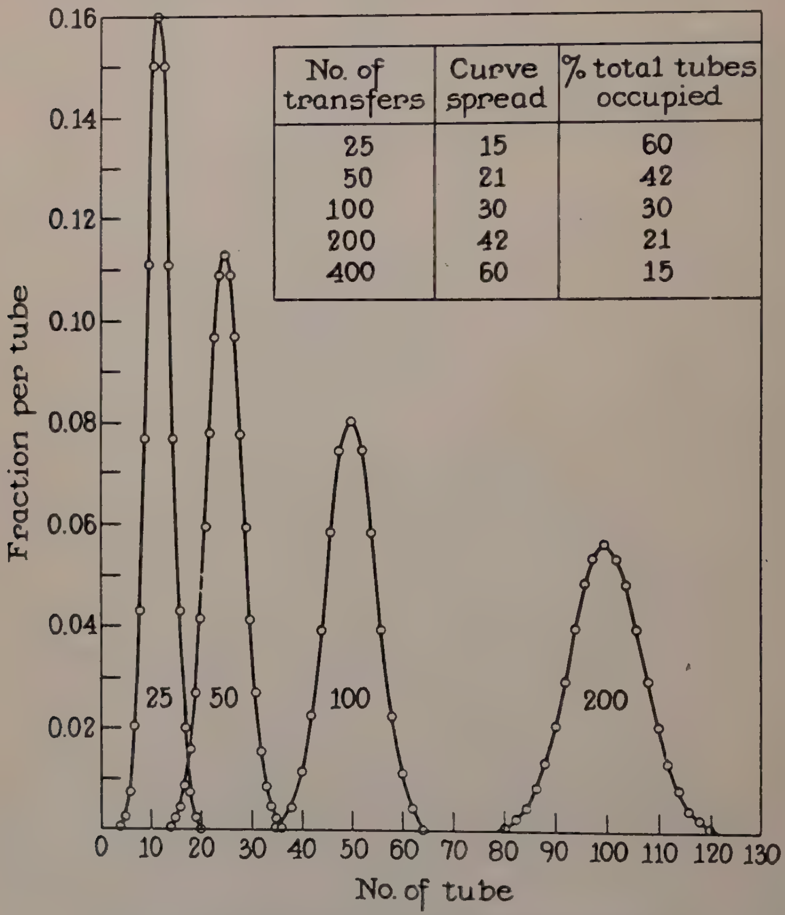

No. of transfers	Curve spread	% total tubes occupied
25	15	60
50	21	42
100	30	30
200	42	21
400	60	15

FIGURE 3. Theoretical curves for $K = 1$ and various numbers of transfers.

$$N = n\left(\frac{K}{K+1}\right). \tag{2}$$

This continuous function is an approximation as applied to the discontinuous distribution process and is not satisfactory for n less than about twenty or for values of K far from unity. Under those conditions, more exact and cumbersome calculations based on the binomial expansion must be used. The position of the peak of a pure substance in a distribution is the most accurate measure of its partition ratio, much more so than any determination based on a single partition.

The available number of contacting cells limits the number of transfers which can be done in this simple way. But the operation can be carried further by an extension of the procedure, which is called "withdrawal."[4, 5] After the cells are filled, following the scheme of FIGURE 1, further transfers give upper phases emerging at the right hand end of the series, while fresh upper phases are fed in from the left at each stage. The effect produced is that of an unlimited series of upper phase portions passing over a fixed and limited set of lower phases. Similarly, a series of lower phases can be made to pass under the fixed uppers, or the two effects can be combined to allow both phases to be withdrawn on alternate transfers. Since each withdrawn fraction has experienced a different and progressively increasing number of transfers, the curve of a pure solute, when it passes into the withdrawn series, is not quite symmetrical. The situation can be dealt with mathematically by simple approximations, and the withdrawal curves can be interpreted as readily as the curves in the basic part of the distribution. This aspect will be treated fully elsewhere.

For distributions of twenty-four transfers or less, and, in any case, where part of the solute remains in the first or last tube, so that its curve is not symmetrical, the exact formula of the binomial expansion must be used in constructing curves. The fraction of the solute in any tube r can be found from formula 3, and there are many other relationships which simplify the calculations.[3]

$$T_{n,r} = \frac{n!}{r!\,(n-r)!}\left(\frac{1}{K+1}\right)^{n}(K)^{r}. \tag{3}$$

On the other hand, for large numbers of transfers, the arithmetic becomes unnecessarily cumbersome. The exact binomial curves then approach normal distribution curves so closely that the mathematics of probability can be substituted as a very excellent approximation. The only formulas needed for calculating a theoretical curve are the following:

$$y_0 = \frac{1}{\sqrt{2\pi n \dfrac{K}{(K+1)^2}}} \qquad y_x = y_0\, e^{-\left(\frac{x^2}{2n\frac{K}{(K+1)^2}}\right)}. \tag{4}$$

The fraction of the solute in the maximum tube is given by y_0, and y_x represents the fraction in a tube, x tubes distant from the maximum on either side. Only enough values of y_x, suitably spaced, need be calculated so that the curve can be drawn readily.

Another useful quantity, stemming from the mathematics of probability, is the standard deviation, σ. A range of $\pm 3\,\sigma$ about the maximum includes more than ninety-nine per cent of the area of a curve,[6] and, for practical purposes, these are considered the limits of the distribution. In terms of the symbols used in these partition studies,

$$\sigma = \sqrt{n \frac{K}{(K+1)^2}}. \tag{5}$$

For many preliminary calculations and estimations of the outcome of distributions, the widths and positions of the curves as obtained from equations 2 and 5 are sufficient.

Even though the experimental and calculated points are connected by smooth curves, and continuous functions are used for approximation, it should be emphasized that the operation itself is discontinuous, the only real values on the graphs being the points themselves.

Calculated curves have two chief uses, one of which is the construction of hypothetical situations which serve as guides in selecting conditions for actual experiments. In addition, it is possible to interpret the results of distributions by fitting calculated curves to them and determining the minimum number of components required to account for the experimental patterns. A distribution of a mixture of four fatty acids[7] is shown in FIGURE 4. The resulting curve shows four peaks, which can be closely fitted by the sum of the four theoretical curves plotted on the same graph. The validity of the analysis in this case was confirmed by isolation and redistribution of the material in tubes 15, 16, and 17. A curve resulted which was accurately matched by a single theoretical curve. The quantitative aspects of this curve-fitting procedure, when used as a method of determining purity, will be discussed later.

The application of these principles as an analytical method is justified as follows: A single partition between two phases is sufficient in theory to cause a partial separation of a mixed solute if there is any difference whatever in the partition ratios of the components. Simply determining the mass of material in each phase is not revealing at this stage. It is necessary to use a more specific analysis which can, in its own right, differentiate between the components of the mixture. If more partitions are done, that is, if a distribution is made, then the mere determination of weight in the various fractions is enough to establish whether species with different partition ratios are present. In this way, weight, the most fundamental and impartial measurable property, is made to give very specific analytical information. Weight is the preferred analytical unit for interpreting most distributions, especially for exploring new situations where some component of a mixture might be overlooked if a more specific analytical method such as spectrophotometry, titration, or bioassay were relied upon.

In this or any other partition method, the sensitivity and separating power are functions of two experimental conditions: the number of effective or equivalent partitions which can be applied, a mechanical problem, and the obtainable difference between the partition ratios in a mixture. The latter involves the careful study of solvents and their effects. The greater the number of transfers in a distribution, the more individual operations contribute to the final result, which then represents the average of a larger number of single partitions. This minimizes the effect of incidental errors in transfers and manipulation. For example, in a routine distribution using fifty-four cells and four hundred transfers, well over 20,000 useful extractions are performed. It is evident that the experimental curves bear a real relationship to the normal distribution or probability curves on which the mathematical treatment rests.

Consequently, one aspect of the subject which has received much attention in this laboratory is the design of apparatus to simplify making large numbers of transfers. Stainless steel countercurrent distribution instruments have been in use for some time.[4, 8] The one shown in FIGURE 5 contains fifty-four tubes arranged in a circle. The open tops and bottoms are all closed simultaneously by two large glass discs, and a sliding joint between the upper and lower sections of the tubes allows all the upper sections to be shifted as a unit with respect to the lower ones about the central shaft. The lower phase exactly fills each lower section, and the upper phases are carried around from one to the next. At each stage, the solvents are thoroughly mixed by tumbling the whole assembly on the side bearings, the equivalent of shaking fifty-four separatory funnels all at once.

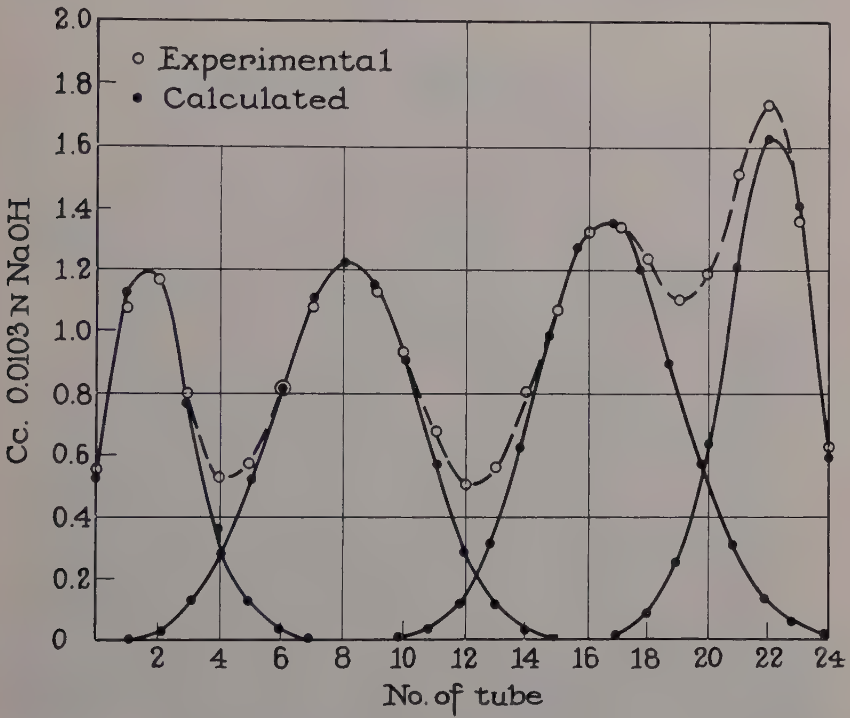

FIGURE 4. Twenty-four transfer distribution of a mixture of (left to right) acetic, propionic, butyric, and valeric acids. ○, experimental curve; ●, theoretical curves.

With a fifty-four tube instrument, up to three or four hundred transfers can be made profitably using one of the withdrawal procedures. Such a run, together with the analysis of the results by evaporating aliquots and weighing the residues, requires three to four man-days of work. There are many fractionation problems for which this would be more than ample, but as more difficult situations are undertaken and more separating power is needed, methods are being developed for making still more transfers quickly and easily. An all-glass apparatus, operating on a simple principle of decantation, has been designed[8] and has already established its usefulness.* A single unit or tube is seen in FIGURE 6. The equilibration is made in chamber A by rocking the tube about 30° above and below the horizontal.

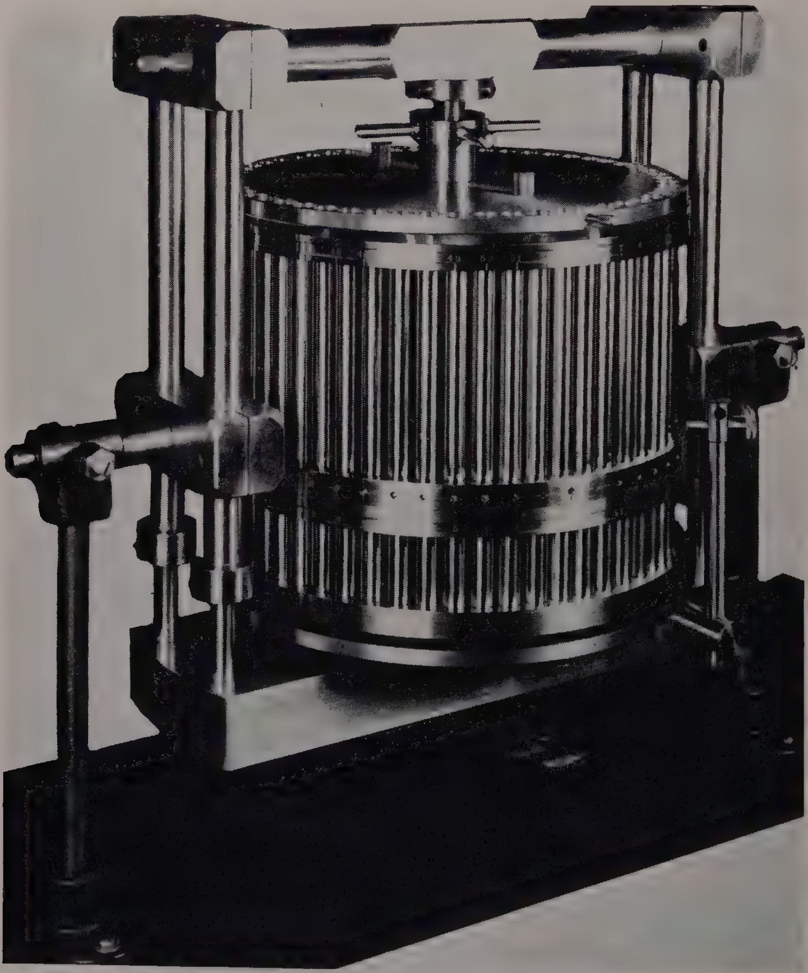

FIGURE 5. Fifty-four tube stainless steel distribution instrument.

---

* A more recent design may be found in: CRAIG, L. C. 1950. Anal. Chem. 22: 1346.

After the phases have separated, the unit is tilted backward 90° so that all the upper phase runs out into the auxiliary transfer chamber, C. The lower phase remains in the end section of A, which it fills exactly. When the tube is righted, the upper phase runs out into the next unit in line. Extension of the train is virtually unlimited, as any number of units may be set up side by side.

FIGURE 7 shows an assembly containing one hundred and eight tubes. Transfers can usually be made at the rate of thirty to forty per hour, which means about 4,000 individual extractions per hour. The advantages of glass construction and the absence of moving or sliding parts are obvious. The assistance of Mr. Otto Post has been invaluable in the design and construction of these instruments.

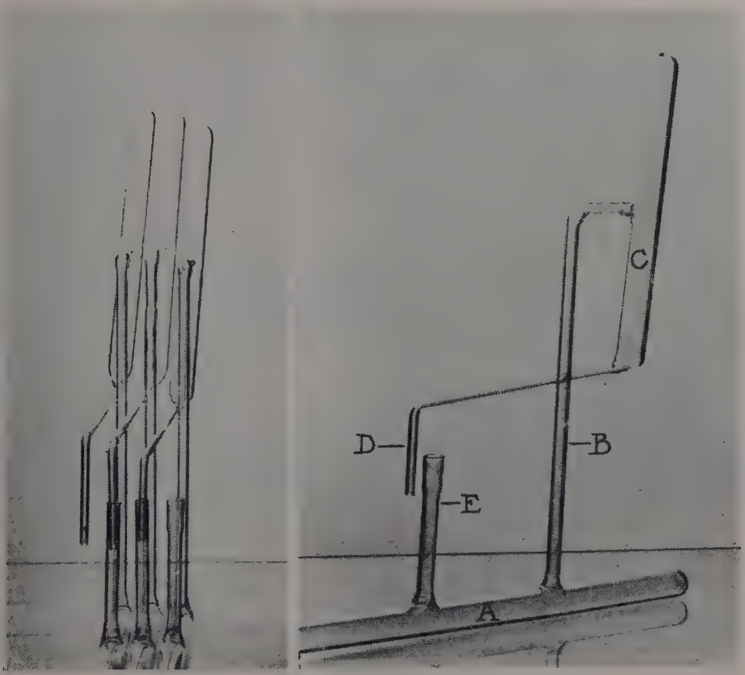

FIGURE 6. Units from glass distribution instrument.

It is interesting to compare certain aspects of such an apparatus with a continuous liquid-liquid extraction column. With regard to rates, when solvent is being fed in at one end of the train and extract withdrawn from the other, the throughput may be more than 400 ml. per hour. There are two important respects, however, in which the method differs from any continuous process: this distribution operates unquestionably at equilibrium, and the exact number of stages (which are practically theoretical stages) is known, so that no assumptions are necessary for the mathematical interpretation.

The practical working range of partition ratios depends on the purpose of the distribution and on the number of transfers which can be applied to to the solute. The maximum separation per transfer of a binary mixture occurs when the partition ratios of the two species are reciprocals of each other.[9, 10] Even though the curves are broadest when the K's are near unity, transfers have the greatest effect on the solutes in this region, and differences in their properties are exploited to the utmost. For general preparative purposes, however, in a small distribution of twenty-four transfers, the working range of K might be approximately 0.2 to 5, for one hundred transfers 0.1 to 10, and for one thousand transfers 0.01 to 100. Although efficiency is lost when the K is either high or low, the fact that many transfers can now be made quickly offsets the disadvantage to some extent and makes it practical to handle a much wider variety of solutes for which systems have not been found giving K's in the optimum range.

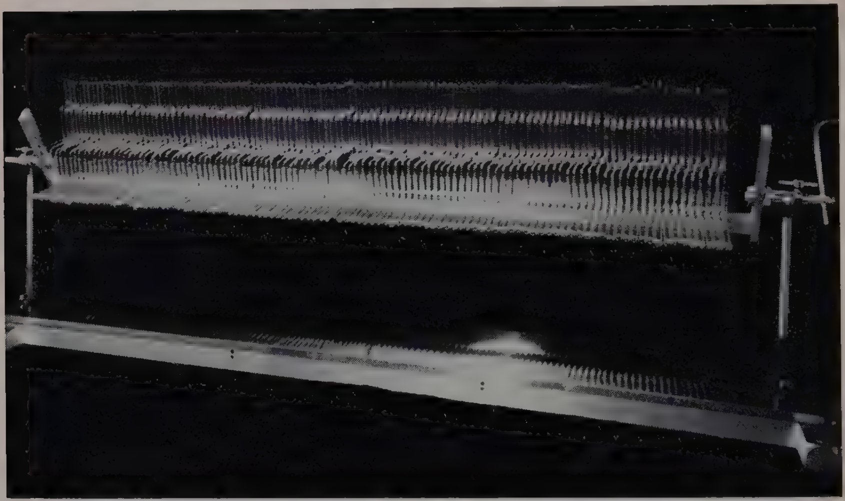

FIGURE 7. 108-Tube glass distribution instrument.

Many amino acids and peptides, for example, can be distributed between an aqueous phase and a partially miscible alcohol,[11] even though most of them greatly favor the aqueous phase.

Several questions arise in connection with the applicability of countercurrent distribution. How many transfers are necessary to separate a given pair of solutes to a given degree of completeness? What is the smallest proportion of a given impurity which can be detected under conditions likely to be encountered? What is the relationship between the nature of a solvent system and its ability to separate particular types of mixtures? The mathematics of the binomial expansion answers the former points. The problem of the specificity of solvents is not so simple, and some generalities and intuitive ideas must suffice for the present.

In order to represent the separations which can be attained, calculated curves have been set up for various situations. For the sake of simplicity, a mixture of two species in equal amount may be assumed, distributed under the most favorable conditions. This means that the partition ratios are reciprocals, the resulting curve being symmetrical about the center of the whole distribution. If a degree of separation is arbitrarily chosen such that fifty per cent of each component is recovered essentially pure, the distance between the peaks is equal to one half the width of either curve, or 3 σ, as in FIGURE 8. The separability or "separation factor" of the two components may conveniently be represented by β, the ratio of the larger K to the smaller. In this special case, $\beta = 1/K^2$. This quantity is analogous to α, the term used in distillation theory for the ratio of the vapor pressures in a binary mixture. When $\beta = 1$, separation is impossible in the given solvent system, and, as β increases, separation becomes easier. The relationship between β and the number of transfers required to achieve this particular spread may be derived as follows (the positions of the maxima are given by formula 2):

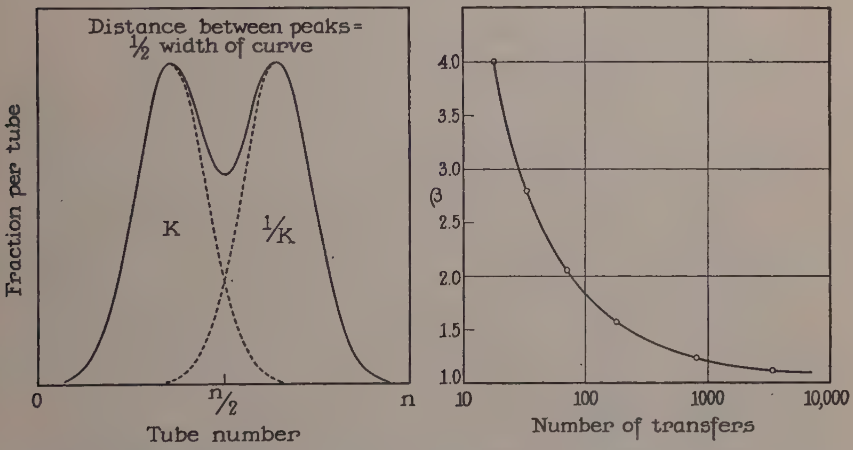

FIGURE 8. Relationship between separability of a binary mixture and number of transfers required for arbitrary degree of separation.

$$N = n\left(\frac{K}{K+1}\right) \quad \text{and} \quad N' = n\left(\frac{1/K}{\frac{1}{K}+1}\right) = n\left(\frac{1}{K+1}\right). \tag{6}$$

The distance between the maxima is:

$$N' - N = 3\sigma \quad \text{or} \quad n\left(\frac{1}{K+1}\right) - n\left(\frac{K}{K+1}\right) = 3\sqrt{n\frac{K}{(K+1)^2}} \tag{7}$$

$$\text{whence} \quad n(1-K) = 3\sqrt{nK} \quad \text{and} \quad n = \frac{9K}{(1-K)^2}. \tag{8}$$

From this relationship and the graph in FIGURE 8, it is seen that the required number of transfers increases very rapidly as β decreases in the region between two and unity. No matter what the β, if the postulated degree of separation is attained and all the material is recovered in two fractions by dividing at the minimum of the curve, each part will be better than ninety-three per cent pure. If essentially complete separation were demanded, the distance between the peaks would have to be 6 σ, with corresponding changes in the formulas.*

When a distribution is used for preparative isolation, it is usually desirable to start with as much solute as possible. The danger then arises of overloading the solvent system to the point where the partition ratio is no longer sufficiently constant and the resulting curve is distorted or skewed. This may be largely offset by scattering the solute initially in several adjacent tubes. In a one hundred-transfer distribution, if the solute is started in seven tubes, the result will be the sum of the seven small overlapping curves in FIGURE 9, given by the solid line. If the same amount of solute were started all in one tube, the dashed curve would result. Unless the ultimate in accuracy is required, the difference in these results may be dis-

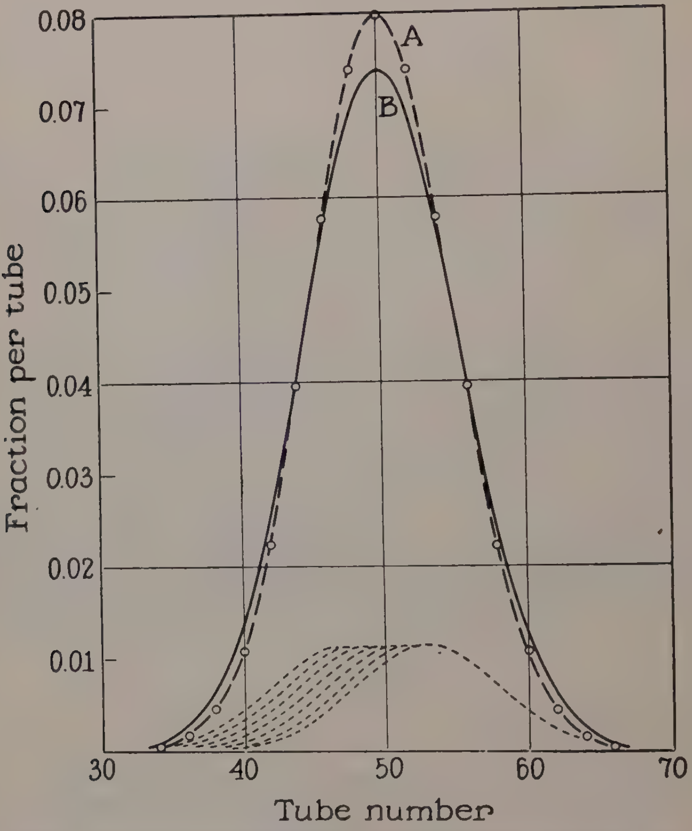

FIGURE 9. 100-Transfer distribution; effect of scattering solute initially in seven tubes.

---

* Since the preparation of this paper, there has appeared a more elaborate development of this approach: NICHOLS, P. L., JR. 1950. Anal. Chem. **22:** 915.

regarded, and the advantages of beginning with only one seventh the concentration may be very great. The discrepancy will be no worse than this if the material is scattered in a number of tubes equal to about twenty per cent of the ultimate width of the curve at the end of the distribution. When $K = 1$, one hundred transfers gives a curve thirty tubes wide, which would allow starting in six or seven tubes.

So far, this discussion has been from the point of view of separation and isolation from gross mixtures. The study of purity is essentially the same problem, with the understanding that contaminants are usually in smaller proportion and that emphasis is on the analytical results. Since the absolute purity of a substance can never be proved and can be confirmed only by continued failure to find impurity, the definition of purity must be an operational one in terms of the specific techniques involved. Although a great deal may be accomplished on a preparative scale, even when the partition isotherm is not linear and the curves are slightly skewed, for sensitive detection of small amounts of impurity it is essential to work at low concentrations and under the most ideal conditions attainable. No distribution can reveal a mixture if the components have identical K's, or if the amount of impurity is below the limit of sensitivity of the measurements used to

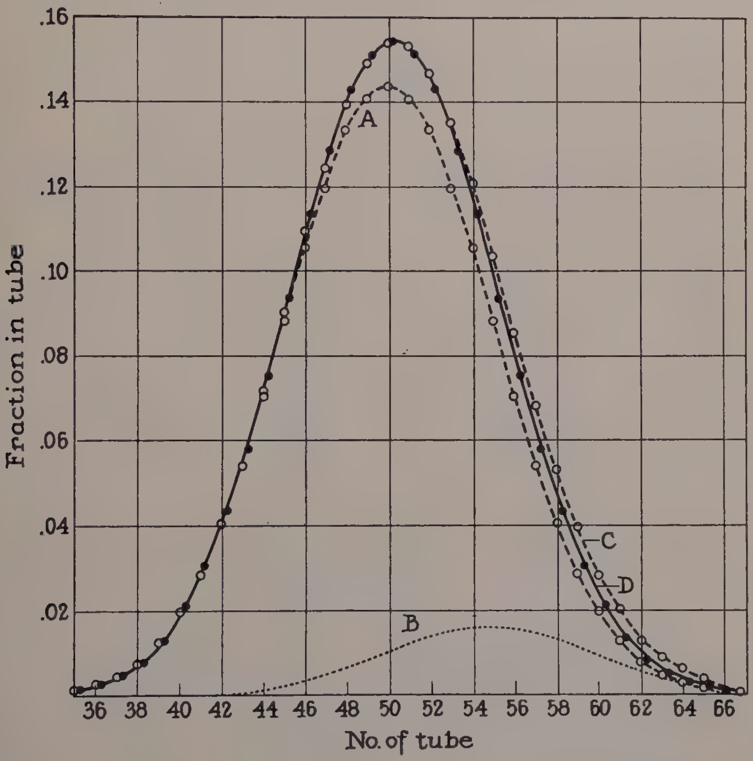

FIGURE 10. Hypothetical 100-transfer distribution of a mixture of 90 per cent compound A ($K = 1.0$) and 10 per cent compound B ($K = 1.2$). $C = A + B$. D = theoretical curve for single substance fitted to C.

obtain the distribution curve. Identical partition ratios are certainly unlikely (except for optical enantiomorphs) especially if more than one solvent system can be applied, but it is important to know exactly what degree of sensitivity may be expected.

In order to form an idea of the limits to which the technique can be carried, the situation in FIGURE 10 may be considered.[12] An impurity of ten per cent should be detectable, using one hundred transfers, if the solvent system is selective enough to give a β of 1.2. The outer curve is the one which would be found on weight analysis of such a distribution. With only this information, a theoretical curve would be calculated to fit as closely as possible. The experimental curve deviates most from the theoretical in the region of the impurity, and the difference here is significant provided the weight determination has a sensitivity at least as good as one per cent of the maximum weight.

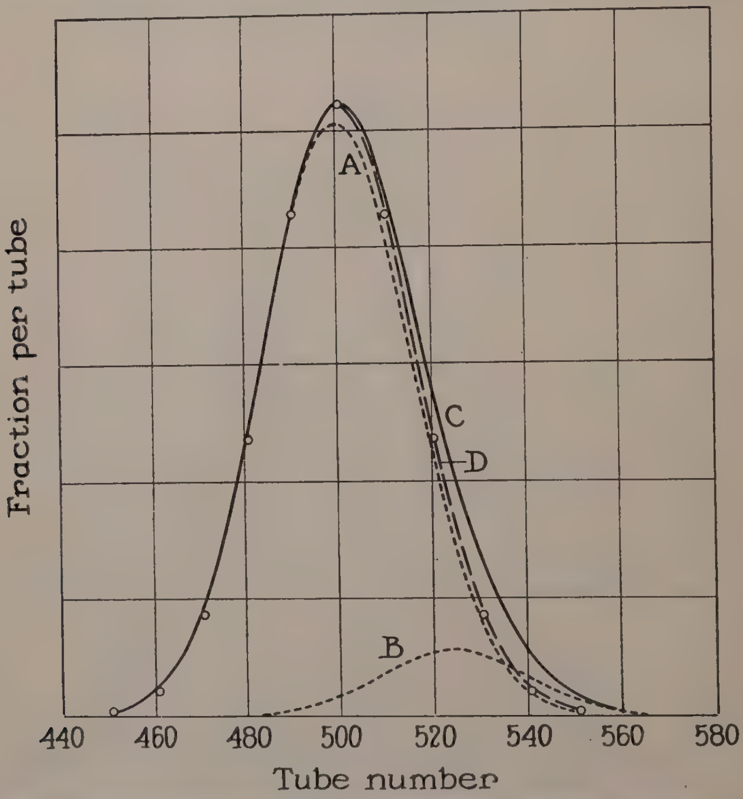

FIGURE 11. Hypothetical 1000-transfer distribution of a mixture of 90 per cent compound A ($K = 1.0$) and 10 per cent compound B ($K = 1.1$). $C = A + B$. D = theoretical curve for single substance fitted to C.

If the β is lowered to 1.1, however, as in FIGURE 11, the number of transfers needed to show an impurity of ten per cent approaches one thousand. In general, one might expect to find such a low β only in the case of very closely related isomers, or else as a coincidence which might be eliminated by changing to a different system. If the β- values were higher in these examples, of course, impurities present in much smaller amount would be observable. A valuable characteristic of countercurrent distribution in purity studies is that the impurities receive the same treatment as the major component and are often as readily isolated.[13]

The sensitivity of the method as outlined here is based on analysis by weight alone. This quantity should always be used when possible because it is all-inclusive, but other methods which differentiate between the components can supplement weight and greatly increase the sensitivity of the results. A specific analysis such as bioassay is often useful in the isolation of natural products, as shown in FIGURE 12, which represents the separation in a single operation of a penicillin from a crude extract of the culture.[14]

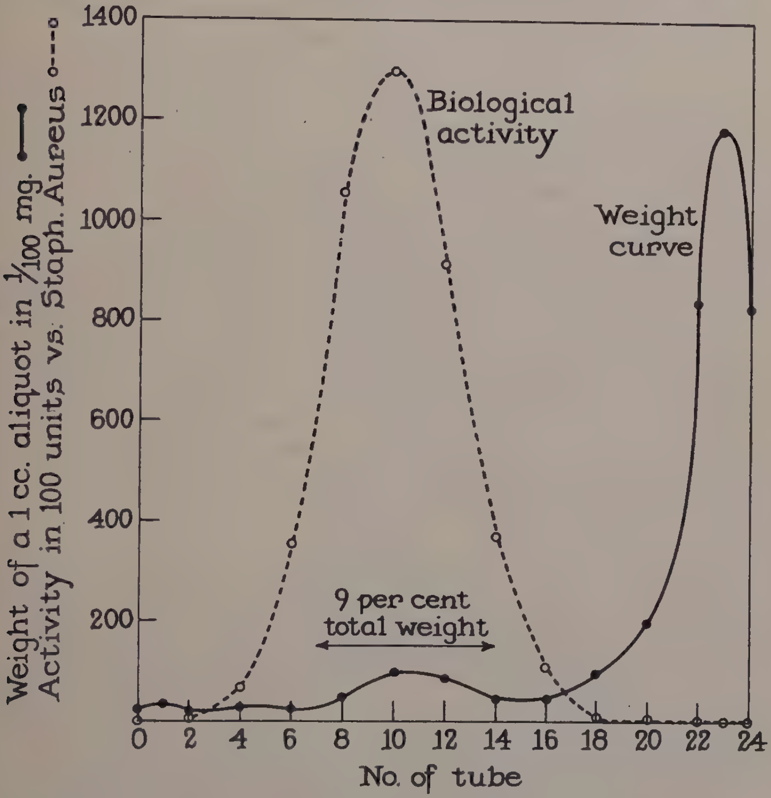

FIGURE 12. Isolation of a penicillin from a crude extract of a culture medium.

With respect to solvents, the only basic requirement is a pair of phases between which the material to be investigated has a reasonably constant partition ratio in the working range at a suitable temperature. The only restriction in the nature or number of solvents which make up the system is that two phases must result, when they have all been shaken to equilibrium, which do not cause transformation of the solute and which do not interfere with the determination of the results, or, in preparative work, with the isolation of the fractionated products. The whole procedure can be done in the cold room if it is necessary to protect labile substances, or at any other particular temperature which may have been found to give useful solvent properties.

In general, it may be said that the greatest specificity is attained when the two phases show the strongest competition for the solutes. Also, the phases should be as different as possible, perhaps as measured by their relative dielectric constants. Specificity is generally, though not always, reduced when solvent combinations which are nearly miscible are used. In the latter case, the composition of the phases is more susceptible to distortion by the presence of the solute and by small temperature changes. In dealing with acidic or basic solutes, a system composed of an aqueous buffer and an organic solvent is often very effective,[9] since it takes advantage of subtle differences in acidity or basicity, and since the partition behavior can be regulated conveniently through the pH of the buffer.

In this brief discussion of countercurrent distribution, the analytical specificity of the method has been shown to depend on the following factors: (a) the number of transfers which can be practically applied (at the present time, apparatus is being developed which greatly increases this number); (b) the selectivity of the solvent systems, a field in which empirical data and experience are the best guides so far; (c) the ideality of the solvent systems, so that partition ratios remain constant, giving results which are predictable by simple mathematics and without assumptions; and (d) the sensitivity and specificity of the measurements used to evaluate the results of the distributions.

Bibliography

1. Craig, L. C., C. Golumbic, H. Mighton, & E. Titus. 1946. Science **103:** 587.
2. Barry, G. T., Y. Sato, & L. C. Craig. 1948. J. Biol. Chem. **174:** 209.
3. Williamson, B. & L. C. Craig. 1947. J. Biol. Chem. **168:** 687.
4. Craig, L. C. 1944. J. Biol. Chem. **155:** 519.
5. Craig, L. C., G. H. Hogeboom, F. H. Carpenter, & V. du Vigneaud. 1947. J. Biol. Chem. **168:** 665.
6. Kenney, J. F. 1939. Mathematics of Statistics. D. Van Nostrand. New York.
7. Sato, Y., G. T. Barry, & L. C. Craig. 1947. J. Biol. Chem. **170:** 501.
8. Craig, L. C. & O. Post. 1949. Anal. Chem. **21:** 500.
9. Craig, L. C., C. Golumbic, H. Mighton, & E. Titus. 1945. J. Biol. Chem. **161:** 321.
10. Bush, M. T. & P. M. Densen. 1948. Anal. Chem. **20:** 121.
11. Barry, G. T., J. D. Gregory, & L. C. Craig. 1948. J. Biol. Chem. **175:** 485.
12. Craig, L. C. 1948. Fed. Proc. **7:** 469.
13. Craig, L. C., H. Mighton, E. Titus, & C. Golumbic. 1948. Anal. Chem. **20:** 134.
14. Sato, Y., G. T. Barry, & L. C. Craig. 1948. J. Biol. Chem. **174:** 217.

For further discussion and mathematical treatment consult: Craig, L. C. & D. Craig. 1950. Technique of Organic Chemistry. **III.** A. Weissberger, Ed. Interscience. New York; and Stene, S. 1944. Arkiv. Kemi. Mineral. Geol. **18A** (18).

METHOD AND APPLICATION OF DIFFERENTIAL THERMAL ANALYSIS*

By Ralph E. Grim
Division of Clay Resources and Clay Mineral Technology, State Geological Survey, Urbana, Illinois

The method of differential thermal analysis determines, by suitable apparatus, the temperature at which thermal reactions take place in a material when it is heated continuously to an elevated temperature and, also, the intensity and general character of such reactions. Because of dehydration, oxidation reactions, destruction of lattice structure, change in crystalline phase, *etc.*, many substances undergo thermal reactions when they are heated. The temperature of the thermal reactions, their intensity, and their general character are characteristics of a particular material and therefore provide criteria for its identification. Further, since such thermal reactions result from changes within the material heated or from other reactions between components of a mixture, the differential thermal method affords a means of studying high-temperature phase changes or reactions.

Thermal reactions of very low intensity can be utilized in the method if they begin abruptly and are completed in a short temperature interval. The results are recorded generally in the form of a continuous curve on which endothermic reactions are conventionally deflected downward and exothermic reactions upward from a horizontal base line.

History of Method

In an investigation of the components of clays in 1887, Le Chatelier[7] appears to have set up, for the first time, simple apparatus to measure and record thermal reactions taking place in a material when heated and to have used these reactions as analytical criteria for studying the components of a material. Following Le Chatelier, thermal reaction studies of clays were made by several investigators.[1, 31, 38, 44, 45] In these early studies, the procedure generally used was to place the material in a small platinum crucible with a single thermocouple junction in the center of the material. The whole mass was placed in a furnace and heated at a rapid and relatively uniform rate. The thermocouple was attached to a galvanometer which was read or recorded photographically at short intervals. Thermal reactions in the material caused variations in the galvanometer record as compared to that obtained when the furnace contained no sample. The record obtained showed the thermal reactions of the material superimposed on the heating curve for the furnace alone (FIGURES 1 and 2). In some of this early work,[38] the method consisted essentially in taking the time-temperature record of a thermocouple embedded in the specimen and comparing it with the record given by a second couple placed in a reference substance alongside it. In still other[37] early work, the so-called Saladin-Le Chatelier apparatus was used, which permitted the recording of two galvanometers (one attached to a thermocouple in the sample, the other in the standard substance) on a single record.

---

* Published with the permission of the Chief, Illinois State Geological Survey.

In 1899, Roberts-Austen[39] devised the differential thermocouple method for measuring differences between a material and a reference unit material. Burgess[5] elaborated the principle of the difference thermocouple and suggested simple, adaptable, and usable differential thermocouple circuits.

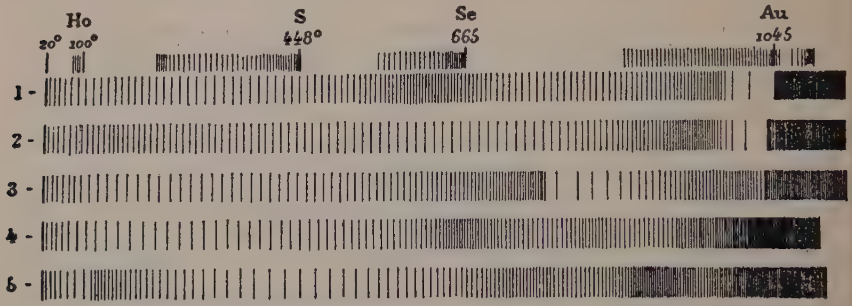

FIGURE 1. Thermal reactions in clay superimposed on furnace heating rate as recorded by Le Chatelier.[7]

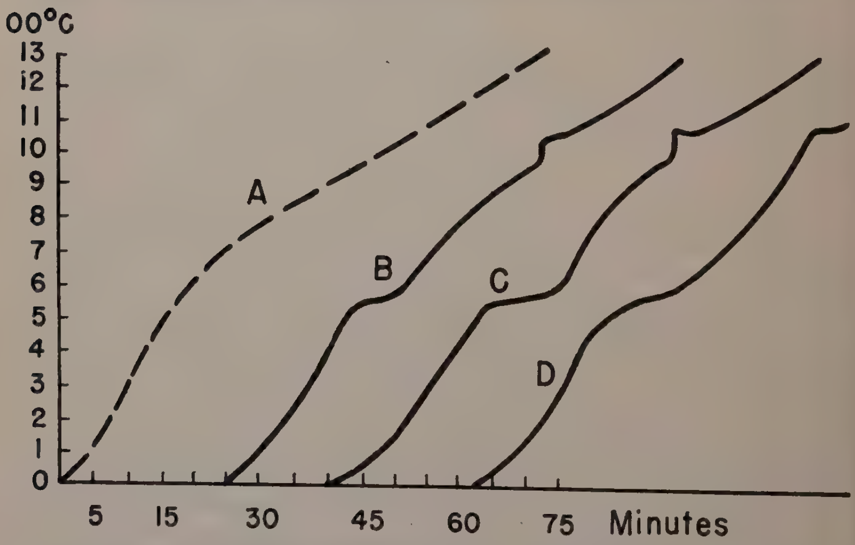

FIGURE 2. Thermal reactions in clay superimposed on furnace heating rate as recorded by Wohlin.[45] Curve A is furnace heating curve. Curves B, C, and D show furnace heating rate with thermal reactions for clays superimposed.

Since the work of Roberts-Austen, the difference thermocouple has been widely used in the field of metallurgy. Fenner,[11] however, in his study of the stability relations of the silica minerals, reported in 1913, appears to have been the first to apply this differential thermocouple procedure to the study of thermal reactions outside of the field of metallurgy. The technique devised by Fenner is substantially that used today, with some elaboration and refinement. After Fenner's report, the differential thermocouple method was used sporadically in the study of high-temperature phase changes, notably by Kracek[29] and others, [30] and frequently in the study of the constituents of clay by various investigators, including Houldsworth and Cobb,[24] Satoh,[41] Orcel,[34] and Kournakov and Tchernick.[28]

In 1933 and 1935, excellent papers by Orcel[35, 36] emphasized clearly the applicability of the method to clay mineral researches. Since that time, many investigators in many different countries have used the method in clay researches. In that field, it has now become a common research tool.

In very recent years, the method has been shown to be a valuable analytical tool for many materials other than clays. It is still used to a considerable extent in the study of high-temperature phase changes and reactions. It is also used widely as a plant control and raw material control instrument and for a quick evaluation of mineral prospect samples.

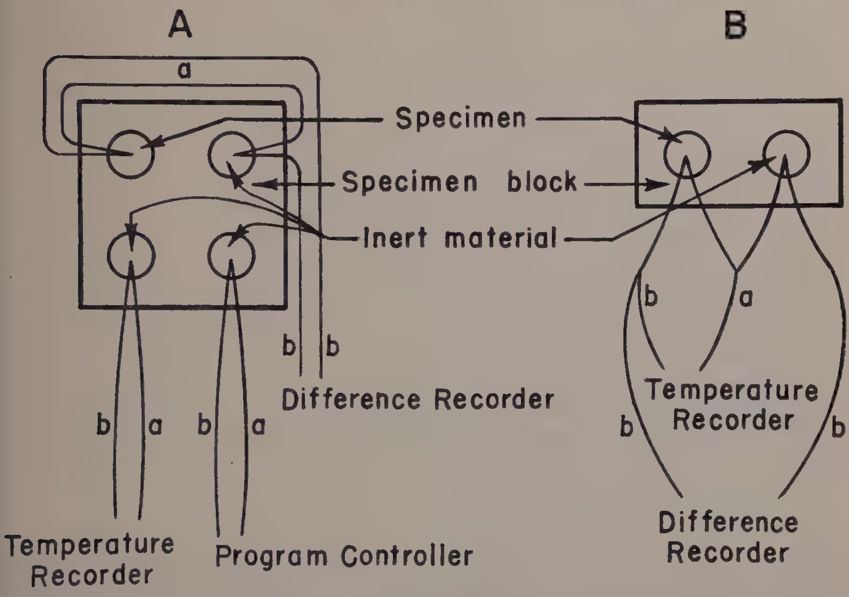

FIGURE 3. A—thermocouple set-up as used today; B—thermocouple set-up as used in early work and in some[2] current work. a = Pt-10 per cent Rh wire; b = Pt wire.

Description of Method

In the method as generally used today, the sample to be studied is placed in one hole of a specimen holder. An inert material that experiences no thermal reactions when heated to the temperature of the experiment, usually calcined aluminum oxide (αAl_2O_3), is placed in the other hole of the specimen holder. One junction of the difference couple (FIGURE 3A) is placed in the center of the sample and the other junction in the center of the inert material. The holder and thermocouple are placed in a furnace so controlled as to get a uniform rate of temperature increase. The temperature of the inert material increases regularly as the temperature of the furnace increases. When a thermal reaction takes place in the sample, the temperature of the sample is greater or less than that of the inert material, depending on whether the reaction is exothermic or endothermic, for an interval of time until the reaction is over and the temperature of the sample again comes to the temperature of the furnace. Consequently, for an interval of time, the temperature of one junction of the difference couple is different from that of the other, and an emf is set up in the differential thermocouple circuit which is recorded as a function of time or of the temperature of the furnace. The record may be made manually with a potentiometer or galvanometer, photographically with a galvanometer, or automatically with some electronic device. When no thermal reaction is taking place in the specimen, the temperature at both junctions of the difference couple is the same, and no emf is set up. The direction of the emf in the differential thermocouple circuit depends on whether the temperature of the sample is above or below that of inert material, and, consequently, the recording mechanism moves in opposite directions for exothermic and endothermic reactions.

Figure 4 shows a differential thermal curve for kaolinite and an equilibrium dehydration curve for the same material. The endothermic reaction between about 500 and 700°C. obviously corresponds to the dehydration of the mineral. A comparison of the curves illustrates that the differential method is a dynamic rather than a static method. The thermal reactions are not instantaneous and are recorded as functions of time or as functions of the furnace temperature, which is continuously increasing as the reaction takes place. The temperature at which the dehydration begins corresponds to the start of the endothermic deflection. The temperature of the peak of the endothermic deflection varies, depending on the details of the procedure followed, the character of the reaction involved, and the material being studied.

An attempt has been made by Speil[42] to analyze mathematically the differential method. As will be shown, certain inherent limitations, due to factors of experimentation and material being studied, restrict mathematical treatment.

Equipment Used

Specimen Holder. A considerable variety of specimen holders has been used by various investigators. In early work by Le Chatelier[7] and others, the specimen was placed in a platinum crucible. Norton,[33] one of the first to apply the method in this country, used a heavy nickel block because "it tends to neutralize thermal gradients." Other investigators have used ceramic specimen holders, and Grimshaw[16] claims they are more desirable than metal because the thermal reactions are larger and more sharply defined. This is due to slow transfer of heat between the test sample and surrounding material because of low heat conductivity of the ceramic material. Grimshaw[16] uses a holder composed of recrystallized alumina, bonded with a little clay and fired to 1600°C.

Orcel[35] and his followers[6] in France have placed the materials in fused silica crucibles. Herold and Planje[21] have described a platinum cup container which also serves as thermocouple, and it is claimed to simplify the experimental procedure, particularly for high-temperature studies. Recently, Gruver[17] has claimed advantages for thin-walled platinum containers because the high heat conductivity of the metal permits the material to reach furnace temperature quickly and because the thin walls provide little heat capacity. According to Gruver,[17] thickwalled containers with higher heat capacity act as heat reservoirs which tend to lower the intensity and sharpness of some reactions.

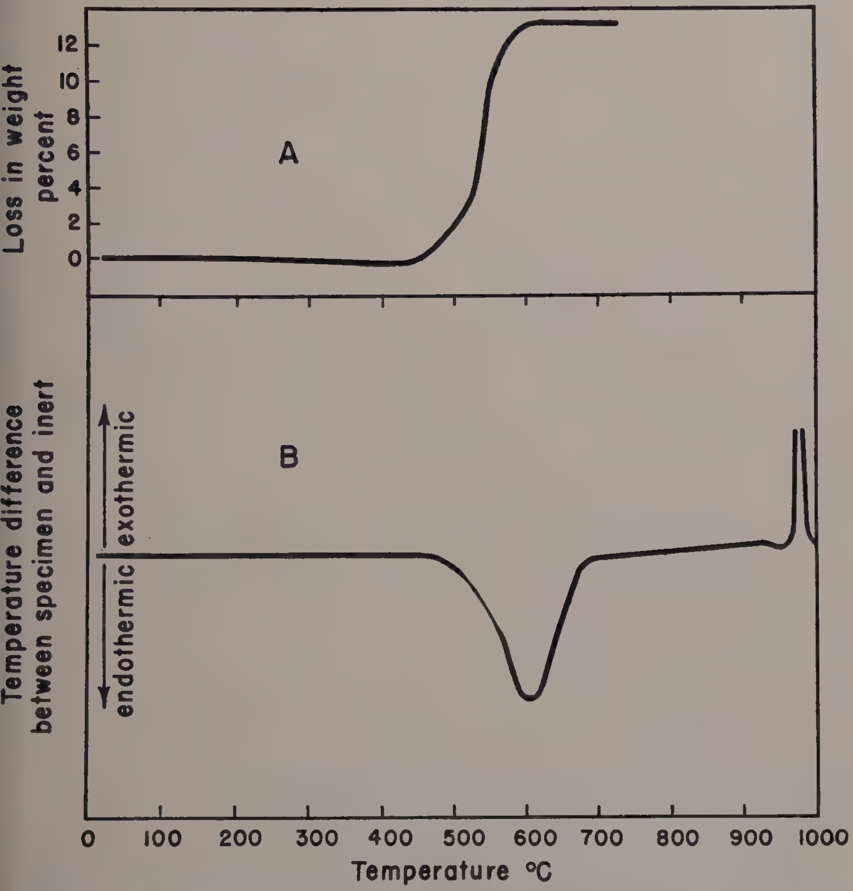

FIGURE 4. A—equilibrium dehydration curve for kaolinite; B—differential thermal curve for kaolinite (after Speil[42]).

Blocks of nickel have been used by most American investigators, and, in general, they have been found satisfactory. Ceramics holders have been used widely in England. Obviously, the ceramic block must not itself react with the material being investigated, and for certain types of material they would prove unsuitable. In the writer's laboratory, a nickel block or a platinum block (for high-temperature studies) has provided adequately sharp reactions. The metal block has the advantage of strength. This is important because many materials being studied vitrify or melt in the course of the analysis, so that there is the problem of removing the fused button from the block. It would seem that a metal holder with walls as thin as is consistent with adequate mechanical strength might be the best type of block.

Thermocouples. FIGURE 3A shows the thermocouple circuit most widely used at the present time. FIGURE 3B shows the circuit used by Fenner[11] and Kracek[29] and still used for analytical work by some European investigators, notably the Russians.[2] In this latter circuit, the sample temperature rather than the furnace temperature is taken as the reference temperature. The present tendency is to use the circuit in FIGURE 3A with a separate thermocouple to measure furnace temperature for calibration. It seems probable that more reproducible results, with less variation between results from different laboratories using slightly different equipment and techniques, are obtained by use of the circuit shown in FIGURE 3A.

Early investigators used platinum-platinum 10 per cent rhodium thermocouples, and such couples are very widely used today. Chromel-alumel couples[3] have been used satisfactorily for temperatures up to 1000°C. for many materials, and they have the great advantage over noble metal couples in developing higher emf and thereby providing greater sensitivity. Kracek[29] has used gold-palladium *vs.* platinum-rhodium thermocouples, which yield about 50 microvolts per 1°C. in the elevated temperature range and are, therefore, about five times as sensitive as platinum *vs.* platinum-rhodium. Au-Pd *vs.* Pt-Rh would undoubtedly be more satisfactory for some materials than the sensitive base metal couples.

Berkelheimer[3] has indicated that the size of the thermocouple bead should be held approximately constant, because "the size of the beads in the difference couple controls the slope of the base line of the differential temperature curve."

The intensity of the thermal reactions varies greatly in different materials. Consequently, it is desirable to have a resistance placed in series in the differential thermocouple circuit, which permits some variation and control of the sensitivity of the apparatus.

Furnace Design. It is necessary to have a furnace with a uniform-temperature hot zone of sufficient size, so that the sample holder and any calibrating thermocouple junction are all subjected to the same temperature. The author[15] has found a horizontal furnace mounted on rollers, so that it can be easily rolled over an alundum tube containing the specimen holder, to be very satisfactory. This design permits easy access to the specimen holder for inserting the sample and for any thermocouple replacements. It also permits the use of more than one furnace with a single specimen-holding arm and a single recording mechanism.

Obviously, the furnace must have enough capacity to permit the desired heating rate up to the desired temperature. Several authors[3, 16, 33] have described satisfactory furnaces in detail.

Furnace Temperature Program Controller. A wide variety of homemade and automatic types of program controllers has been used to get a uniform heating rate. The use of an auto transformer,[3, 14] driven by a motor through a speed reducer in such a way as gradually and continuously to increase the voltage into the furnace, has been found quite satisfactory and economical in many laboratories for furnaces with alloy windings. The method does not supply a uniform heating rate for platinum-wound furnaces because of the change in resistance of platinum with temperature. With the autotransformer-type control apparatus, heating rates varying less than 1°C. ± at a rate of 12°C./min. can be obtained for temperatures up to 1000°C.

A considerable variety[17, 21, 27, 43] of automatic controllers has been described. They are necessary for platinum-wound furnaces or when close reproducibility of heating rate is desired. In general, the automatic controller must be "tailor-made" for the furnace it is to control. This is particularly essential for controllers of the "on-off" type. When such controllers are used with inside-wound furnaces, or even with outside-wound furnaces if the furnace tube is thin, there is a tendency for the on-off impulses to get onto the differential thermocouple record, making it irregular.

Recording Mechanism for Differential Thermocouple. In the early use of the method, the emf set up in the differential thermocouple was determined at regular intervals by means of a potentiometer, and the data were plotted against time or temperature. Besides being time consuming, the method had the disadvantage of missing some slight reactions of low sensitivity which might be significant. It is very important that the recording be continuous.

A photographic method is used in many laboratories in which a reflecting galvanometer is arranged so that a spot of light is reflected from the galvanometer mirror onto a piece of photographic paper attached to a drum rotating at a certain speed. With this method, high sensitivity can be obtained by increasing the distances between the galvanometer and the drum. It has the disadvantage that the record can not be seen as it is made and that it requires a dark room or some rather elaborate light-tight equipment to handle the photographic paper.[3]

Experience in the author's laboratory on a wide variety of materials indicates that recording equipment must be sensitive enough to yield a deflection of at least two inches in length for a reaction at about 600°C. when the temperature difference between the junctions of the difference couple is no more than 10°C. For platinum-platinum rhodium thermocouples, this is an emf of 0.1 M.V., and there has been difficulty getting recorders with this sensitivity. With base metal couples, the emf is larger, and automatic equipment of adequate sensitivity is available readily. Recently, Gruver,[17] Kerr and Kulp,[27] and Rowland and Jonas[40] have described automatic recording mechanisms which have given satisfactory results. The automatic recorders should be equipped with variable resistances, so that their sensitivity can be varied and controlled.

Calibrating Devices. Some means are necessary to determine the temperature of the thermal reactions shown by the difference couple record. This may be done by placing a regular thermocouple in the specimen block (FIGURE 3) and taking temperature readings at specified intervals. In the photographic method of recording, these furnace temperatures may be printed on the same paper as the difference record by placing a light in front of the box containing the recording drum with the light connected to a switch through which it can be lighted momentarily when the furnace has reached certain temperatures. Honeybourne[23] has constructed a device whereby the light in front of the drum is lighted by an automatic program controller at specified temperature intervals.

In the photographic method of recording, it is difficult to correlate the height of the thermal deflections with the temperature difference at the time of the reactions, *i.e.*, to set up a vertical scale for the difference curve. Grim and Rowland[14] have constructed curves applicable to their apparatus based on measuring the swing of the galvanometer for known temperature differences.

Faust[10] has recently presented a method of determining the temperature of the thermal reactions based on the inversion temperature of α and β quartz and the trace of the furnace heating rate recorded on the paper, along with the difference record, by means of a second reflecting galvanometer. When an automatic recording mechanism is used, the problem is that of calibrating the instrument for the thermocouples used.

Experimental Factors Influencing Results

It is proposed here to consider the experimental factors that can be varied by the operators and that can influence the results obtained.

Packing of Sample. Gruver[17] states that the sample needs only loose packing in the specimen holder. Many other users of the method, including the author, prefer solid packing. All samples should be packed in as nearly the same way as possible, so that there is the least chance of a variation in thermal diffusivity because of variation in density. The thermocouple bead should always be of about the same size, and it is very important to have it centered in the center of the sample. The specimen holder should be placed in the furnace so that the sample and inert material are always in the same position.

In the author's experience, it is most convenient to bring the thermocouples into the specimen from the side rather than from the top or bottom, because this permits more uniform packing, while retaining the junction in the center of the sample.

Thermocouples. Relatively fine wire (gauge 22) should be used to reduce conductance of heat through the wire. The wire should be well insulated, particularly where it goes through the specimen block.

Preparation of Sample. The particle size of the sample packed into the furnace is of no importance unless the material is all relatively coarse (+60 mesh) or extremely fine-grained (−2 microns). A range of particle size permitting dense packing is advantageous. The author has found it good practice to grind all coarse samples to pass a 60-mesh sieve before analysis. The overall objective is to get reproducible density of packed samples in the block.

Materials with the property of adsorbing water must be brought to equilibrium at a definite relative humidity before analysis, if reproducible results in the initial part of the curve are to be obtained. FIGURE 5 presents two curves for the same clay (prepared at different relative humidities), showing the difference obtained in the initial part of the curve when samples have not been brought to equilibrium at a given R.H. In studying clays, the author follows the practice of allowing all samples to remain in a desiccator with 46 per cent R.H. (saturated $Ca(NO_3)_2 \cdot 4H_2O$ solution) for four days before running the analysis.

Heating Rate. Both Norton[33] and Speil[42] have investigated the effect of heat rate on the difference curve. As shown in FIGURE 6, the slower the heating rate, the broader the peak and the lower the peak temperature. The area under the curve for a given reaction and the temperature at the start of the reaction are independent of the rate of heating.

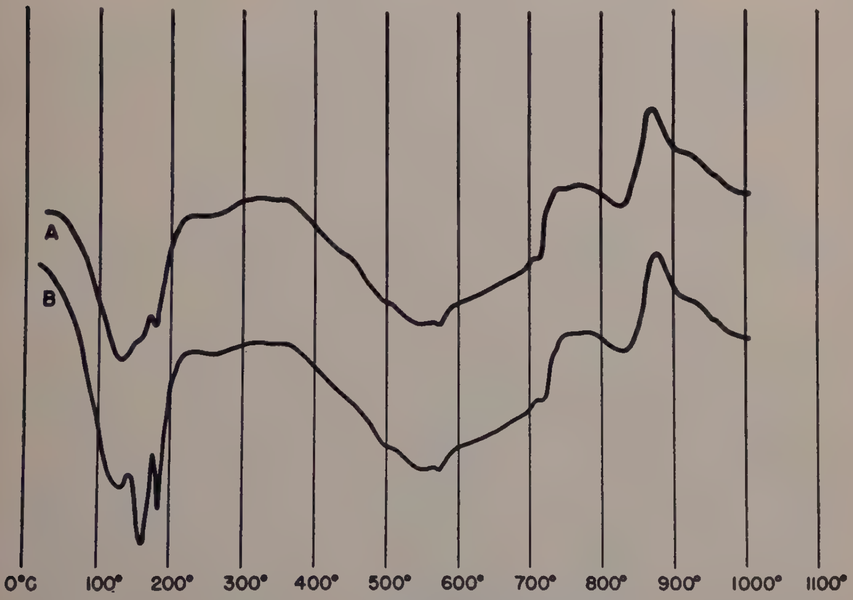

FIGURE 5. Differential thermal curves of same clay sample treated at different relative humidities before running analyses.

The experience of many operators has shown that a heating rate in the range of 10° to 15°C. per minute is most satisfactory. A slower heating rate reduces the sharpness of the reactions and prolongs unnecessarily the time required for an analysis. A faster heating rate is apt to cause too much overlapping of reactions in samples that are mixtures.

The heating rate must be uniform. Even small changes in the rate of heating, if they are relatively sudden, will be reflected in the differential curve.

Furnace Atmosphere. In order to obtain reproducible results for many materials, the furnace atmosphere must be kept constant. For materials that are subject to oxidation reactions, it is important that samples be prepared and placed in the furnace in such a way that they always have the same ease of oxidation. Rowland and Jonas[40] have shown how variations in particle size, packing, covering of block, and dilution of sample, in addi-

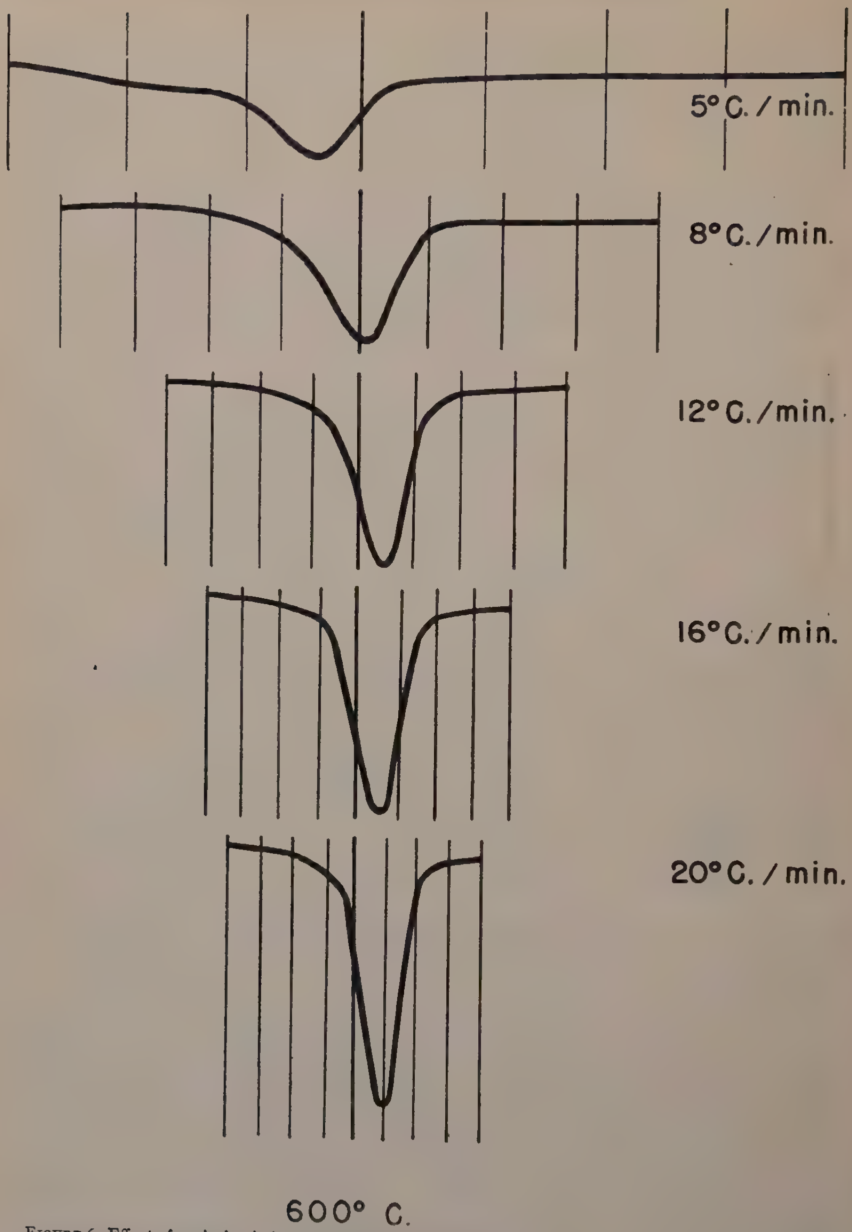

FIGURE 6. Effect of variation in heating rate on the endothermic reaction for the dehydration of kaolinite (after Speil[42]).

tion to furnace atmosphere, influence the ease of oxidation of the iron in siderite and, hence, the curves obtainable from the mineral (FIGURES 7 and 8).

Material Factors Influencing Results

It is proposed here to consider the variations within the material to be analyzed, over which the operator has little or no control.

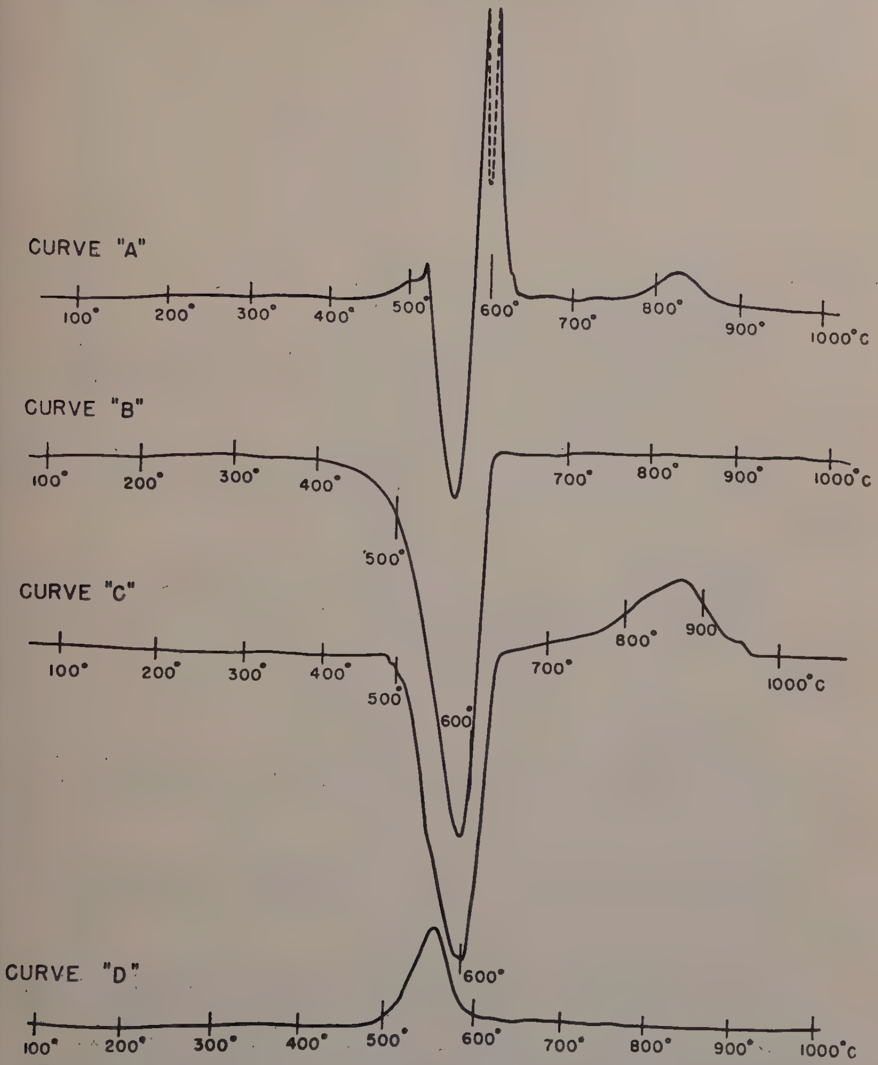

FIGURE 7. Differential thermal curves for siderite: A—firmly packed without cover on sample holder; B—firmly packed without cover run in nitrogen atmosphere; C—firmly packed with cover on specimen holder; D—very finely ground, loosely packed, and without cover (after Rowland and Jonas[40]).

Thermal Diffusivity. The temperature at the junction of the difference thermocouple depends to some extent on the coefficient of thermal diffusivity of the material in which it is imbedded. The rate at which a point in a hot body will cool under definite surface conditions is known as thermal diffusivity[17] and is equivalent to $\frac{k}{dC_p}$, where k is the conductivity, d, the density, and C_p the specific heat. The diffusivity of the sample to be analyzed may be different from that of the inert material. Furthermore, the diffusivity of the sample may change as it is heated, because of the formation of new phases at higher temperatures. The effect on the differential curve will be to produce a sloping base line or a rather sharp offset in the curve, depending on the suddenness of the change. In the curve for quartz (FIGURE 9), the base line is shifted upward after the reaction for the α and β inversion because of a difference in coefficient of thermal diffusivity.

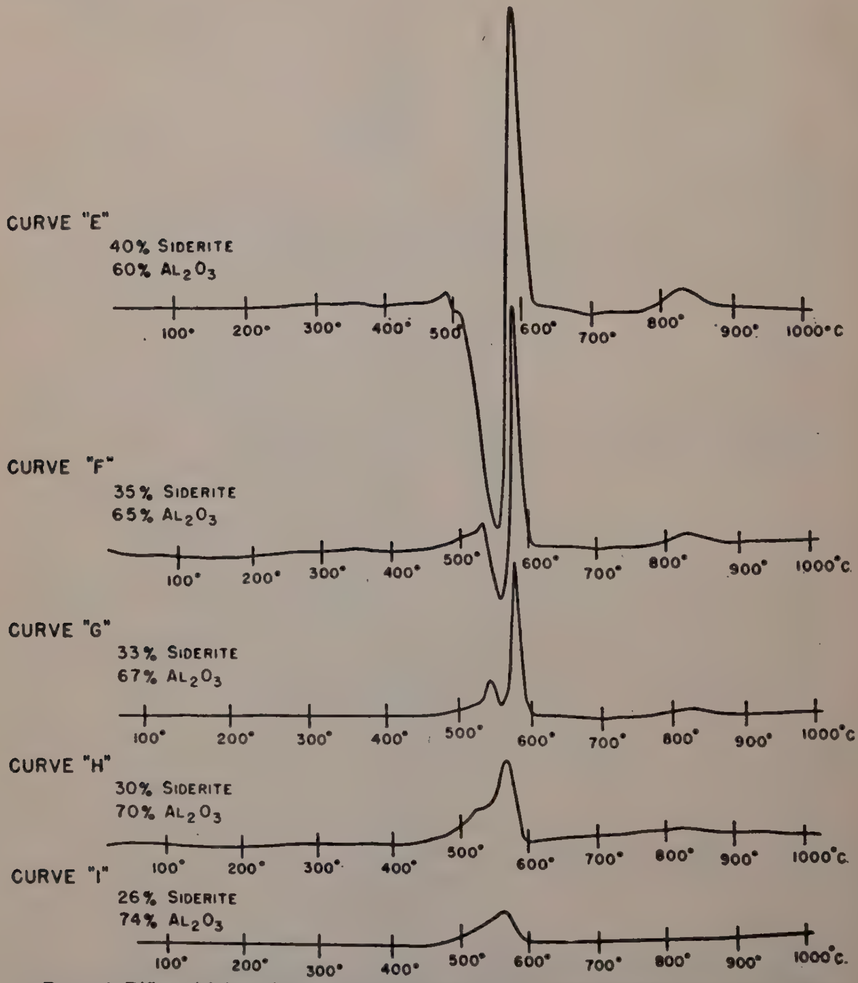

FIGURE 8. Differential thermal curves for siderite show effect of dilution of sample on curves of a material containing an oxidizable component (after Rowland and Jonas[40]).

In order to take account of this variable, Grimshaw[16] would use a precalcined sample as the reference material. For materials without reversible heat effects this might be satisfactory. Mitchell and Henry[32] suggested making a second run on the calcined material, without disturbing the setup, and then subtracting the second run from that of the first. Again, any reversible inversions would interfere with this method. Jeffries[25] suggested using weights of sample and reference material based on their specific heats. This is obviously impossible when unknown mixtures are analyzed and would only be valuable if the sample and inert material held the same ratio between their specific heats throughout the temperature interval of the run.

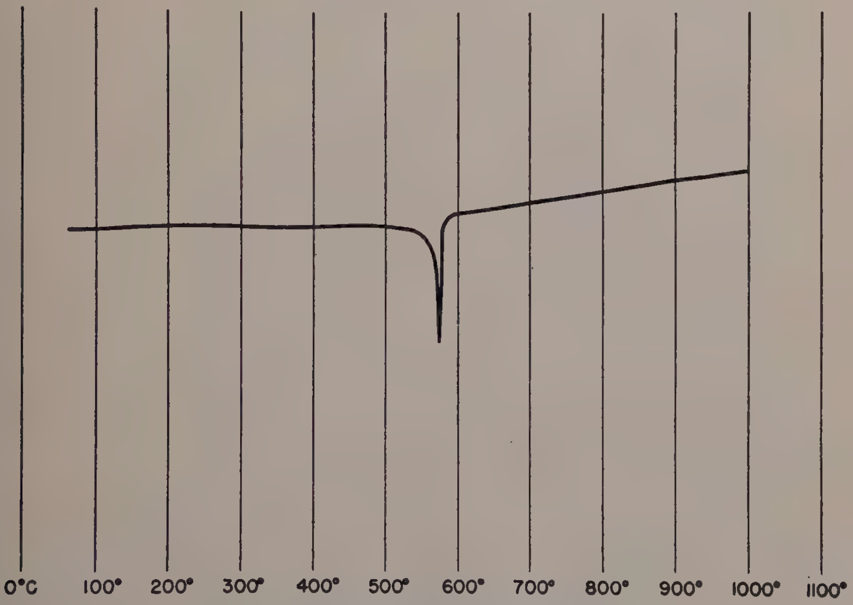

FIGURE 9. Differential thermal curve for quartz.

The matter of thermal diffusivity is very significant in the differential thermal method and has not yet been given the critical study that it deserves.

Changes in Volume of Sample on Heating. Shrinkage or swelling of a sample on heating will obviously affect the coefficient of thermal diffusivity and, therefore, alter the difference curve. In some materials, the sample may shrink away from the specimen holder with an attendant shift in the curve because of a difference in heat transfer to the sample as compared to the inert material.

Variations with Particle Size. Speil[42] has shown that, for some materials, the thermal curve varies with the particle size of the component minerals in the size range below about 2 microns. In general (see FIGURE 10), the size of the thermal reaction and the temperature of the peak decrease as the particle size decreases.

In some instances, decrease in particle size is accompanied by a decrease in the perfection of the crystallinity of the material. Curve C of FIGURE 11 shows a curve for a kaolin composed of well-crystallized particles of kaolinite of about one micron in diameter. Curves A and B of FIGURE 11 are for kaolins composed of particles of kaolinite less than about 0.1 micron in which there is some distortion of the lattice. The intensity of the reactions and the temperature of the peak decrease as the perfection of crystallinity decreases.[13] This influence of crystallinity may be a disturbing factor in some cases, but it has considerable analytical value in others.

Variations in Quantity of Material in a Mixture. FIGURE 12, after Speil,[42] presents a series of curves for varying quantities of kaolinite. The size of the reaction and the temperature of the peak decrease as the amount of material decreases. In mixtures, therefore, the temperature of the peak cannot always be used to identify the components.

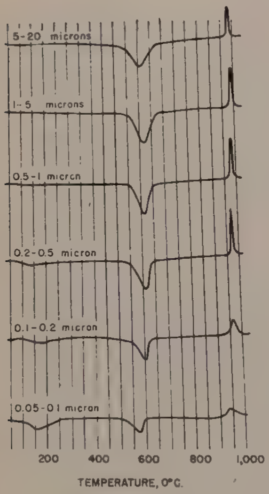

FIGURE 10

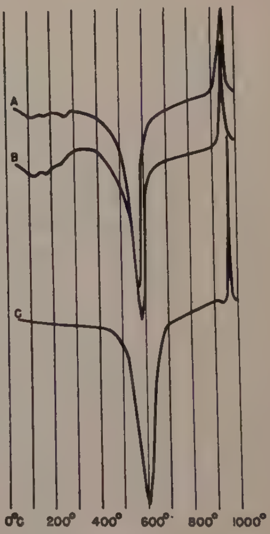

FIGURE 11

FIGURE 10. Differential thermal curves for kaolinite showing variations resulting from differences in particle size (after Speil[42]).

FIGURE 11. Differential thermal curves for kaolin composed of very fine grained poorly crystalline kaolinite A and B, and for kaolin composed of well-crystallized, relatively coarse-grained kaolinite C (after Grim[13]).

Intimacy of Mixing of Components. Grim[13] has shown that the characteristics of the curves for mixtures of some minerals depend somewhat on the intimacy of the mixing of the components. In clay minerals, there is considerable difference between the curves for mixtures of discrete particles of clay mineral of several microns or more in diameter and an intimate interlayering of considerably smaller units, such as is frequently found in nature. Arbitrary curves set up on the basis of dry mixtures of clay minerals, therefore, are frequently of no value in evaluating curves of natural clays which are mixtures.

In general, the thermal reactions for the individual components decrease in intensity and sharpness of reaction as the intimacy of mixing increases.

Overlapping of Reactions. Many clays contain organic material which burns out over a long period of time, causing an exothermic reaction which effectively masks any endothermic reactions which may be taking place for other components at the same time.[15] Frequently, this difficulty can be overcome by firing the material beforehand to a temperature adequate to burn the organic material but below that of the significant reactions of the other components. In some materials, the organic material can be removed by a solvent or H_2O_2 treatment.

The overlapping or the concurrence at the same temperature of the thermal reactions characteristic of the components in a mixture may make the method unworkable for some materials. Grimshaw[16] has overcome this difficulty, in some cases, by diluting the inert material with the estimated amount of one of the components of the mixtures, which causes the reaction for that component to be cancelled out of the difference record. Obviously, this procedure could be used only if the identity and approximate abundance of the conflicting components were known.

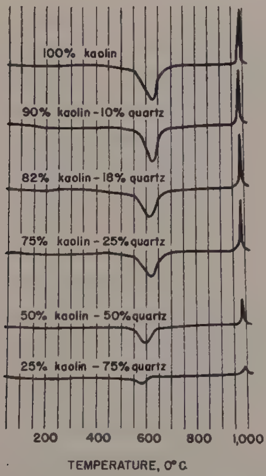

FIGURE 12. Differential thermal curves for kaolinite diluted with varying amounts of quartz (after Speil[42]).

Influence of Minor Constituents and Impurities. The thermal curves of some molecules, particularly the clay minerals, are sensitive to the presence of very small amounts of some non-clay materials. Hendricks and his colleagues[20] have pointed out the variation in the initial endothermic reaction of montmorillonite clay minerals resulting from differences in the character of the exchangeable base. Caillére and Hénin[6] and unpublished work in the author's laboratory have shown that relatively large variations in the thermal curve for the clay minerals may result from the presence of small amounts of salts of various kinds which may be present in clays.

Quantitative Interpretations

Care in the preparation of material for analysis and in making the analysis itself will provide reproducible curves which permit quantitative interpretations. FIGURE 5 shows two curves, substantially alike in all details in the region above 250°C., which were run on the same sample at an interval of two months. In the region below 250°C. they are not alike, because the samples were not brought to equilibrium at the same R.H.

It is obvious from the foregoing discussion of the limitations of the method that its accuracy for quantitative analysis is limited. The accuracy varies with the kind of material being analyzed, but, for many substances, values ±2–5 per cent are obtainable, depending on the relative abundance of the components. In some mixtures, less than 5 per cent of certain components can be identified.

Use of the method for quantitative analysis requires setting up standards by the analysis of prepared samples which contain known amounts of the components to be sought in the analysis. The standards must be obtained on the apparatus to be used in the work, and tests must be run according to a standard procedure. For the quantitative analysis of some natural materials, it is difficult to obtain satisfactory standards because of the difficulty in duplicating extremely fine particle size or the intimacy of mixing of the components.

In general, the quantitative evaluations are based on the area under the peaks which correspond to reactions of components. It may be difficult to measure accurately the area of some peaks because of the difficulty of establishing precisely the start of a reaction or a definite base line. Measuring an area is simple for reactions which begin and end abruptly, such as for the α and β quartz transition, but, unfortunately, many reactions (such as those accompanying the dehydration of many hydrous micaceous minerals) begin gradually, end rather gradually, and are of low intensity. Berkelheimer[4] has presented a method of measuring the area beneath deflections on curves which is workable for reactions that are at least moderately sharp and intense. Dean[9] has used a trigonometric function of the peak angle for quantitative analysis which is workable also for materials giving relatively sharp and intense reactions.

Recently, the International Committee for the Study of Clays (Comité International pour l'Étude des Argiles, CIPEA) has organized a subcommittee which will study in detail the variations in the method due to experimentation procedure, equipment, and material being analyzed. On the basis of this study, the subcommittee hopes to recommend a standard procedure that will enhance the quantitative value of the method.

Application of Differential Thermal Analysis

A few differential thermal curves are presented to illustrate some of the various substances that have been studied by the method. No attempt is made to illustrate all types of the various substances that have been studied, nor even all the fields to which the method has been applied.

FIGURE 13 shows curves for a mica and several clay minerals. Differential thermal analysis has been applied more extensively to the study of clays than to any other material, and numerous investigators[14, 16, 18, 33, 35, 42] have published many curves for specific clay minerals and natural clays. All of the clay minerals are characterized by an endothermic reaction somewhere between 500° and 700°C. due to loss of (OH) water. Some are also characterized by an initial endothermic reaction due to loss of adsorbed water, by a high-temperature endothermic reaction due to destruction of the lattice, and by a high-temperature exothermic reaction resulting from the crystallization of a new phase. The difference in the initial endothermic reactions of the montmorillonite clays (D and E of FIGURE 13) is a consequence of a difference in the exchangeable base carried by these minerals. For some samples, data concerning the character of the exchangeable base can be determined from the thermal curve, because the amount of adsorbed water is related to the adsorbed ion.[20]

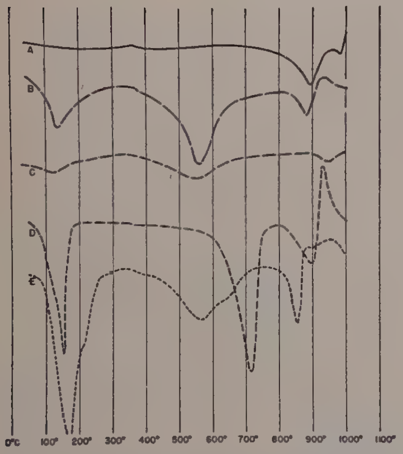

FIGURE 13

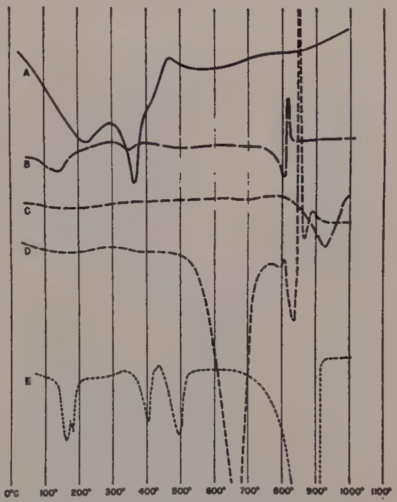

FIGURE 14

FIGURE 13. Differential thermal curves for: (a) muscovite, coarse grained, University of Illinois collection; (b) illite, Fithian, Illinois; (c) glauconite, Gloucester County, N. J.; (d) montmorillonite, Clay Spur, Wyoming; and (e) montmorillonite, Pontotoc, Mississippi.

FIGURE 14. Differential thermal curves for: (a) heulandite, Sonora, Mexico; (b) sepiolite, Ampandrandava, Madagascar; (c) talc, Vermont; (d) clinochlorite, Chester, Massachusetts; and (e) wall plaster.

FIGURE 14 presents curves for a zeolite, sepiolite, talc, and chlorite to illustrate that these minerals are amenable to the method. It should be emphasized that other types of these minerals, for example, zeolites other than heulandite, will give different curves. Curve E in FIGURE 14 is from a sample of plaster and shows an initial reaction characteristic of gypsum and endothermic reactions at about 400°C., 500°C., and 800–900°C., resulting respectively from magnesium hydrate, calcium hydrate, and a carbonate. The method works particularly well for hydrates and carbonates because they give sharp, intense, thermal reactions, and it is a simple matter to get a horizontal base line. Quantitative application of the method for such materials is possible with relatively high accuracy. Cuthbert and Rowland[8] and Kerr and Kulp[27] have published curves for a variety of carbonate minerals.

FIGURE 15 shows curves for dolomite, limonite (ferric hydrate), bauxite, and alunite. The bauxite is a mixture of gibbsite which provides the endothermic peak at 300–360°C. and the halloysite-type clay mineral. The method works well quantitatively for bauxite (Hendricks, Goldich, and Nelson[19] have described portable differential thermal equipment used in bauxite prospecting). The method has the great advantage of speed, permitting a relatively close estimation in the field of the Al_2O_3 content of bauxite samples in a little more than an hour. Thus, the promising samples can be selected quickly from the less promising or worthless ones for chemical analysis. Kerr and Kulp[27] have described equipment in which six analyses can be run simultaneously.

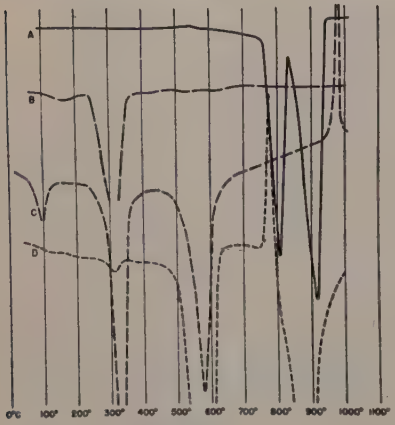

FIGURE 15

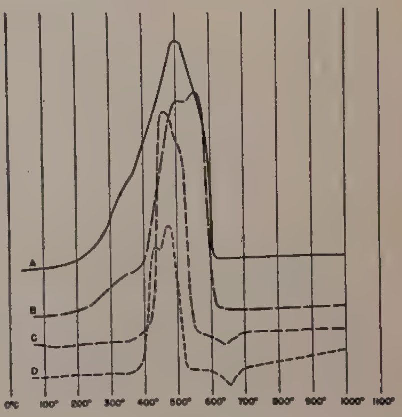

FIGURE 16

FIGURE 15. Differential thermal curves for: (a) dolomite, Candan, Ohio; (b) limonite, University of Illinois collection; (c) bauxite, Irvington, Ga.; and (d) alunite, locality unknown.

FIGURE 16. Differential thermal curves for: (a) vitrain, diluted with 95 per cent inert (αAl_2O_3); (b) clarain, diluted with 95 per cent inert (αAl_2O_3); (c) pyrite, diluted with 95 per cent inert (αAl_2O_3); and (d) marcasite, diluted with 95 per cent inert (αAl_2O_3).

Curve D in FIGURE 15 is for alunite ($K_2O \cdot 3Al_2O_3 \cdot 4SO_4 \cdot 6H_2O$). The method should be applicable generally to hydrous salts of all kinds, but, so far, the differential thermal characteristics of such materials have been little investigated.

FIGURE 16 presents curves for two sulphides, pyrite and marcasite, showing distinct exothermic reactions for the oxidation of the sulphur. The method should be applicable generally to sulphides other than the iron sulphides.

The differential thermal method is applicable also to the study of organic compounds. Hollings and Cobb[22] applied the method to the study of the combustion of coal. Curves A and B in FIGURE 16 show the records for vitrain and clarain constituents of Illinois coal made in the author's laboratory. The exothermic reaction for such material is so great that the sample must be diluted with an inert material for analysis. Jordan[26] has used the method in the study of organic materials adsorbed by the montmorillonite clay mineral, as shown in FIGURE 17. The amines studied by Jordan show

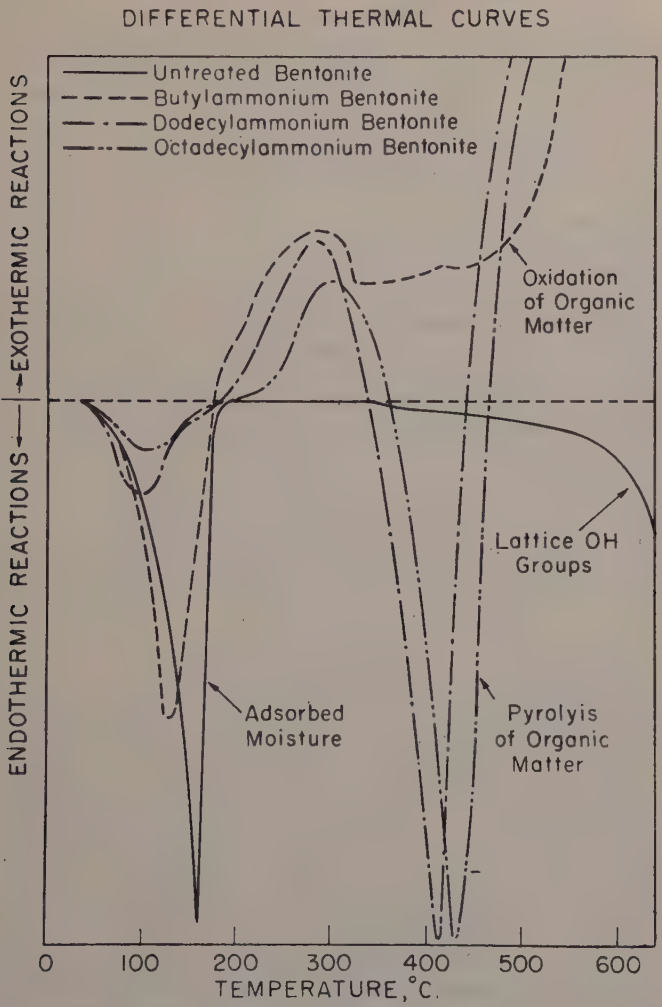

FIGURE 17. Differential thermal curves of montmorillonite with adsorbed amine compounds (after Jordan[26]).

an endothermic reaction due to the fractionation of the organic molecule superimposed on the exothermic reaction due to oxidation. Vold[43] has applied the method to the study of soaps (FIGURE 18) and has followed the difference-temperature record on cooling as well as heating.

The method is applicable to the study of phase changes[11] taking place as substances are heated and to high-temperature reactions in phase equi-

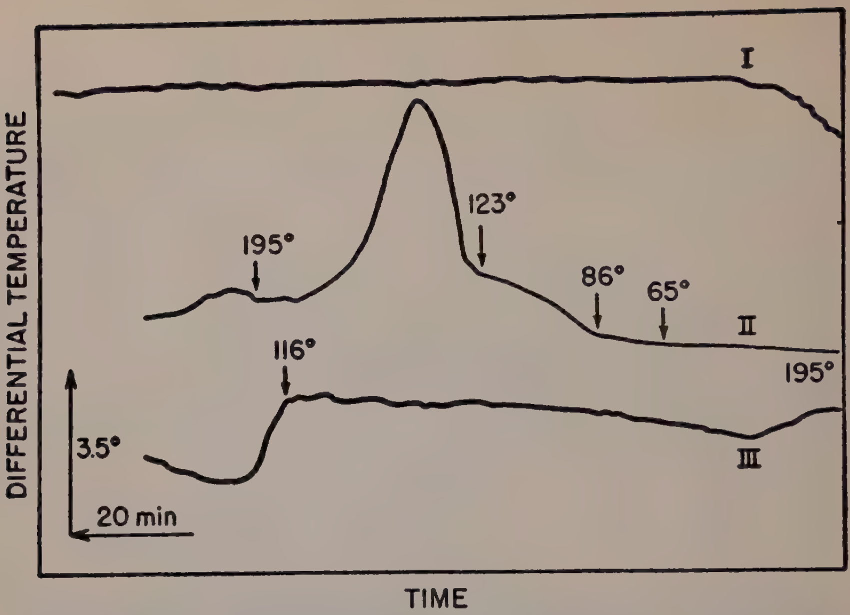

FIGURE 18. Differential thermal analysis of anhydrous crystalline calcium stearate. Curve I—base line obtained with Nujol in both sample and reference cell. Curve II—heating Ca(Str)₂ at 1.5°/min. Curve III—cooling Ca(Str)₂ at from 2.5°/min. at 200° to 0.5°/min. at 100°. Temperatures of increase or decrease of △T as marked, indicate transitions (after Vold[43]).

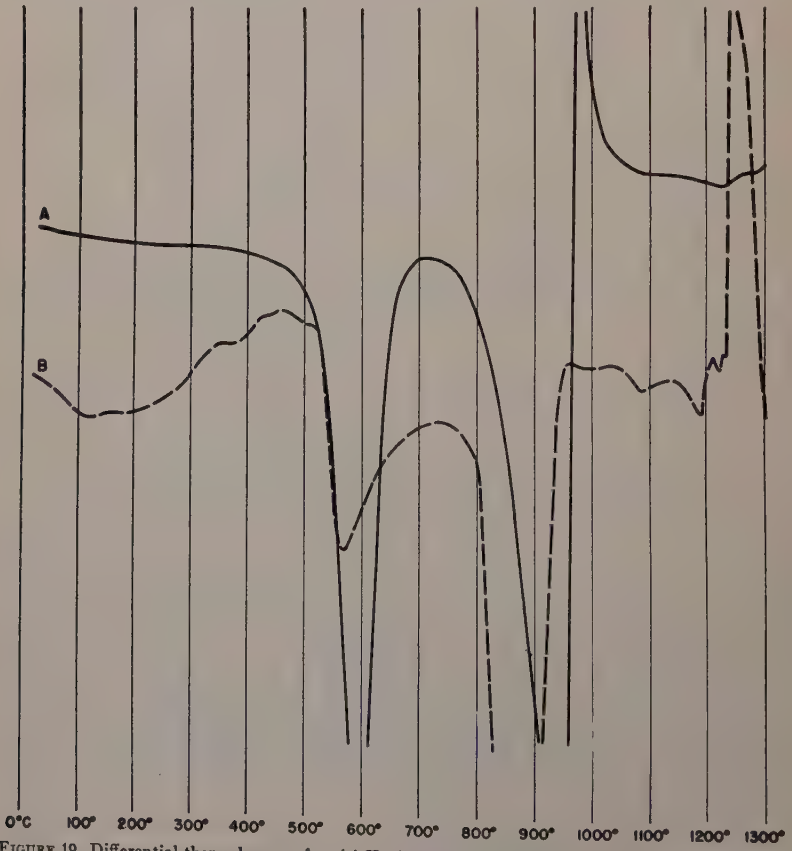

FIGURE 19. Differential thermal curves for: (a) Kaolinite-calcite mixture; and (b) Illite-soda ash-calcite mixture.

librium studies,[30] provided the change takes place abruptly and a modest amount of energy is involved. FIGURE 9 shows an endothermic reaction corresponding to the change from α to β quartz, and FIGURE 11 shows an exothermic reaction corresponding to the formation of a new high-temperature phase from kaolinite at about 975°C.

FIGURE 19 shows differential thermal reactions for a clay-lime mixture (A) and a clay-soda-lime mixture (B) made in the course of a study of a part of the problem of the extraction of alumina from clays.[12] Curve A (kaolinite clay and calcite) shows an endothermic reaction at about 600°C. due to loss of (OH) water from the kaolinite and an endothermic reaction at 800–970°C. corresponding to loss of CO_2 from the lime carbonate, followed immediately by an exothermic reaction, which X-ray diffraction data indicate as resulting from the formation of gehlenite ($Ca_2Al_2SiO_7$). X-ray data show that pentacalcium trialuminate and dicalcium silicate have formed by 1400°C., but they are not reflected in the curve, which suggests that they formed slowly. Curve B (illite clay, soda ash, and calcite) shows an initial endothermic reaction due to loss of adsorbed water, a second endothermic reaction due to loss of (OH) from the illite, and a third endothermic reaction corresponding to loss of CO_2 from the carbonates, followed by a series of endothermic and exothermic reactions which could not be fully interpreted, except that the final, most intense one represents, at least in part, the formation of dicalcium silicate. The method has been used very little to study reactions of mixtures at high temperatures, but it appears to have considerable promise, particularly when used in conjunction with X-ray diffraction and optical analyses to identify the phases corresponding to the thermal reactions.

Bibliography

1. ASHLEY, H. E. 1911. The decomposition of clays, and the utilization of smelter and other smoke in preparing sulphates from clays. J. Ind. Eng. Chem. **3:** 91–94.
2. BERG, L. G., V. I. NIKOLAIEV, & E. Y. RODE. 1944. Thermographia. Acad. Sci. U.S.S.R: 25.
3. BERKELHEIMER, L. H. 1944. An apparatus for differential thermal analysis. U. S. Bur. of Mines. Rept. Rept. Inv. **3762**.
4. BERKELHEIMER, L. H. 1944. Differential thermal analyses of quartz. U. S. Bur. of Mines. Rept. Inv. **3763**.
5. BURGESS, G. K. 1908–09. On methods of obtaining cooling curves. U. S. Bur. of Standards. Bull. **5:** 199–225.
6. CAILLÉRE, S. & S. HÉNIN. 1945. Application de l'Analyse Thermique Differentielle a l'Etude des Argiles des Sols. Ann. Agronomiques.
7. LE CHATELIER, H. 1887. De l'action de la chaleur sur les argiles. Bull. Soc. Franc. Min. **10:** 204–211.
8. CUTHBERT, F. L. & R. A. ROWLAND. 1947. Differential thermal analyses of some carbonate minerals. Am. Min. **32:** 111–116.
9. DEAN, L. A. 1947. Differential thermal analyses of Hawaiian soils. Soil Science **63:** 95–105.
10. FAUST, G. T. 1948. Thermal analyses of quartz and its use in calibration in thermal analysis studies. Am. Min. **33:** 337–345.
11. FENNER, C. N. 1913. The stability relations of the silicate minerals. Am. Jour. Sci. 4th Series **36:** 331–384.
12. GRIM, R. E., J. S. MACHIN, & W. F. BRADLEY. 1945. Amenability of various types of clay minerals to alumina extraction by the lime sinter and lime-soda sinter process. Illinois State Geol. Survey, Bull. **69**.

13. Grim, R. E. 1947. Differential curves of prepared mixtures of clay minerals. Am. Min. **32**: 493–501; 1948. Ill. Geol. Surv. Rept. Inv. **134**.

14. Grim, R. E. & R. A. Rowland. 1942. Differential thermal analyses of clay minerals and other hydrous materials. Am. Min. **27**: 746–761, 801–818; 1942. Ill. Geol. Surv. Rept. Inv. **85**.

15. Grim, R. E. & R. A. Rowland. 1944. Differential thermal analyses of clays and shales, a control and prospecting method. Jour. Am. Cer. Soc. **27**: 65–76; 1944. Ill. Geol. Surv. Rept. Inv. **96**.

16. Grimshaw, R. W., E. Heaton, & A. L. Roberts. 1945. Constitution of refractory clays, II. Thermal analysis methods. Trans. Ceramic Soc. (Great Britain) **44**: 76–92.

17. Gruver, R. M. 1948. Precision method of thermal analysis. Jour. Am. Cer. Soc. **31**: 323–328.

18. Hendricks, S. B. & L. T. Alexander. 1939. Minerals present in soil colloids. I. Descriptions and methods for identification. Soil Science **48**: 257–271.

19. Hendricks, S. B., S. S. Goldich, & R. A. Nelson. 1946. A portable differential thermal analysis unit for bauxite prospecting. Econ. Geol. **41**: 64–76.

20. Hendricks, S. B., R. A. Nelson, & L. T. Alexander. 1940. Hydration mechanism of the clay mineral montmorillonite saturated with various cations. Jour. Am. Chem. Soc. **62**: 1457–1464.

21. Herold, P. G. & T. J. Planje. 1948. Modified differential thermal analysis apparatus. Jour. Am. Cer. Soc. **31**: 20–22.

22. Hollings, H. & J. W. Cobb. 1915. A thermal study of the combustion process. Trans. Chem. Soc. **107**: 1106–1115.

23. Honeybourne, D. B. 1948. Building Research Station, Harpenden, Great Britain. Personal communication.

24. Houldsworth, H. S. & J. W. Cobb. 1922–23. The behavior of fire clays, bauxites, *etc.*, on heating. Trans. Ceram. Soc. (Great Britain) **22**: 111–137.

25. Jeffries, C. D. 1944. Quantitative approach to study of thermal characteristics of clays. Soil Sci. Soc. Am. Proc. **9**: 86–91.

26. Jordan, J. W. 1949. Alteration of the properties of bentonite by reactions with amines. Mineralogical Magazine. (In press.)

27. Kerr, P. F. & J. L. Kulp. 1948. Multiple differential thermal analysis. Am. Min. **33**: 387–419.

28. Kournakov, N. S. & V. V. Tchernick. 1928. Physico-chemische Untersuchungen einiger wasserhaltigen Eisenoxyde und Tonerdesilikate. Mem. Soc. Russ. Mineral LVII: 62–73.

29. Kracek, F. C. 1929. The polymorphism of sodium sulphate: I. Thermal analysis. Jour. Phys. Chem. **33**: 1281–1303.

30. Kracek, F. C., N. L. Bowen, & G. W. Morey. 1929. The system potassium-metasilicate-silica. Jour. Phys. Chem. **33**: 1857–1879.

31. Mellor, J. W. & A. D. Holdcroft. 1911. The chemical constitution of the kaolinite molecule. Trans. Cer. Soc. (Great Britain) **10**: 94–120.

32. Mitchell, L. & E. C. Henry. 1943. Nature of Georgia kaolin: II. Evidence of mineralogical analysis. Jour. Am. Cer. Soc. **26**: 113–119.

33. Norton, F. H. 1939. Critical study of the differential thermal method for the identification of the clay minerals. Jour. Am. Cer. Soc. **22**: 54–63.

34. Orcel, J. 1927. Analyse thermique des chlorites. Bull. Soc. franc. Min. **50**: 278–322.

35. Orcel, J. 1936. L'emploi de l'analyse thermique differentielle dans la determination des constituants des argiles, des laterites, et des bauxites. Congr. Internat. Mines, Met. Geol. Appl. 7 Session. Paris 1935. **1**: 359–373.

36. Orcel, J. & S. Caillére. 1933. L'Analyse thermique differentielle des argiles a montmorillonite (bentonites). Compt. Rend. **197**: 774–777.

37. Rengade, E. 1909. Analyse Thermique et Metallographique Microscopique. Vol. 1. Paris.

38. Rieke, R. 1911. Einige Berbactungen uber den Gluhverlust von Kaolen und Tonen. Sprechsaal **44**: 637–640.

39. Roberts-Austen. 1899. Fifth Report of the Alloys Research Committee. Proc. Inst. Mech Eng: 35.

40. Rowland, R. A. & E. C. Jonas. 1949. Variations in differential thermal analysis curves of siderite. Am. Min. (In press.)

41. Satoh, S. 1923. Heat effects on fire clays and their mixtures. Science Reports Ser. III. Tohoku Imp. Univ. **1**: 157–203.

42. Speil, S., L. H. Berkelheimer, J. A. Pask, & B. Davies. 1945. Differential thermal analysis—its application to clays and other aluminous minerals. U. S. Bur. of Mines Tech. Paper **664**.

43. Vold, R. D., J. D. Grandine, & M. J. Vold. 1948. Polymorphic transformations of calcium stearate and calcium stearate monohydrate. Jour. Colloid Sci. **3:** 339–362.

44. Wallach, H. 1913. Analyse thermique des argiles. Compt. Rend. **157:** 48–49.

45. Wohlin, R. 1913. Beitrage zur Kenntnis der thermischen Analyse von Tonen, Bauxiten und einigen verwandten Korper. Sprechsaal **46:** 719–21, 733–35, 749–51, 767–9, 781–3.

OPTICAL PROPERTIES OF SURFACE FILMS

By Alexandre Rothen
Rockefeller Institute for Medical Research, New York, N. Y.

"Having proved that the superficial viscosity of water was due to a greasy contamination, whose thickness might be much less than one millionth of a millimeter, I too hastily concluded that films of such extraordinary tenuity were unlikely to be of optical importance." These words of Rayleigh were written about sixty years ago.[1] The feeling which he had when he first considered the optical influence of films of such tenuity is still the feeling of most of us when confronted with the same problem. We are prone to think that the yardstick should not be of a larger magnitude than the dimension to be measured. Influenced in part by the theory of resolution of optical instruments, we think of the wavelength of light as the order of magnitude below which no dimension can be measured by optical means. As we shall see, the problem of optical resolution in two dimensions is entirely different from that of estimating an optical path, which can be determined to within an extremely small fraction of one wavelength of light.

In this review, we shall be concerned with optical phenomena occurring on reflection of light from a metallic surface coated with a film, and especially with the application of these optical events to the determination of the optical thickness of the film. The optical parameters which characterize a film are: (1) the optical thickness, that is, the product of its real thickness by the index or indices of refraction; and (2) the absorption coefficient. Absorption occurs in metallic, that is, conductive films as well as in certain dielectric films whose molecules possess, for example, a system of conjugated double bonds.

Let us consider the case of a transparent film deposited on a reflecting metallic surface. Obviously, if the film thickness is such that a path difference of the order of $\lambda/2$ occurs between the light reflected from the upper surface of the film and the light reflected from the metal surface, interference phenomena occur. On this basic fact, Blodgett and Langmuir[2] developed a method some years ago to determine the thickness of transferred films on metallic surfaces. In their method, enough layers of a reference film are deposited on a polished metal slide, barium stearate, for example, so that the added thickness produces an optical path difference of slightly less than $\lambda/2$ when the light is reflected at an angle of incidence of 70° to 80°. Additional layers are then deposited stepwise so that the difference in thickness between two adjacent steps is equal to two monolayers. Measurement consists in determining the angle of incidence at which two adjacent steps appear equally illuminated. When a film of unknown thickness is deposited on a slide covered with such an optical gauge, the angle of incidence must be shifted in order to reëstablish equal darkening of two adjacent steps. The thickness is then calculated from this shift of angle of incidence. The light used is linearly polarized and is vibrating perpendicular to the plane of incidence (the reason for this choice will be discussed later on). This method is thus based on a phase shift close to 180° between the electric vector corresponding to the waves reflected at the air-film and film-metal interphases. To be sensitive, the method requires that the change in phase shift versus thickness should be large, in the neighborhood of a 180° phase shift.

This technique can be considered as a particular case of a more general method. Instead of producing nearly complete interference with light polarized in, *or* perpendicular to, the plane of incidence, one can illuminate the surface with light polarized at 45° to the plane of incidence, that is, light having components both in, *and* perpendicular to, the plane of incidence. In so doing, partial interference can be produced between these two components vibrating at right angles, the term "interference" being understood in the broadest sense.

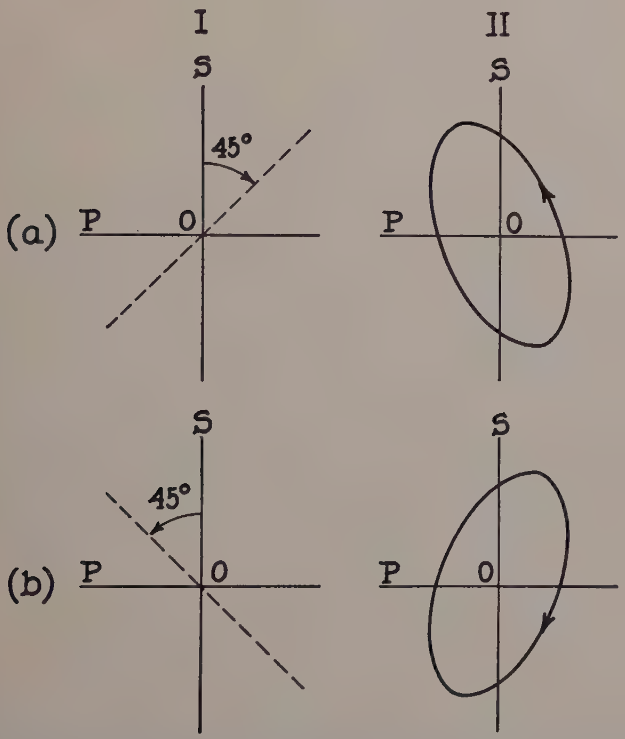

FIGURE 1. The coordinates are the directions perpendicular (OS) and parallel (OP) to the plane of incidence. IIa and IIb are the ellipses obtained after metallic reflection at an angle of incidence of approximately 70°. The ellipses are symmetrically placed with respect to the plane of incidence and rotate in opposite direction.

Suppose that light linearly polarized at 45° to the plane of incidence is sent on a metallic surface. Before reflexion, the electric vectors can be looked upon as made up of two components which, in this case, are of equal magnitude vibrating in phase, one in the plane of incidence (*p*), the other perpendicular to it (*s*). After reflection from the metal, the light becomes elliptically polarized. The two components suffer a phase difference as well as a change in relative magnitude. The phenomenon is illustrated in FIGURE 1, in which the plane of the figure is perpendicular to the direction of the light. OP and OS are the components in, and perpendicular to, the plane of incidence, respectively. FIGURE 1, II, illustrates the conditions after reflection. OP is smaller than OS and is in advance of more than 90° over OS. Depending upon the quadrants in which the linear vibration is localized before reflection, the light becomes dextro- or levo-elliptically polarized.

Let us now consider a metal surface covered with a transparent film. How will the film affect the ellipticity of the reflected light? It was to the great merit of Drude[3] to show that a film produces a change in phase and amplitude of both components *p* and *s*. Moreover, the two components are unequally affected by the presence of the film. The ratio, ψ, of their amplitude, and the difference of their phase, $\Delta = \delta^p - \delta^s$, are functions of the thickness of the film. It is also important to realize that this property does not depend upon the anisotropy of the film. The effect occurs even when the indices of refraction along OP and OS are the same. The separate determination of a change in phase and amplitude for each component is not easy, except under special circumstances, as in Langmuir and Blodgett's method. It is, however, very easy to determine a slight change in the ratio of the amplitudes of the components as well as in the difference of their phase, $\Delta = \delta^p - \delta^s$. Qualitatively, a thin film will alter the ellipticity of the reflected light, but the problem solved by Drude was that of calculating this change in ellipticity as a function of the thickness and index of refraction of the film.

Starting from Maxwell equations and the appropriate boundary conditions, Drude obtained the following equation:

$$\frac{\rho^{p,s}}{I^{p,s}} e^{i\delta^{p,s}} = \frac{r_f^{p,s} + r_m^{p,s} e^{-ix}}{1 + r_f^{p,s} r_m^{p,s} e^{-ix}} \tag{1}$$

In this equation, I and ρ are the amplitudes of the electric vectors (square root of light intensity) of incident (I) and reflected (R) light; δ is the phase, r_f is the real Fresnel coefficient for reflection at the film surface, and r_m is the complex Fresnel coefficient for reflection at the metal surface. The superscripts, ^{p,s}, indicate that this formula holds for each component separately. The variable x is equal to $4\pi n \cos \varphi \frac{l}{\lambda}$, in which n is the index of refraction of the film, φ is the angle at which the light is reflected at the film metal interphase, l is the thickness of the film, and λ is the wave length of the light used.

Writing the above formula for the two components, *p* and *s*, separately, and taking the ratio, one obtains:

$$tg\psi e^{i\Delta} = \frac{(r_f^p + r_m^p e^{-ix})(1 + r_f^s r_m^s e^{-ix})}{(1 + r_f^p r_m^p e^{-ix})(r_f^s + r_m^s e^{-ix})} \tag{2}$$

In this equation, $\psi = \frac{\rho^p}{\rho^s}$ and $\Delta = \delta^p - \delta^s$.

It is apparent from the above formula that ψ and Δ are periodic functions of the thickness l of the film. It is difficult to say more than this qualitative statement without expanding the equation. The equation was developed by Drude using the first term of a serial development. He obtained the following linear relationships between Δ or ψ and the film thickness:

$$\begin{aligned} \Delta - \Delta' &= -A\left(1 - \frac{1}{n^2}\right)\frac{l}{\lambda} \\ 2\psi - 2\psi' &= B(1 - C)\left(1 - \frac{1}{n^2}\right)\frac{l}{\lambda} \end{aligned} \tag{3}$$

In this equation, Δ' and ψ' are the values of Δ and ψ, when there is no film; A, B are functions of the angle of incidence and the optical constants of the metal; and $C = n^2 \cos^2 \varphi$, n being the refractive index of the film and φ the angle of incidence. Tronstad[4] was the first to test such relationships with thin films of known thickness. He used films of fatty acids adsorbed on a mercury surface and found good agreement between experimental and theoretical values. With the advent of Langmuir and Blodgett's method for the transfer of films by the dipping method, it became much easier to test Drude's formulas. We used films of multilayers of barium stearate deposited on stainless steel slides. The following values could be calculated from formulas (3) for one monolayer of barium stearate 24.4 Å thick and in which $n_{5893} = 1.495$ (TABLE 1).

TABLE 1

Angle of incidence:	49.2	69.2	74.2
$\psi - \psi' =$	0.00	0.34	0.61
$\Delta' - \Delta =$	1.37	3.6	3.55

It was found[5] that these values are in complete agreement with the experimental data obtained for thin films. At large angles of incidence, there is an appreciable deviation for films thicker than 50 Å, although the agreement is still good at 50° incidence with films up to 250 Å in thickness.

Drude's approximations, or similar approximations,[6] are thus valid for films which are thin with respect to the wavelength of light, but the approximations obviously cannot hold for thick films. Hauschild[7] obtained a better approximation by using a two-term development. This procedure, however, is unsatisfactory. Fortunately, formulas (1) or (2) can be developed explicitly without approximation. This has been done by Vasicek[8] for the case of films deposited on a transparent medium. The same method can be used for films deposited on metallic surfaces,[5] but the algebraic equations are a little more cumbersome since the coefficients $r^{p,s}_m$ are complex and must be split into two parts $r^{p,s}_m = X^{p,s} + iY^{q,s}$. The development of formula (1) consists of separating the real from the imaginary quantities.

$$\frac{\rho^{p,s}}{I^{p,s}} e^{i\delta^{p,s}} = \frac{r_f^{p,s} + [X^{p,s} + iY^{p,s}] \cos x - i[X^{p,s} + iY^{p,s}] \sin x}{1 + r_f^{p,s}[X^{p,s} + iY^{p,s}] \cos x - ir_f^{p,s}[X^{p,s} + iY^{p,s}] \sin x}$$

$$= \frac{r_f^{p,s} + X^{p,s} \cos x + Y^{p,s} \sin x - i[X^{p,s} \sin x - Y^{p,s} \cos x]}{1 + r_f^{p,s} X^{p,s} \cos x + r_f^{p,s} Y \sin x - ir_f^{p,s}[X^{p,s} \sin x - Y^{p,s} \cos x]}.$$

Writing this formula for the two components separately, and substituting the subscripts $_1$ and $_2$ for the superscript ^{p}, and subscripts $_3$ and $_4$ for the superscript ^{q}, one obtains:

$$\frac{\rho^p}{I^p} e^{i\delta^p} = \frac{\alpha_1 - i\beta_1}{\alpha_2 - i\beta_2} \quad \text{and} \quad \frac{\rho^s}{I^s} e^{i\delta^s} = \frac{\alpha_3 - i\beta_3}{\alpha_4 - i\beta_4}.$$

Taking the ratio,

$$\frac{\rho^p}{I^p} e^{i\delta^p} \frac{I^s}{\rho^s} e^{-i\delta^s} = tg\,\psi e^{i\Delta} = \frac{(\alpha_1 - i\beta_1)(\alpha_4 - i\beta_4)}{(\alpha_2 - i\beta_2)(\alpha_3 - i\beta_3)}$$

$$= \frac{(\alpha_1 - i\beta_1)(\alpha_2 + i\beta_2)(\alpha_4 - i\beta_4)(\alpha_3 + i\beta_3)}{(\alpha_2^2 + \beta_2^2)(\alpha_3^2 + \beta_3^2)}$$

$$= \frac{(\alpha_1\alpha_2 + \beta_1\beta_2 + i\alpha_1\beta_2 - i\alpha_2\beta_1)(\alpha_3\alpha_4 + \beta_3\beta_4 + i\alpha_4\beta_3 - i\alpha_3\beta_4)}{(\alpha_2^2 + \beta_2^2)(\alpha_3^2 + \beta_3^2)}$$

$$= \frac{(A + iB)(A' + iB')}{(\alpha_2^2 + \beta_2^2)(\alpha_3^2 + \beta_3^2)}.$$

Since

$$tg\,\psi \cos \Delta = \frac{AA' - BB'}{(\alpha_2^2 + \beta_2^2)(\alpha_3^2 + \beta_3^2)}$$

and

$$tg\,\psi \sin \Delta = \frac{AB' + A'B}{(\alpha_2^2 + \beta_2^2)(\alpha_3^2 + \beta_3^2)},$$

hence

$$tg\,\Delta = \frac{AB' + A'B}{AA' - BB'} \tag{4}$$

In this last equation,

$$A = r_f^p[1 + X^{p^2}\, ty^{p^2}] + X^p[1 + r_f^{p^2}] \cos x + Y^p[1 + r_f^{p^2}] \sin x;$$

$$A' = r_f^s[1 + X^{s^2} + Y^{s^2}] + X^s[1 + r_f^{s^2}] \cos x + Y^s[1 + r_f^{s^2}] \sin x;$$

$$B = -X^p[1 - r_f^{p^2}] \sin x + Y^p[1 - r_f^{p^2}] \cos x;$$

and $B' = X^s[1 - r_f^{s^2}] \sin x - Y^s[1 - r_f^{s^2}] \cos x.$

The coefficients $r^{p,s}_f$ can be calculated from Fresnel equations, since the angle of incidence and the index of refraction of the film are known. The quantities $X^{p,s}$, $Y^{p,s}$ are related to the phase shifts δ_m^p, δ_m^s (abbreviated $\delta_m^{p,s}$) of the components after reflection from the uncoated metal surface by the following formulas: $tg_m^{\delta p,s} = Y^{p,s}/X^{p,s}$, $\rho_m^{p,s} = [X^{p,s} + Y^{p,s^2}]^{\frac{1}{2}}$. The correct sign should be taken for the coefficients $X^{p,s}$, $Y^{p,s}$. It turns out that X^p is positive, Y^p is negative, X^s is negative, and Y^s is positive. The quantities $\delta_m^{p,s}$ and $\Delta_m = \delta_m^p - \delta_m^s$ as well as $\rho_m^{p,s}$ can be computed from the optical constants of the clean metal surface by means of equations which can be found, for instance, in the Handbuch der Physik, **20**: 242. Thus, *tg* Δ can be calculated for any film thickness from equation (4), since the coefficients A, A', B, and B' can be computed. FIGURE 2 shows that there is good agreement between the experimental and theoretical curves of Δ plotted against the thickness of film. As indicated in (4), the change in phase Δ is not a sinusoidal function of x, since the function contains $\sin^2 x$, $\cos^2 x$, $\sin x \cos x$, terms corresponding to a periodicity of $2x$. The theoretical number of monolayers of barium stearate which produces a path difference of 5893 Å at the angles of incidence of 50°, 69.2°, and 80° are 93.3, 102.5, and 105, respectively. These figures compare favorably with the experimental values of 92.5, 102.2, and 105 monolayers at which the periods describing the change of phase are completed. Furthermore, the curves of FIGURE 2 show that the change of phase with increasing thickness is especially large for films equivalent to 40 to 50 monolayers of barium stearate. In that range of thickness, an increment of 24 Å brings about a change of phase $\Delta = 48°$ at 80° incidence. Since a change of phase Δ can be measured within $\pm 0.04°$, it follows that a variation in thickness of less than 0.1 Å can still be appre-

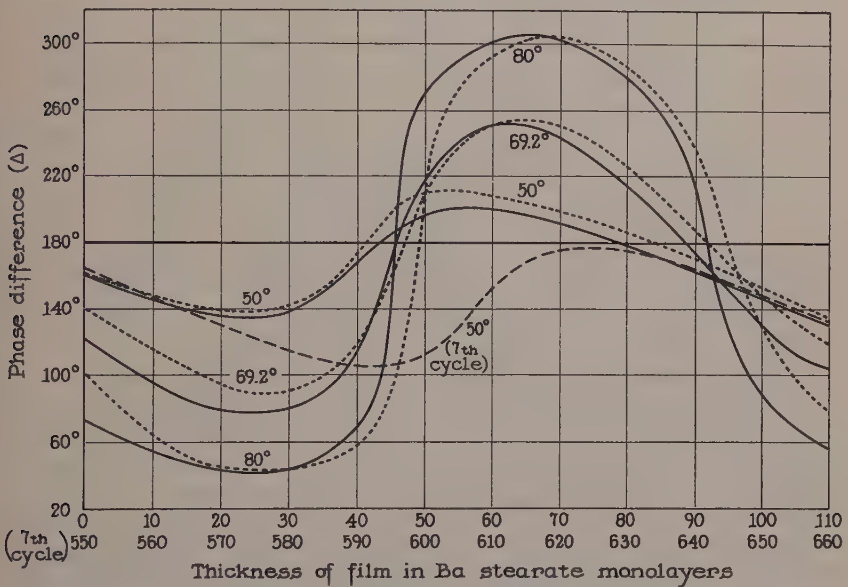

FIGURE 2. Phase shift Δ produced by films of Ba stearate at 50°, 69.2°, and 80° incidence. The dotted curves are theoretical, and the solid and dashed lines are experimental.

ciated. When the film is about 600 Å or 1500 Å thick, the phase changes very little with the small increment in thickness.

It is interesting to note that, because of the skewness of the curve, the coefficient $\frac{\delta\Delta}{\delta N}$, which is maximum at 45 layers, is also large at 95 layers, but appreciably smaller than at 45 layers. This means that δ^p and δ^s taken separately are different functions of x. These absolute phase shifts δ^p and

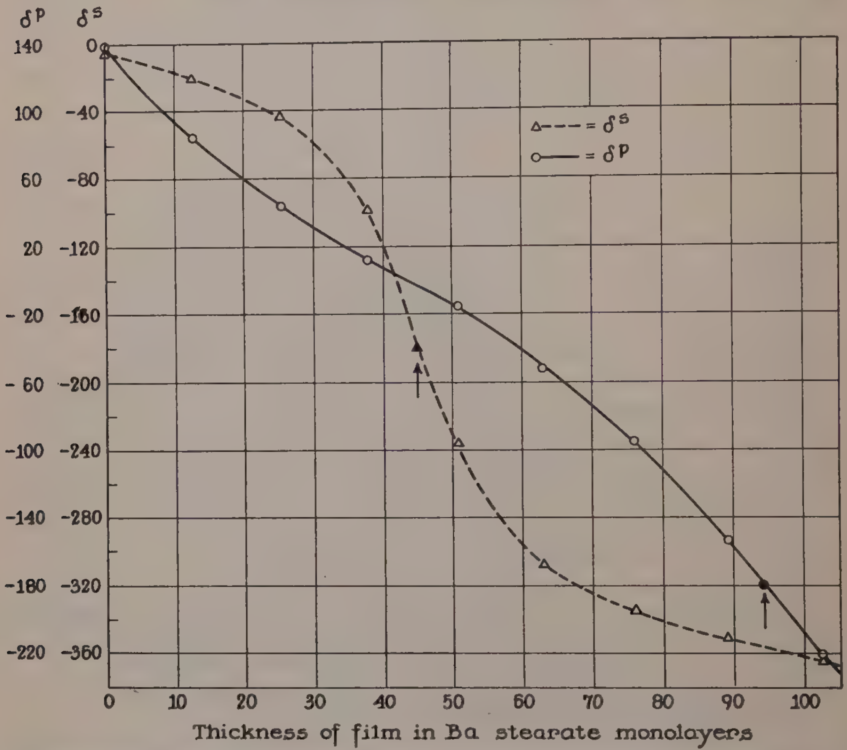

FIGURE 3. Absolute phase shift δ^p, δ^s of each component produced by films of Ba stearate at 69.2° incidence.

δ^s can be calculated from equation 1 as Δ was calculated above. The calculations give:

$$tg\,\delta^p = \frac{\alpha_1\beta_2 - \alpha_2\beta_1}{\alpha_1\alpha_2 + \beta_1\beta_2} \quad \text{and} \quad tg\,\delta^s = \frac{\alpha_3\beta_4 - \alpha_4\beta_3}{\alpha_3\alpha_4 + \beta_3\beta_4}.$$

The results have been plotted in FIGURE 3 for the angle of incidence of 69.2°. The difference of the two curves gives the corresponding Δ curve seen in FIGURE 2. The curves of FIGURE 3 show that there is a phase shift of 180° for the components s and p, for thicknesses equivalent to 46.8 and 94.1 monolayers of barium stearate, respectively. This means that a minimum does occur in the intensity of the light corresponding to the components s and p at these thicknesses. The figure also shows that the curve δ^s is much steeper than the curve δ^p when their respective phase shift is 180°. This is why it is much better to use the component s, rather than p, in the method of Blodgett and Langmuir described above. The required phase change of 180° occurs for both of them at the appropriate thicknesses, but the sensitivity (change in δ *versus* change in thickness) is much greater for s. Blodgett and Langmuir[2] indeed have noticed that the useful range of angles of incidence is much smaller for p than s in accord with these theoretical curves.

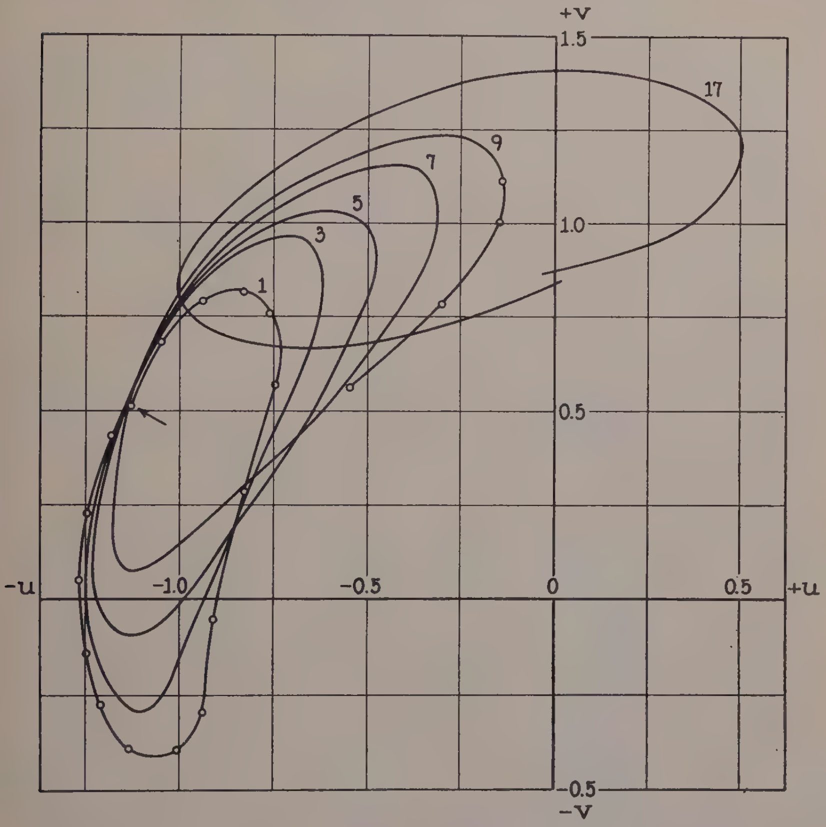

FIGURE 4. Ellipticity of reflected light at 50° incidence produced by films of Ba stearate from 0A up to the equivalent of 17 wavelengths of light (λ5893). Arrows indicate beginning of the first cycle. All cycles are described clockwise. The points indicated on the initial cycle correspond to thickness intervals of 146 Å (six monolayers of Ba stearate).

As already indicated, there is a corresponding periodic change in the value of ψ. Since the change in ψ is, in general, smaller than the change in Δ, we shall not consider it here.

Films Producing an Optical Path Difference Greater Than One Wavelength of Light. With the increase in the thickness of the film, formula (2) predicts that the changes in ψ and Δ are truly periodical and repeat the same cycle each time the thickness is equivalent to a path difference of one wavelength of light. To test this point, experimental data were obtained for film thickness up to 40,000 Å of barium stearate. Both ψ and Δ were determined. The results obtained at 50° are represented graphically in FIGURE 4 according to the method of Poincaré. The plane of the figure is the complex plane. The coordinates u + iv of each single point are:

$$u = \cot \psi \cos \Delta; \qquad v = \cot \psi \sin \Delta; \qquad \text{and } u + iv = \cot \psi e^{i} \,.$$

With this representation, all points on the u axis correspond to linear vibrations, whereas all points on the v axis correspond to ellipses whose axes are oriented along OS and OP. The points, $u = 0$, and $v = \pm 1$, are two circular vibrations of opposite sense. It is apparent that each cycle corresponds to an optical thickness of one wavelength of light, but the successive cycles precess clockwise around the origin as the approximate center of rotation. This lack of superposition cannot be predicted by formula (2). It may be due in part to the birefringence of the film which has hitherto been neglected.

We have reviewed so far the optical phenomena occurring with transparent films. In the case of absorbing films, the general formula (1) of Drude is still valid except that the exponential coefficient x includes the absorption coefficient. This case will not be discussed since no experimental data have yet been obtained for absorbing films of known thickness.

Apparatus to Measure the Ellipticity of Reflected Light. The basic principle of all the apparatus developed up to the present depends on a change from the elliptically polarized light to linearly polarized light by the introduction of a supplementary phase shift by means of a compensator (Babinet compensator or mica $\lambda/4$ plate). In order to be sensitive, the apparatus should be equipped with a half shadow device. In our own apparatus, built specifically for thickness determination, the half shadow is produced on the reflecting surface itself.[9] With such an apparatus it is an easy matter to determine an optical thickness of a thin film to less than 1 Å. The theoretical limit is $\simeq \pm 0.1$ Å under the most favorable conditions (when $\dfrac{\delta \Delta}{\delta N}$ is maximum).

Conclusions. It has been shown that a film as thin as 0.1 Ångström unit produces some noticeable effect on the parameters characterizing the light reflected from the surface upon which the film is deposited. The thickness of the film can be calculated from the magnitude of this optical effect. It may be well to emphasize that such a thickness is an overall thickness. Apparatus built with the purpose of determining such small thickness may be compared to a one-dimensional microscope, with a one-dimensional resolution far greater than that achieved in the best electronmicroscope. Unfortunately, it is only one dimensional. The resolution in the other two dimensions perpendicular to the thickness is limited by the ordinary laws of optics.

Bibliography

1. Rayleigh. 1892. Phil. Mag. **33:** 1.
2. Blodgett, K. B. & I. Langmuir. Phys. Rev. **51:** 964.
3. Drude, P. Ann. Phys. u. Chemie. **36:** 865.
4. Tronstadt, L. 1935. Trans. Faraday Soc. **31:** 1151.
5. *Rothen, A. & M. Hanson. 1949. Rev. Sci. Inst. **20:** 66.
6. Lucy F. A.. 1948. J. Chem. Physics **16:** 167.
7. Hauschild, H. 1920. Ann. Phys. u. Chemie. **63:** 816.
8. Vasicek, A. 1947. J. Opt. Soc. America. **37:** 145.
9. Rothen, A. 1945. Rev. Sci. Inst. **16:** 26.

* In this article, a misprint occurred in the Drude formula appearing on page 67. The formula should read $\Delta' - \Delta$, instead of $\Delta - \Delta'$.

MEASUREMENT OF PROPERTIES OF THIN FILMS ON CHROMIUM BY THE REFLECTION OF POLARIZED LIGHT

By J. B. Bateman and Margaret W. Harris
Camp Detrick, Frederick, Maryland

Thin films coating a plane polished metal surface can be characterized in terms of their effect upon the optical properties of the surface. Drude[7] demonstrated sixty years ago that the effect is readily measurable and the experimental arrangement used by him in his studies of metallic reflection has survived without substantial modification through the several subsequent investigations in which optical examination of surface films has been attempted. If a specimen of the clean polished metal is available, the measurement generally presents no great difficulty, and it may afford a convenient method of following surface changes brought about by various agencies. More often, it is desirable to derive values for the thickness and refractive index of the film from the measured quantities and to interpret these ultimately in terms of molecular dimensions and molecular orientation.

Difficulties of interpretation have been the chief drawback in the wider use of polarization optical methods in the study of surface configurations. Several approximations of the general equations, applicable only to very thin films, are available. These should describe the observed behavior of such films, provided it is possible to specify the boundary conditions which operate. Until very recently, however, no experimental test had been made, because acceptable independent methods of determining the film constants were not available.

Increasing realization of the importance of thin films in electrochemistry, electronics, applied optics, and biophysics has made it desirable to establish the range of application of the theoretical equations of the optical study of films. Fortunately, the circumstances which give particular interest to the problem have also provided an excellent experimental method with which to attack it. Blodgett[2] has shown how to transfer almost any desired number of monolayers of stearic acid and other long chain fatty acids from the liquid surface on which they were formed to a glass or metal plate, and has measured the thickness and refractive index of the transferred films.[3, 5] A study of their effects upon the optical properties of the metal base, with an obvious bearing upon the applicability of the theoretical equations, would also clearly serve as an empirical means of correlating the observed effects with film thickness and refractive index in the event that discrepancies between experimental and theoretical data should render the equations of doubtful practical value in their present form.

This paper presents the results of polarization measurements on aliphatic acid layers transferred to chromium by Blodgett's method. The data were obtained with the above considerations in mind, and with the special object of determining the conditions most favorable to the precise simultaneous measurement of thickness and refractive index. To this end, it proved necessary to extend the measurements to thicker films than those which had been used for the purpose of comparison with the approximate theoretical equations, most of which apply only when the film thickness is much less than the wavelength of the light in which they are observed.

Approximate Equations of Film Optics

Polarimetric methods permit the measurement of the relative changes in phase and amplitude brought about by reflection of a plane-polarized beam resolved into components whose electric vectors vibrate parallel (ray *op*) and perpendicular (*os*) respectively to the plane of incidence. If the two components are initially equal in phase and amplitude, the ellipse defining the reflected vibrations is represented by the relative reflection coefficient, $\tan \psi \cdot \exp (i\Delta)$, the real part of which is the ratio of the reflected amplitudes, R_p/R_s, while the imaginary part, Δ, gives the difference between the absolute phase changes, $(\delta_p - \delta_s)$.

The effect of a thin film upon the relative reflection coefficient of a metal is conveniently represented by

$$\frac{\tan \psi}{\tan \psi_0} \exp i(\Delta - \Delta_0)$$

in which the subscript 0 refers to the uncoated metal. Typically, when light is reflected at an angle of incidence 70° from the surface of a metal covered with a film of refractive index 1.5 and thickness 20 AU, $\tan \psi/\tan \psi_0$ is about 1.01 and $(\Delta - \Delta_0)$ has a negative value of two or three degrees. The available theoretical equations predict correctly the sign and order of magnitude of these changes but differ among themselves as to the exact relationship with film thickness and refractive index.

The experimental studies reported here have been guided by reference to only two of the theoretical approximations, the earliest by Drude[8] and a recent modification given by Lucy.[10]

Drude's equations are linear in film thickness, L:

$$\frac{\tan \psi}{\tan \psi_0} - 1 = BLa_1^1 \frac{n^2 - 1}{n^2} (1 - n^2 \cos^2 \varphi) \qquad (1)$$

$$\Delta - \Delta_0 = -BL \frac{n^2 - 1}{n^2} (\cos^2 \varphi - a_1) . \qquad (2)$$

In these equations, $B = \dfrac{4\pi}{\lambda} \cdot \dfrac{\cos \varphi \sin^2 \varphi}{(\cos^2 \varphi - a_1)^2 + a_1^{12}}$;

$$a_1 = \frac{1 - \kappa_0^2}{n_0^2(1 + \kappa_0^2)^2}; \qquad \text{and} \qquad a_1^1 = \frac{2\kappa_0}{n_0^2(1 + \kappa_0^2)^2}.$$

In these equations, φ represents angle of incidence, λ is the wavelength, n is the film refractive index, and n_0 and κ_0 are the refractive index and absorption coefficient of the metal base, respectively. The presence of the term $n^2 \cos^2 \varphi$ in equation 1 establishes the possibility, in principle, of determining both L and n from a single measurement of $\tan\psi/\tan\psi_0$ and $\Delta - \Delta_0$, these quantities being related by the equation:

$$-(\Delta - \Delta_0) = \frac{\cos^2\varphi - a_1}{a_1^1(1 - n^2\cos^2\varphi)}\left[\frac{\tan\psi}{\tan\psi_0} - 1\right] \tag{3}$$

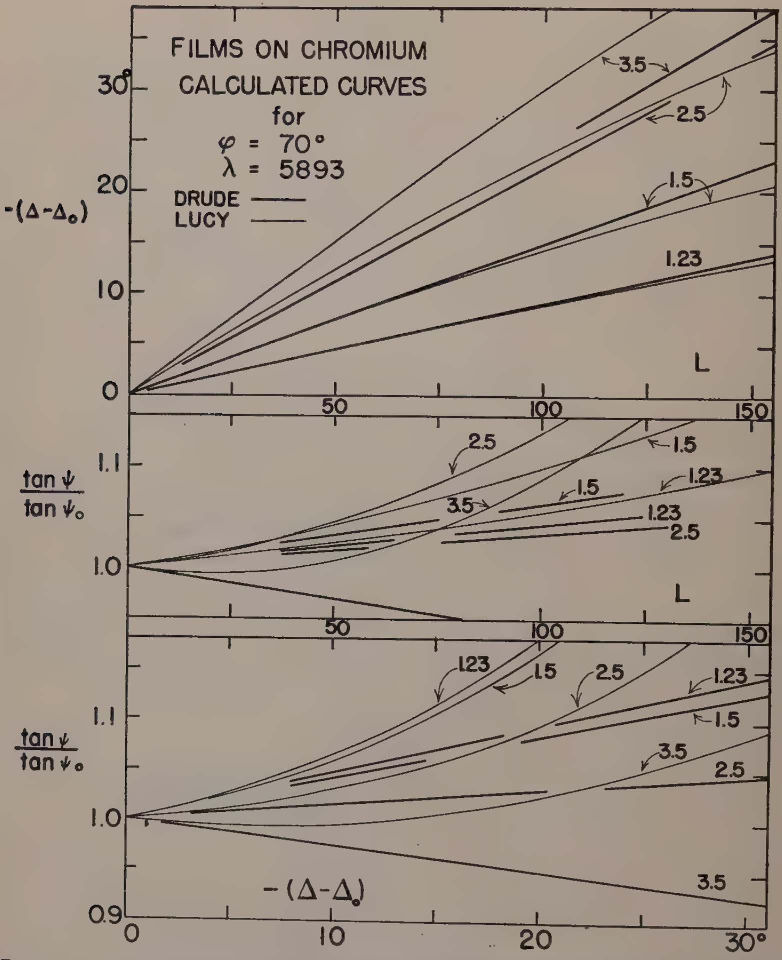

FIGURE 1. Optical properties of film-coated chromium: theoretical curves for films of refractive index 1.23, 1.5, 2.5, and 3.5 on chromium, viewed in sodium light, angle of incidence 70°. Heavy lines calculated from the Drude equations; thin curves from the Lucy equations. Top section: abscissa, film thickness; ordinate, $\Delta - \Delta_0$. Middle section: abscissa, film thickness; ordinate, $\tan\psi/\tan\psi_0$. Bottom section: abscissa, $\Delta - \Delta_0$; ordinate, $\tan\psi/\tan\psi_0$.

It is apparent from equation 3 that $(1 - n^2 \cos^2 \varphi)$ is least sensitive to changes of film refractive index when the latter approaches unity; the lines in FIGURE 1 illustrate this and show that the method is rather unsuitable for measurement of the refractive index of films of unknown thickness in the range below 1.5.

Equations 17 to 22 given in Lucy's paper[10] can be rearranged in the following form for the convenient calculation of theoretical curves:

$$\frac{\tan^2 \psi}{\tan \psi_0} = (1 - M_1)^2 + M_2^2 \tag{4}$$

$$\cos (\Delta - \Delta_0) = (1 - M_1) [(1 - M_1)^2 + M_2^2]^{1/2} \tag{5}$$

In the equations,

$$M_1 = \frac{4\pi}{\lambda} \cdot \frac{\sin \varphi \tan \varphi}{r^2 + s^2} \cdot \frac{n^2 - 1}{n^2} \cdot L \cdot [(\alpha s - \beta r)n^2 + (\beta^2 - \alpha^2)s + 2\alpha\beta r];$$

$$M_2 = \frac{4\pi}{\lambda} \cdot \frac{\sin \varphi \tan \varphi}{r^2 + s^2} \cdot \frac{n^2 - 1}{n^2} \cdot L \cdot [(\alpha r + \beta s)n^2 + (\beta^2 - \alpha^2)r - 2\alpha\beta s];$$

$\alpha = n_0^2(1 - \kappa_0^2)$; $\beta = 2n_0^2\kappa_0$; $r = (\alpha - 1)(\alpha - \tan^2 \varphi) - \beta^2$; and $s = \beta(2\alpha - \tan^2 \varphi - 1)$.

As in the Drude equations, the film thickness term always involves the product $L \cdot (n^2 - 1)/n^2$, while the refractive index also occurs elsewhere in the definitions of M_1 and M_2. It is also evident that the equations can be solved in principle for n and L, and that the refractive index effect is not large in the case of films of refractive index less than 1.5 (see FIGURE 1). The curves of FIGURE 1 also show that, in the case of films of low refractive index, although the Drude and the Lucy equations give concordant values of the limiting slope at zero film thickness, deviations from the linear relationship may be expected to appear in the case of the phase change when the film thickness exceeds 50 AU, and in the case of the amplitude factor at thicknesses as low as 10 AU. When the film refractive index is greater than 2.5, discrepancies are already evident in the values for the limiting slopes.

Experimental Technique

In outline, the following experimental procedure has been followed: Preliminary observations establish the optical constants of a clean metal surface. The desired number of aliphatic acid monolayers is transferred to the surface by dipping. The polarimetric observations are repeated. Further monolayers are transferred and the process continued until the desired film thickness is attained. Detailed descriptions of each operation are available in the literature and the following notes refer to these accounts and to the modifications that have been made in the course of the present work.

Metal Slides. In the first experiments, optically flat polished stainless steel plates formed the reflecting base. It was soon found that the plates could not be polished in such a manner as to give uniform values of the optical constants. Furthermore, the constants were altered by the process of conditioning the plates for the uptake of an initial film when raised through an aqueous interface occupied by a monolayer of barium stearate. As a result, the apparent effect of the first one or two stearate monolayers was highly erratic, since the optical constants of the conditioned surface could not be measured. These difficulties were not encountered when glass slides, coated with chromium by condensation *in vacuo*, were used instead of steel. Satisfactory results were obtained with ordinary lantern slides cut to the desired size. After cleaning in bichromate, followed by rinsing in distilled water, the slides were heated in air or *in vacuo* for several minutes and were then exposed to chromium vapor. A strongly adherent layer was deposited. The optical properties of the surfaces were more reproducible than those of polished steel. Furthermore, the bare chromium will, with few exceptions, pick up one fatty acid monolayer when lowered through a liquid interface covered with such a film, and a second when raised. The optical effects of this *Y*-layer (Blodgett[2]) were reproducible and consistent with those of subsequent *Y*-layers, and were brought about wholly by the transferred monolayers, not by mere immersion of the slide in the substrate. Occasionally, freshly prepared chromium plated slides are wettable. In this condition, they pick up a monolayer when lowered through the film-covered interface and release it when raised. Within a few hours, however, they acquire hydrophobic properties without undergoing any measurable change in optical constants.

Transferred Monolayers: Skeleton Films. Barium stearate-stearic acid and barium palmitate-palmitic acid films were made by spreading the respective acids dissolved in benzene upon water containing barium chloride and buffered with bicarbonate at pH 7 (solution "*a*" of Blodgett and Langmuir[5]). Cadmium arachidate layers were prepared at pH 5.7 as described by Blodgett.[4] After observations had been made upon the continuous films of cadmium arachidate, they were skeletonized by soaking for two minutes in acetone. When measurements on the skeleton films were complete, the original refractive index was re-established by treatment of the slides with a drop of Nujol (bibliographical reference 5, page 980), and a further series of measurements provided assurance that no significant loss of thickness had accompanied the skeletonization.

Polarimetric Measurements. The polarimetric assembly consisted of the usual elements mounted upon a spectrometer base in the following order: sodium arc, filter, iris diaphragm, collimator pinhole, collimating lens, Glan-Thompson polarizer, reflecting plate, Soleil-Babinet compensator, Glan-Thompson analyzer, focusing lens, and eyepiece pinhole. In the earlier measurements, Rothen's half-shade device was employed,[11] consisting of an optical gauge of barium stearate* incorporated in the reflecting base. This method gave very satisfactory empirical calibrations in terms of film thickness. Matching of the fields occurs, not at some unique setting of compensator and analyzer azimuths, but over a wide range of settings. Consequently, it is possible to select arbitrarily some constant setting of the compensator and to determine the variation of the analyzer readings at which the fields match, as a function of film thickness. This procedure is less suited to the exact determination of the phase and amplitude factors.

---

* An excellent half shade can also be made by condensing a thin layer of silicon dioxide on one half of the slide.

Rothen[13] achieved the latter end in his studies of thick films by adjusting both quarter-wave plate and analyzer to "a position of maximum uniform darkness." In our hands, this procedure proved insensitive. Better results were obtained by discarding the optical gauge and adjusting compensator and analyzer to extinguish the reflected beam. Careful alignment of the optical elements of the instrument gave scale correction data, and further allowance for the effects of any remaining lack of symmetry was made by taking readings with polarizer settings of 45° and 315° (Drude[6]). The equations for calculating tan ψ and Δ from the observed compensating azimuths are given in convenient form by Lucy.[10]

Results and Discussion

Optical Properties of Chromium. The optical constants of uncoated chromium were calculated from Δ and tan ψ by means of the approximate formulae (bibliographical reference 7, page 544, and bibliographical reference 9, page 363). Theoretical curves for comparison with our film data were obtained by using the values, $n_0 = 3.10$, and $\kappa_0 = 1.22$, as the optical constants of the uncoated chromium base. When the calculations were made, these were selected as the most frequently occurring values. Later averages, based upon measurements of 48 plates, were $n_0 = 2.963$ and $\kappa_0 = 1.132$. On the other hand, calculations of Δ and tan ψ for filmed plates were made using the appropriate values of n_0 and κ_0 for each individual plate. The extreme values, approached only in a few instances, were $n_0 = 2.626, 3.264$; and $\kappa_0 = 0.986, 1.264$.

Behavior of Thin Aliphatic Acid Films on Chromium. An example of the observed optical behaviour of barium stearate films on a single chromium-plated slide, as the film thickness is increased in steps of two monolayers from zero to one thousand AU, is shown in FIGURE 2. The observations were made in sodium light at an angle of incidence of 70°. Whereas Δ reaches a maximum value around 600 AU and tan ψ begins to increase sharply at about 800 AU, the approximate theoretical equations predict a continuous decrease of Δ and a steady increase of tan ψ (FIGURE 1). The comparison of experimental and theoretical data must be confined to films less than 400 AU thick (optical thickness of the order 0.1 λ).

In FIGURE 3, the experimental data for barium stearate and barium palmitate films are plotted, together with the appropriate theoretical lines calculated from the Drude and Lucy equations. The scale of thickness, L, for the experimental data is based upon values of 48.8 and 44.0 AU, respectively, for the thickness of double molecular layers[5] of barium stearate and barium palmitate, while the calculated curves are for films of a refractive index of 1.5.

Both the Drude and Lucy formulations are consistent with the experimental values of $\Delta - \Delta_0$ for film thicknesses up to 100 AU. At this point, deviations from the linear relationship become evident; up to 200 AU, the points follow the Lucy curve within the limits of experimental error. Deviations from linearity in the case of tan ψ/tan ψ_0 are anticipated by the Lucy formulation for quite thin films, and, in practice, are already suggested by the points for one double layer of barium stearate of a thickness of 48.8 AU, and are quite definite at 88 AU. Quantitatively, it seems that the Lucy formulation for tan $\psi/\tan \psi_0$ over-corrects for deviations from the linear relationship.

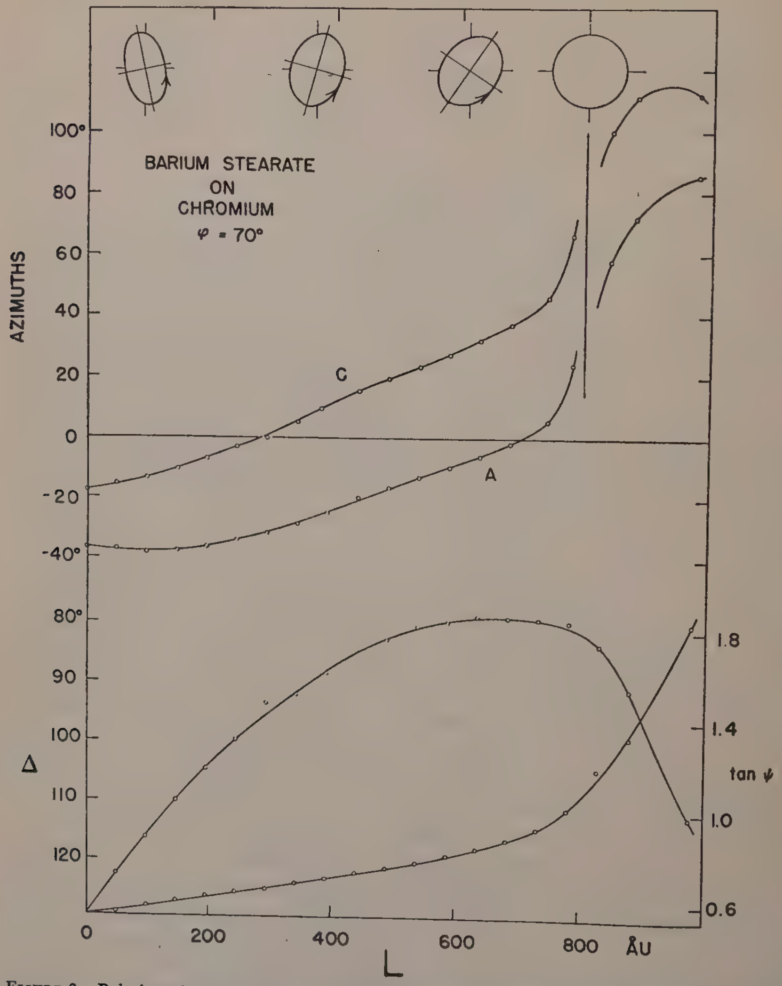

FIGURE 2. Polarimetric observations on a single chromium plate covered with barium stearate-stearic acid: sodium light, angle of incidence 70°. Abscissa, film thickness. The upper pair of curves gives the compensator (C) and analyzer (A) azimuths at which the elliptically polarized reflected light is compensated, the compensator retardation setting being 90°. The corresponding values of Δ and tan ψ are shown by the lower pair of curves, the one which is concave to the axis of abscissae being Δ. The small figures at the top represent the reflected light at selected values of film thickness; here the horizontal axis corresponds to the electric vector *op* and the vertical axis to *os*; the observer is looking toward the light source.

In FIGURE 3, each type of symbol corresponds to a single metal-coated slide upon which films were deposited in steps of two monolayers, readings being taken in the polarizing assembly at each step. It will be observed that the scatter among the experimental points is made up partly of systematic differences between the slides and partly of irregularities in the effects of successive double layers. The former are partly accounted for by differences in the optical constants of the uncoated metal surfaces. Since such differences are of importance, the data should be compared with theoretical zones corresponding to the range of values of n_0 and κ_0 encountered in the measurements, rather than with the single curves shown in FIGURE 3. These differences are less important, however, than the variable effects of successive double layers upon a single slide. Irregularities in the character of the monolayers when spread on the original liquid substrate, and variations in the configuration they assume when transferred to the chromium slide, are probably responsible for the most serious optical inconsistencies, the causes of which have not been fully determined. Variations in the purity of the water used in the aqueous substrate, in the rate and temperature of transfer, and in the dust content of the air are contributory factors which will require careful control in any attempt to obtain more precise data.

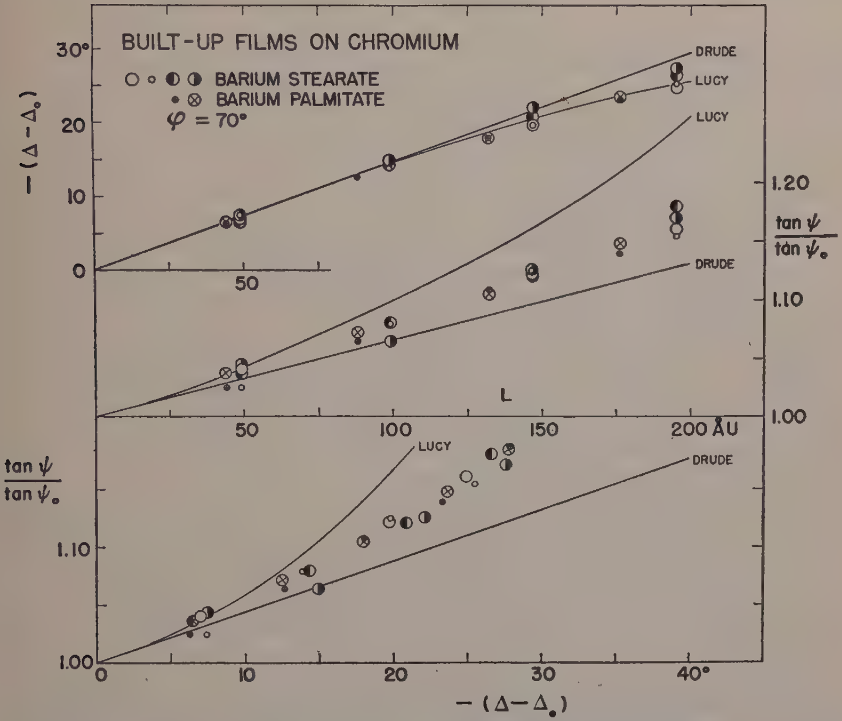

FIGURE 3. Thin films of barium stearate and barium palmitate on chromium: comparison of experimental and theoretical data for wavelength 5893 AU, angle of incidence 70°. Lines calculated for films of refractive index 1.5 upon a reflecting base with optical constants n_0, 3.10; κ_0, 1.22 from equations of Drude and Lucy. Experimental points are for films of barium stearate and barium palmitate, each type of symbol representing a single reflecting plate. The optical constants of the metal base had the following values for the plates used in these measurements: barium stearate plates, $n_0 = 3.130, 3.137, 3.177, 3.264$; $\kappa_0 = 1.167, 1.168, 1.154, 1.139$; barium palmitate plates, $n_0 = 3.119, 3.080$; $\kappa_0 = 1.164, 1.208$.

Errors referable to variations in the metal base and the transferred films outweigh those arising from the technique of optical measurement and from uncertainties in the values chosen for film thickness and refractive index. The thickness scale may require slight revision. The value 48.8 AU for the thickness of a double molecular layer of barium stearate was obtained

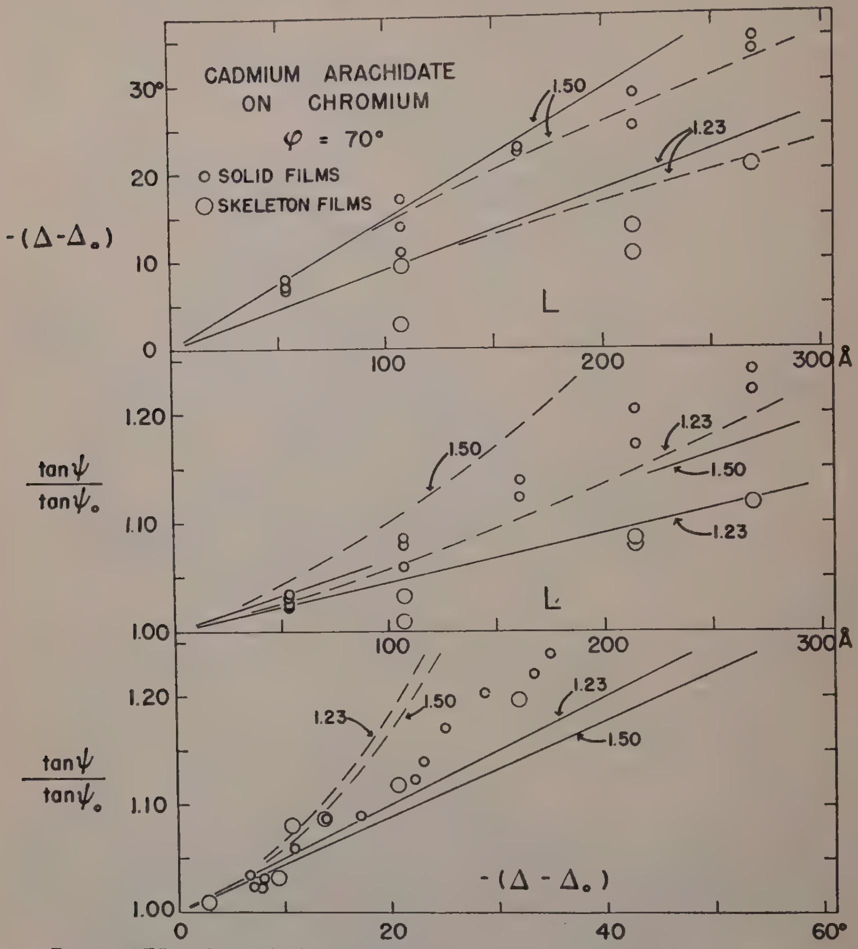

FIGURE 4. Effect of refractive index difference on optical behavior of thin films on chromium: comparison of experimental and theoretical data for wavelength 5893 AU, angle of incidence 70°. Continuous lines are calculated from Drude equations for films of refractive index 1.5 and 1.23. Broken lines, from Lucy equations. Small experimental points are for mixed films of cadmium arachidate-arachidic acid; large points are for the cadmium arachidate films prepared by skeletonizing the mixed films with acetone. Each individual small circle represents a separate plate (contrast data in FIGURE 3).

by Blodgett and Langmuir[5] by observation of the intensity minima of the ordinary ray, R_s, reflected from barium stearate films on chromium-plated brass, assuming the refractive index of the films for the R_s ray to be 1.491, the value measured for similar films on glass. The length of the double molecule of stearic acid in monoclinic crystals is 49.6[14] and that of rhombic sodium stearate, 51.8 AU.[15] Although the effect of the barium atom in the mixed stearic acid-barium stearate films is not known, these figures suggest that the chains in the transferred layers on chromium are not quite vertical. The tilt has been taken into account in the values 44.0 AU assumed for the double molecule of barium palmitate and 53.6 (*q.v.*) for cadmium arachidate. These figures are subject to slight revision when more direct measurements of thickness become available. The refractive index, 1.5, used in calculating the theoretical curves, is the effective value for the angle of incidence, 70°, calculated from n_1 and n_3, the refractive indices of the birefringent film as measured by Blodgett and Langmuir.[5]

Skeleton Films of Cadmium Arachidate. Films of cadmium arachidate-arachidic acid on chromium showed the same behavior in relation to the theoretical curves as barium stearate and barium palmitate (FIGURE 4), although the films were more erratic in their optical properties. When the mixed films were converted by the action of a solvent to skeleton films of the metallic arachidate, $\Delta - \Delta_0$ and $\tan \psi/\tan \psi_0$ changed to values characteristic of much thinner continuous films. This effect is predicted by the theoretical equations. The curves for films of refractive index 1.23, the figure given by Blodgett[4] for skeleton films prepared by her method, are shown in FIGURE 4 for comparison with the experimental points. The changes are somewhat greater than those anticipated on theoretical grounds, and are more marked in the case of the thinner films.

Treatment of skeleton films with Nujol restored their optical properties to those of the original continuous films, except in the case of plates covered with only two monolayers, which seemed to be removed completely by the briefest contact with acetone. With this exception, therefore, it seems that the exaggerated effects of the solvent upon the thinner films cannot be explained by detachment of entire monolayers from the upper surface, but must be due to removal of cadmium arachidate or residual amounts of the free acid from the body of the film. Observations on thicker films suggest, however, that this process does not occur uniformly throughout the depth of the film, since prolonged immersion in solvent does result in a decrease in the measured thickness of the Nujol-filled skeleton (bibliographical reference 5, page 980).

A Semi-Empirical Linear Relationship Based on Lucy's Equations. Lucy's equations lead to a simple expression involving $(\Delta - \Delta_0)$ and $\tan \psi/\tan \psi_0$ as a linear function of L and $(n^2 - 1)$:

$$[\cos(\Delta - \Delta_0) + k' \sin(\Delta - \Delta_0)]\cdot \tan \psi/\tan \psi_0 = k''L(n^2 - 1) - 1 \quad (6)$$

In this equation,

$$k^2 = [(\alpha^2 - \beta^2)s + 2\alpha\beta r]/[(\beta^2 - \alpha^2)r - 2\alpha\beta s] \quad (7)$$

$$k'' = \frac{4\pi}{\lambda}\cdot \sin \varphi \tan \varphi \cdot \beta(\beta^2 + \alpha^2)/[(\beta^2 - \alpha^2)r - 2\alpha\beta s] \quad (8)$$

The symbols have the definitions given for equation 5. Under the conditions of our experiments, k', by equation 7, should be 0.354. A plot of the data for barium stearate, using this value, gives the upper curve in FIGURE 5.

The value of k' can be adjusted empirically to give a straight line for films up to 400 AU thick. The best value of k' is unity, the slope of the straight line, k'', being about one order of magnitude larger than that defined by equation 8.

The same line fits the data for cadmium arachidate (FIGURE 6) and the same value of k' (unity) is applicable to the skeleton films, as shown by the upper line in FIGURE 6, which is consistent with the experimental points up to 800 AU. Comparing the slope of this line with that obtained for the continuous films of cadmium arachidate-arachidic acid, 1.25 is derived as the refractive index of the skeleton films, in good agreement with the value of 1.23, calculated by Blodgett[4] for films from which one half of the substance has been dissolved.

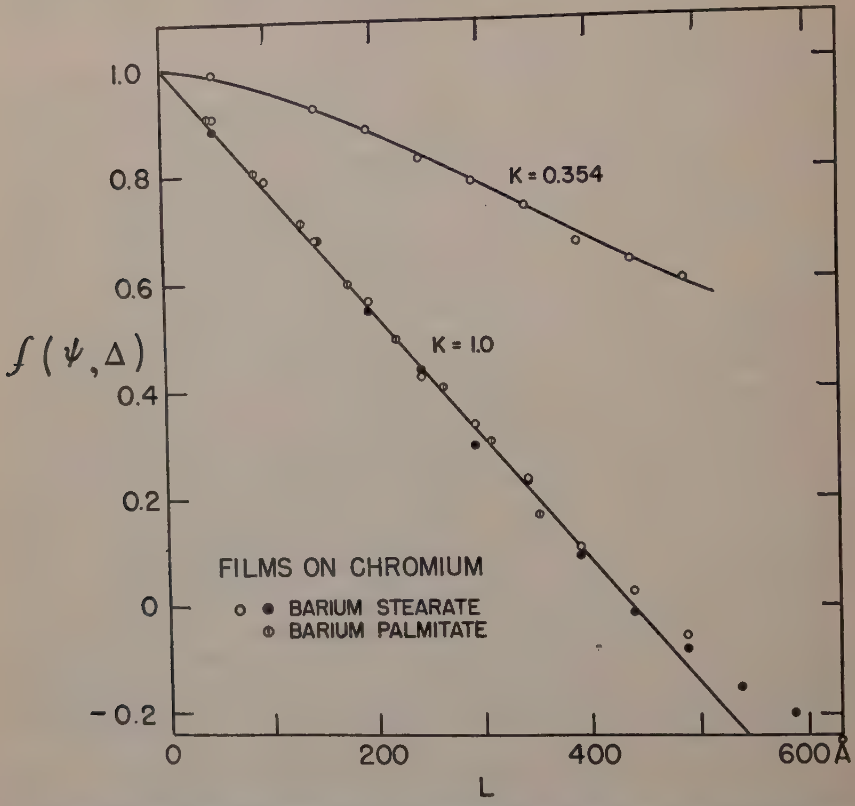

FIGURE 5. Test of equation 6 based upon Lucy's approximation: Upper curve: values of $f(\psi, \Delta)$, using k, calculated from the theoretical equation. Lower curve: empirical version of equation 6 using $k' = 1.0$. The experimental data are the same as those plotted in FIGURE 3.

Measurement of Thickness and Refractive Index of Thin Films. For films of known refractive index around 1.5, measurement of $(\Delta - \Delta_0)$, followed by application of Drude's or Lucy's approximate equations, will permit good estimates of film thickness, if less than 100 AU. When it is between 100 and 200 AU, Lucy's equation is more reliable. In the particular case under consideration ($n = 1.5$), greater accuracy can be achieved empirically, since it is easy to carry out a calibration with barium stearate layers. It is then unnecessary to determine absolute extinction positions or to calculate $\Delta - \Delta_0$. The elegant half-shade method developed by Rothen[11] can be used. In other instances, when the refractive index of the film can be determined by independent methods and is known to differ appreciably from 1.5, the range of usefulness of the two equations is not immediately apparent from the present measurements. It can be safely said, however, (see FIGURE 1) that both equations can be applied to increasingly thick films as the refractive index is decreased.

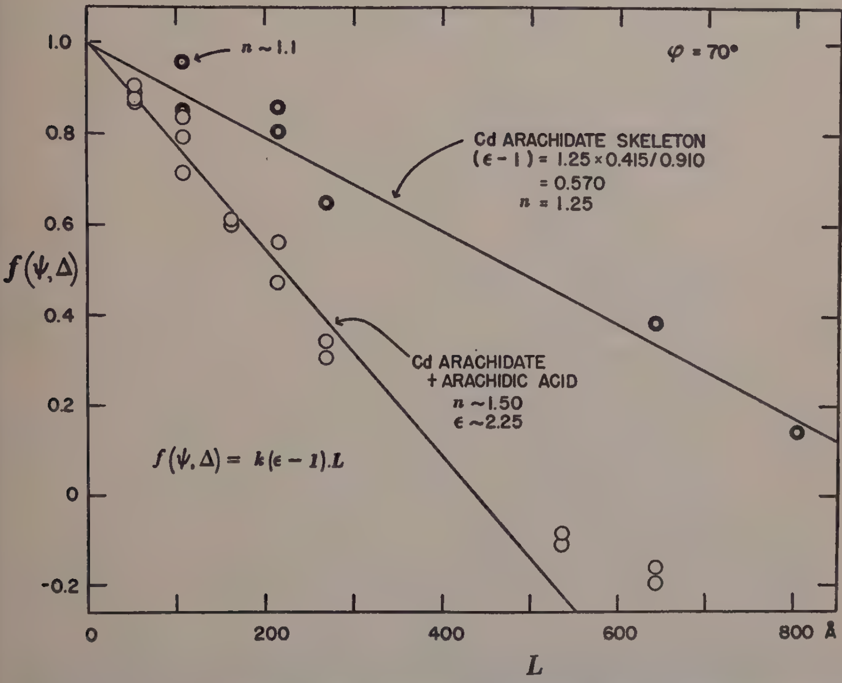

FIGURE 6. Test of the empirical version of equation 6 with experimental data for mixed continuous films of arachidic acid-cadmium arachidate (light circles) and for films of cadmium arachidate produced by skeletonizing the mixed films with acetone (heavy circles). In each case, the value $k' = 1.0$ was used in calculating $f(\psi, \Delta)$. The lower straight line is the same as that shown in the lower portion of FIGURE 5. The upper line was drawn by inspection through the heavy circles. The experimental data are the same as those plotted in FIGURE 4.

Measurements of $\tan \psi/\tan \psi_0$ are of little use in determining film thickness by use of the theoretical equations. The failure of the equations to describe correctly the course of change of $\tan \psi/\tan \psi_0$ implies also that they cannot be used for the simultaneous calculation of film thickness and refractive index, nor are empirical methods of much value in this connection, since the relationship between $\Delta - \Delta_0$ and $\tan \psi/\tan \psi_0$ is very insensitive to changes of refractive index in the range from 1.0 to 1.5. This was suggested by the curves in FIGURE 1 and is evident in the data plotted in the bottom section of FIGURE 4.

In some applications of the optical study of thin films, the film thickness is known or can be determined by an independent method. The success of equation 6, in its empirical form, in describing the behavior of both continuous and skeletonized films, suggests the possibility that this equation will be useful in measurements of refractive index. We hope to test its validity for condensed films of highly refracting substances.

Thick Films of Barium Stearate (up to 1000 AU). The progressive increase in ellipticity of the light reflected from filmed chromium plates with increasing film thickness is illustrated in FIGURE 2, together with the changes in the compensator and analyzer azimuth settings at which the ellipses are compensated, and the corresponding values of Δ and tan ψ. The curves draw attention to the fact that the sensitivity of the azimuth readings to small increments in thickness increases gradually up to a total thickness of about 300 AU, remains roughly constant thereafter, until, at approximately 700 AU, it starts increasing sharply toward the point (800 AU) at which the reflected light becomes circularly polarized. The readings are then indeterminate, and, in a zone on either side of this point, the high sensitivity is offset by the poor definition of the intensity minima, so that the azimuth readings are subject to considerable error. Beyond this zone, for films more than 900 AU thick, is a region (see also FIGURE 7) in which great sensitivity of the phase and amplitude parameters to small changes in thickness is asso-

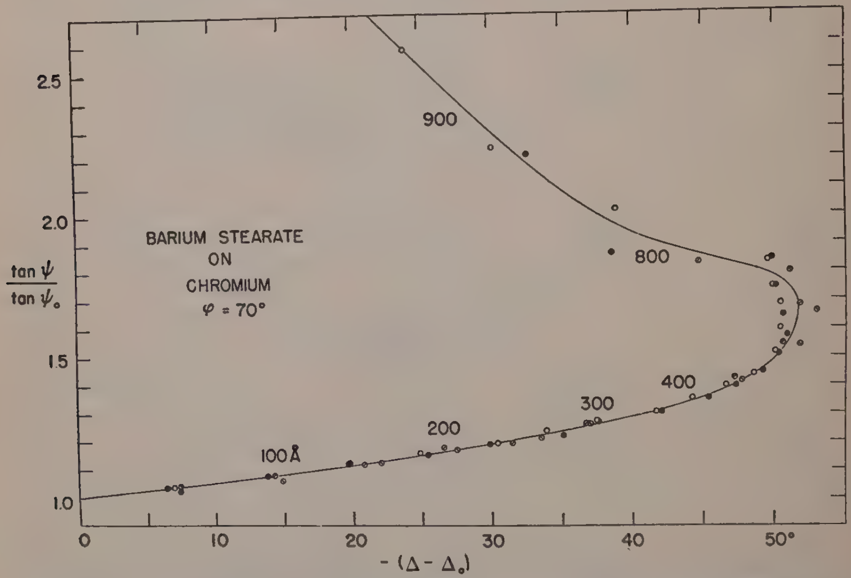

FIGURE 7. Thick films of barium stearate on chromium: *cf.* bottom section of FIGURE 3, which is identical to the initial part of this figure. Here the results of extending the observations to film thickness 900 AU are plotted. The continuous line was drawn through the experimental points by inspection. Film thickness is indicated by numerals on diagram. See text.

ciated with conditions which enable precise adjustments of the instrument to be made. Rothen[13] has indicated this region as one in which thickness increments of 0.1 AU might easily be detected.

Thick Skeleton Films: Measurement of Refractive Index of Thick Films. The minimum value of Δ occurs in the case of barium stearate films at a thickness of about 600 AU and is about 80°, corresponding to $-50°$ for $\Delta - \Delta_0$. At this point, $\tan \psi/\tan \psi_0$ is about 1.65. Since the rise of $\tan \psi/\tan \psi_0$ is continuous, the relationship between the two parameters takes the form shown in FIGURE 7. Essentially the same result was obtained for cadmium arachidate (FIGURE 8). When the arachidate films were skeletonized, it was found that the minimum value of $\Delta - \Delta_0$ was only $-40°$. It occurred when the film thickness was about 800 AU and $\tan \psi/\tan \psi_0$ was 1.4. Up to this point, the curves of $\Delta - \Delta_0$ against $\tan \psi/\tan \psi_0$ for the continuous and the skeleton films had been indistinguishable within the limits of experimental error; thereafter, they diverged (FIGURE 8). Thus, the regions of great sensitivity to changes in film thickness are also characterized by a greatly increased dependence of the phase-amplitude relationship upon film refractive index. A single experimental observation upon a film represented by a point situated anywhere in the upper third of FIGURE 8 should therefore be sufficient to define both L and n. The accuracy attainable remains to be determined.

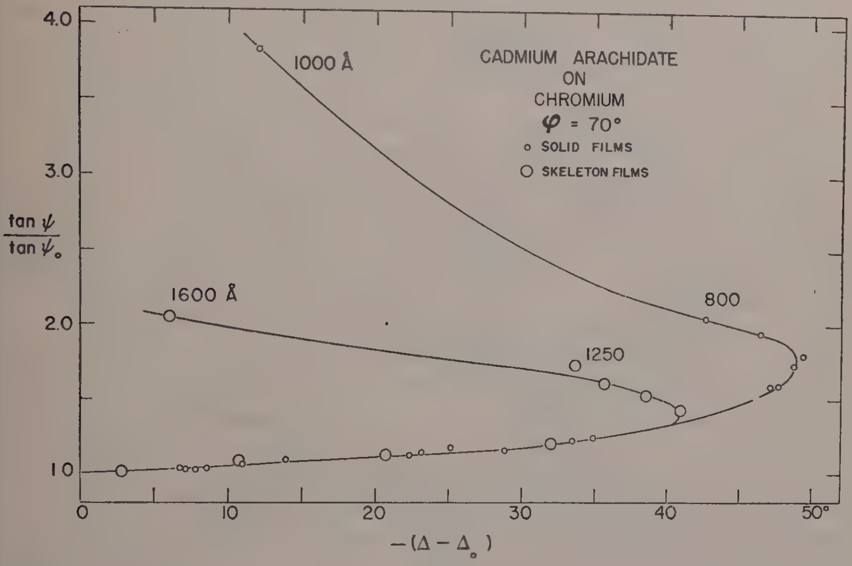

FIGURE 8. Effect of film refractive index on optical behavior of thick films on chromium. The initial portion of this diagram is the same as the bottom part of FIGURE 4. Here the results of extending the observations to thicker films are plotted. Film thickness is indicated by numerals on diagram. See text.

In order to define the limits within which measurement of thickness and refractive index can be made, observations on both continuous and skeletonized cadmium arachidate films have been extended to the point at which the optical distance traversed in the film by light reflected from the film-coated chromium base is about one wavelength. This completes in rough outline a picture of the changes which can be brought about by the presence of non-absorbing films on chromium, except for the effects of birefringence, which have been neglected (*cf.* Rothen[13]). The cyclic nature of the changes can be indicated by plotting tan ψ exp$\cdot(i\Delta)$, as in FIGURE 9.

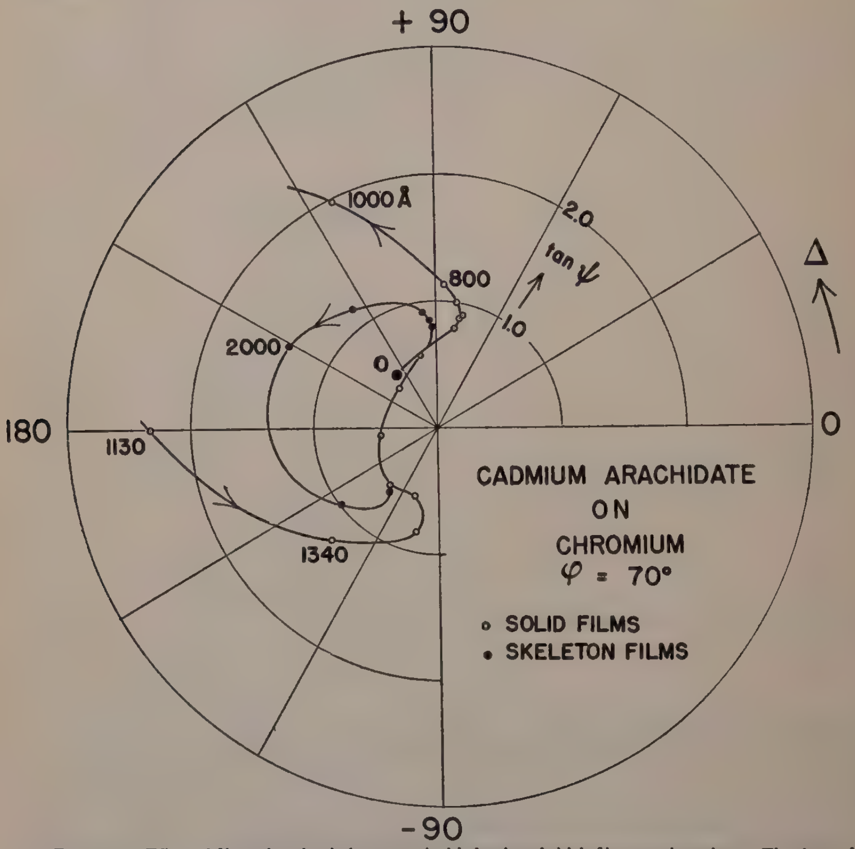

FIGURE 9. Effect of film refractive index on optical behavior of thick films on chromium. The data of FIGURE 8 are extended to include one complete optical cycle. This is represented here by plotting tan $\psi\cdot$exp(i Δ), the origin for clean chromium being at the point O.

It is clear from FIGURE 9 that, for each refractive index value, there will be a definite range of film thickness appropriate for measurement of L and n. Each cycle consists characteristically of a portion common to all films, whatever their refractive index, and an outer arc which shifts with changes in film refractive index. In order to be useful from the present point of view, experimental points must lie in the outer zone. Delimitation of the zones with a view to the setting up of experimental conditions suitable for the optical measurement of particular types of film is much to be desired but scarcely attainable at present with the calibration methods used in this investigation. Diagrams of tan ψ exp $(i\Delta)$ should be available for several values of n, and they should be traversed by lines of equal film thickness to facilitate interpolation. Calculation of theoretical curves from the generalized Fresnel equation (Winterbottom[17]) has been shown by Mr. R. Hartman to give results which are more closely in accord with our experimental data for thin films than the approximate algebraic formulations considered on page 1065; the remainder of the cycle is also correctly reproduced. It is anticipated, therefore, that theoretical calculation will provide an adequate basis for the construction of calibration curves covering a wide range of film characteristics.

Characterization of Double or Laminated Films. The foregoing considerations indicate that the problem outlined on page 1064 can be solved within certain clearly defined limits by polarization optical methods. A single experimental point, suitably placed, is open to an interpretation in terms of film thickness and refractive index which is free of ambiguity, provided the film is known to be optically homogeneous. This is not always the case. Particular interest attaches to the deposition of one film upon another, the optical properties of which may differ considerably from those of the first. The ambiguity which arises when the second film is characterized merely in terms of an "optical," or apparent, thickness has been considered previously[1] in connection with the interference method.[3] The ambiguity exists equally in studies made hitherto by the polarimetric method.[11, 12] It is clear qualitatively from an inspection of FIGURE 9 that in the "outer" zone a sudden change in the refractive index of the film during its gradual increase of thickness will bring about a deviation from the loop characteristic of the material constituting the initial layers and that, if a sufficient amount of the second substance is added, the new curve will gradually approach the closed curve characteristic of films consisting only of this second substance. Vašíček[16] has reduced the mathematics of the laminated film problem to that of a single film. A study by this method is being carried out, together with measurements on heterogeneous films.

Summary

The effects of thin films of proteins and other substances upon the optical properties of polished metals afford a valuable means of studying the molecular characteristics and interactions of such substances. As a preliminary to biophysical studies of this kind, we have investigated the possibilities of the optical method by determining the behavior of multilayers of aliphatic acids deposited upon metal surfaces. These films provide an opportunity for testing the validity of the various approximate theoretical formulations which are available.

Glass slides coated with chromium are examined in a polarizing assembly suitable for the measurement of elliptically polarized light. The desired number of paired aliphatic acid monolayers is then transferred to the slide and the polarimetric measurement repeated.

The relationship between the parameters of the elliptically polarized

reflected light and film thickness has been determined experimentally for barium stearate and cadmium arachidate multilayers (refractive index 1.5) and for skeletonized cadmium arachidate (refractive index 1.2–1.3). The following conclusions have been drawn:

A. The Drude approximate equations represent adequately the limiting slopes of the curves showing the changes of the phase parameter Δ and the amplitude parameter $\tan \psi$ with increasing film thickness. Significant deviations from the Drude curves become apparent in the case of $\tan \psi$ for films 50 AU thick and when the thickness exceeds 100 AU in the case of Δ.

B. The equations given by F. A. Lucy predict correctly that these deviations are in quantitative agreement with our data for Δ. In the case of $\tan \psi$, they represent an over-correction.

C. The Lucy equations imply a certain linear relationship (see equation 6). The experimental data show a similar linearity but the constants of the empirical equation are not those predicted by the theory.

D. Although the measurement of Δ and $\tan \psi$ enables film thickness and refractive index to be determined in principle, the experimental data on films less than 600 AU thick show these quantities to be so insensitive to changes in refractive index that reliable values are not to be expected with present methods.

E. When film thickness is comparable to wavelength, Δ and $\tan \psi$ undergo cyclic changes. In a certain portion of each cycle, the values become very sensitive both to thickness and to refractive index. It is possible to define the circumstances under which this fact can be utilized in the optical study of films by extending the experimental calibration curves with the aid of theoretical curves derived from the generalized Fresnel equations.

Acknowledgment is due to Miss Helen Woods for preparing the chromium-plated slides used in this investigation, to Mr. Richard Hartman for taking part in the work in its final stages, and to Mr. John T. Quynn for design of parts of the polarizing assembly.

Bibliography

1. Bateman, J. B., H. E. Calkins, & L. A. Chambers. 1941. Optical study of the reaction between transferred monolayers of Lancefield's "M" substance and various antisera. J. Immunol. **41:** 321–341.
2. Blodgett, K. B. 1935. Films built by depositing successive monomolecular layers on a solid surface. J. Am. Chem. Soc. **57:** 1007–1022.
3. Blodgett, K. B. 1937. Properties of built-up films of barium stearate. J. phys. Chem. **41:** 975–984.
4. Blodgett, K. B. 1939. Use of interference to extinguish reflection of light from glass. Phys. Rev. **55:** 391–404.
5. Blodgett, K. B. & I. Langmuir. 1937. Built-up films of barium stearate and their optical properties. Phys. Rev. **51:** 964–982.
6. Drude, P. 1888. Beobachtungen ueber die Reflexion des Lichtes an Antimonglanz. Ann. Physik, Neue Folge **36:** 489–531.
7. Drude, P. 1889. Ueber Oberflaechenschichten. I. Ann. Physik, Neue Folge **36:** 532–566.
8. Drude, P. 1889. Ueber Oberflaechenschichten. II. Ann. Physik, Neue Folge **36:** 865–897.
9. Drude, P. 1902. The Theory of Optics. Longmans. Green. New York.

10. Lucy, F. A. 1948. Studies of surface films by reflection of polarized light. I. A more rigorous algebraic method for computing results. J. Chem. Phys. **16:** 167–174.
11. Rothen, A. 1945. The ellipsometer, an apparatus to measure thicknesses of thin surface films. Rev. Sci. Instr. **16:** 26–30.
12. Rothen, A. 1947. Immunological reactions between films of antigen and antibody molecules. J. Biol. Chem. **168:** 75–97.
13. Rothen, A. 1949. Optical properties of surface films. II. Rev. Sci. Instr. **20:** 66–72.
14. Schoon, T. 1938. Polymorphe Formen kristalliner Kohlenstoffverbindugen mit langen gestreckten Ketten (nach Strukturuntersuchungen durch Elektronenbeugung). Z. phys. Chem. **39B:** 385–410; 1938. Strukturber. **6:** 238–240.
15. Thiessen, P. A. & J. Stauff. 1936. Feinbau und Umwandlungen kristallisierte Alkalisalze langkettiger Fettsaeuren. Z. phys. Chem. **176A:** 397–429; 1936. Strukturber. **4:** 288–290.
16. Vašíček, A. 1947. The reflection of light from glass with double and multiple films. J. Opt. Soc. Am. **37:** 623–634.
17. Winterbottom, A. B. 1946. Optical methods of studying films on reflecting bases depending on polarization and interference phenomena. Trans. Farad. Soc. **42:** 487–495.

GONIOMETRIC ANALYSIS OF CRYSTALS

By J. D. H. Donnay
The Johns Hopkins University, Baltimore, Maryland

The methods of goniometric analysis can cope with problems of both determination and identification. The latter consists in checking a hypothesis as to the nature of a crystal (question: "Is X really A?"), the former, in finding what it is without any preconceived idea as to its composition, (question: "What is X?"). In either case, the first step is to obtain determinative data in the form of measured angles.

Several kinds of angles can be measured. The most common one has long been the interfacial angle, usually defined as the supplement of the true dihedral angle between two faces. It is equal to the angle between the two face-normals. In present day practice, the coordinate angles of a face are widely used. They are defined as follows: Imagine the crystal placed inside a sphere of arbitrary radius, with a vertical set of parallel edges or, using geographical language, in the north-south direction. Then, from the center of the sphere, drop a perpendicular onto each face and produce it until it meets the surface of the sphere. The sphere is thus covered with an array of face-poles, the points where the face-normals puncture the sphere. The geographical coordinates (longitude φ and colatitude or polar distance ρ) of a face-pole are the coordinate angles of the corresponding face.

In addition to faces, edges also yield angles. Since a zone is defined as the assemblage of faces parallel to a given edge, the (plane) angle between two edges is an interzonal angle. The inter-edge angle between two edges lying in a face is usually measured in such a way that the face is comprised between the sides of the angle. The interzonal angle is then defined as the supplement of the inter-edge angle.

The type of angles used depends on the kind of crystals to be measured and the equipment at hand.

Obtaining the Data

For large crystals (say, one cm. across or more) with rough or nonreflecting faces, interfacial or interzonal angles can be measured by contact goniometry with an accuracy that rarely attains the half-degree. A contact goniometer is nothing more than a 180° protractor with a moving arm pivoting about the center. The edge of the protractor and the edge of the arm are applied to the angle to be measured. The method is crude and is resorted to only when other methods fail.

If the crystal faces reflect light properly, a crystal, large or small, can be measured on an optical goniometer. Angles are measured with an accuracy of a few minutes, or even a half-minute in exceptional cases. The one-circle goniometer yields interfacial angles, requiring a different setting of the crystal for each zone to be measured. The two-circle goniometer gives the coordinate angles of each face, one setting of the crystal usually being sufficient. This advantage is such that the two-circle instrument has generally supplanted the one-circle model. The techniques of crystal goniometry, measurements and calculations, are readily available from a number of sources.[1-6]

Until recently, the chief obstacle to the use of goniometric methods of crystal analysis had been that goniometers were not commonly available, particularly in this country. This difficulty no longer exists, inasmuch as several firms, since 1946, have built and marketed new two-circle goniometers (L. C. Eichner, Bloomfield, N. J.; Laboratory Associates, Belmont, Mass.[7]; Unicam, Cambridge, England). An interesting improvement of the instrument has been proposed by Terpstra.[8] He places the optical axes of the collimator and telescope in a vertical plane (perpendicular to the horizontal circle), although these two optical axes were horizontal in previous designs. Since the arm that carries the vertical circle swings around the (vertical) axis of the horizontal circle, the Terpstra set-up allows a considerably greater range to the swinging motion.

For small or very small crystals, and for fragments of crystals, with few faces or no face at all, X-ray goniometry, by means of the Weissenberg instrument, for instance, is indicated. This method yields absolute length measurements in addition to angular data. The equipment has become popular, owing to the introduction of the equi-inclination model, designed by M. J. Buerger[9] and manufactured by several firms (Otto von der Heyde, Cambridge, Mass.; Charles Supper, Newton, Mass.; Unicam, Cambridge, England). The crystal carrier of the two-circle optical goniometer should be interchangeable with that of the Weissenberg X-ray goniometer, and this specification is met by the manufacturers mentioned here.

Finally, very small crystals (say, smaller than 0.1 mm.) can be investigated by the methods of microscope goniometry,[10] in which angles are measured by means of the rotating stage of the microscope. Angles between edges (interzonal angles) are measured, either in true value, if the edges lie parallel to the stage of the microscope, or as projected angles, if at least one of the two edges including the angle is oblique to the stage. Projected, as well as true, interzonal angles can be used to solve the crystallographic problem. No special equipment is needed, beyond a microscope with a graduated rotating stage. The accuracy of angular measurements is low, one-third or one-half of a degree. Nevertheless, microscope goniometry is a useful technique that should not be overlooked when a non-destructive method of analysis is a prerequisite.

Using the Data for Determination

It is obvious, of course, that goniometric methods are not designed for the quantitative analysis of mixtures. They can identify only pure chemical compounds occurring as crystals.

Determinative tables in which unknown crystals can be looked up must be used in conjunction with goniometric analysis. The chief problem in the compilation of such tables lies in the choice of the determinative criteria. Either measured values or values calculated from measurements can be used.

The Boldyrev method[11] aims at avoiding all calculations. The crystal angles are measured and looked up as such in an index. No special orientation needs to be figured out. As Haan[12] puts it, the Boldyrev determinative method is crystallographic only in its aim; in essence, it is "purely administrative." The Boldyrev index had not been completed at the time of Boldyrev's death (1946). Only part of it, the section dealing with the tetragonal crystal system, has been published.[13]

Boldyrev's efforts were an attempt at simplifying the determinative method of his master, Fedorov.[14] The celebrated Fedorov index, Das Krystallreich, was completed in 1920. The determinative procedure rests on a proper choice of crystal setting. In Fedorov's mind, the "correct" setting should have structural significance. Essentially, the measured angles (the interfacial angles, for instance) are used to determine the shape of the unit cell. In the most general case, that of a triclinic crystal, five independent angles are necessary and sufficient to calculate the axial elements, namely, the angles between the cell edges (interaxial angles α, β, γ) and the ratios of the lengths of the cell edges to one another (axial ratios $a:b$ and $c:b$). The choice of the axes of coordinates, parallel to edges or possible edges of the crystal, and the choice of the parametral face (or unit face) intersecting all three axes, however, must be governed by a set of rules in order that the unit cell be uniquely determined. It was Fedorov's aim to determine a unit cell that would be similar in shape to the structural unit cell. His rules, based on the classical law of Bravais, were inadequate to solve his structural problem. In so far as uniquely defining a unit cell, however, they were satisfactory, though complicated.[15]

Another, more successful, attempt at simplifying the procedure of crystal determination from angular measurements is that of Barker.[16] In the Barker method, axial elements need not be calculated; angular values are used as determinative criteria. A unique setting of the crystal, however, even though devoid of structural significance, is a prerequisite. It is obtained by applying a number of conventional rules designed for the purpose. Angles between faces with simplest Miller indices (*i.e.*, 0's and 1's) are measured if possible, or, if not, are calculated from other measured angles. The determinative angle in the orthorhombic system, for instance, is the angle $a(100):m(110)$, which is equal to arctan (a/b). It is convenient to be able to look up the angle, rather than its tangent, in the determinative table. The details of the method and references to the literature have been given elsewhere[17]; they can, therefore, be omitted at this point.

After Barker's death (1930), the compilation of his index was continued at Oxford University under the editorship of R. C. Spiller and Mary W. Porter, with the collaboration of a number of crystallographers. The first volume of the index covers all crystal systems, other than monoclinic or triclinic, and it should appear in the very near future. It will contain approximately 3,300 substances. An introduction (by M. H. Hey) will give a full description of the Barker method and the use of the tables. Work on the second volume of the Barker Index is being actively carried on.

Whereas the classical law of Bravais and the Fedorov principles that stemmed from it were not powerful enough to determine the structural unit cell, present-day methods of X-ray diffraction can solve this problem in a straightforward way, and the method of morphological analysis,[18, 19, 20] based on the generalized law of Bravais,[21, 22] although not foolproof, leads to the structural unit cell (and space group) in the vast majority of cases. Moreover, the conventional rules governing the orientation of the unit cell have been revised,[23, 24] so that it is now possible to use the structural unit cell for determinative purposes.

With the help of several co-workers, I have for some years been compiling goniometric data in the form of axial ratios and interaxial angles. The determinative property is the axial ratio a/b, in the conventional setting. In the index now in preparation, other axial elements are also listed, together with absolute lengths of the cell edges (whenever they are known from X-ray results), space group, and specific gravity. When complete, such an index will make it possible to determine a crystal from either relative or absolute unit-cell dimensions.

No matter which index is used, its rôle in the determinative procedure is simply to restrict the number of possible hypotheses. In most cases, the determination of a crystal must be checked by means of an additional test, chemical, optical, *etc.* A combination of several methods is often fruitful. Optical goniometry combined with an X-ray powder pattern, for example, will yield the absolute dimensions of the unit cell. The latter, combined with a specific gravity determination, gives the weight of the cell, from which the molecular weight or a simple multiple of it can be calculated.

Conclusion

As compared with other methods of analysis, crystal goniometry occupies a place of its own. It cannot be expected to be universally applicable, but it will succeed in special cases in which other methods would fail. An example of such a case is that of a pseudomorphous crystal, resulting from the alteration or replacement of a pre-existing crystal of a different chemical composition, whose external form is preserved. The destroyed crystal can still be identified. Crystals containing inclusions (as mechanical admixtures) can be determined by goniometry, since these inclusions do not affect the crystal form. Other advantages of goniometric analysis are fairly obvious: the method is non-destructive; only a very small amount of material is required (a crystal, a fraction of one mm. in its longest dimension will suffice); the determinative data can be obtained in a number of different ways, so that various kinds of equipment can be used; the method is usually fairly rapid (from about fifteen minutes to a few hours); and its specificity is very satisfactory, except in cases of solid solution (mixed crystals of similar compositions have similar angles) and homeomorphism (crystals of different compositions but related crystal structures may show some similarities in their angles).

Goniometric analysis can compete with the X-ray powder method of determination in dealing with crystals of organic compounds, which are apt to have large unit cells and low symmetry, and therefore give powder patterns characterized by a great many closely-spaced diffraction lines.

One limitation of goniometric analysis is its inability to cope with crystals of the isometric (cubic) crystal system, in which the angle between two faces with given Miller symbols is the same, regardless of chemical composition. Even in such cases, however, goniometry is useful, as it enables one to identify the crystal forms (and possibly the space group), which in themselves are of determinative value.

Bibliography

1. Tutton, A. E. H. 1943. Crystallography and Practical Crystal Measurement. 2 Vols. Macmillan and Co. New York, N. Y.
2. Palache, C. 1920. The two-circle goniometer. Am. Mineral. **5:** 23–33; see also: *Ibid.* 67–80, 89–99, 112–120, 129–133, 143–152, 158–166, 173–182, 185–194, 198–208.
3. Terpstra, P. 1931. Kristalmeting als hulpmiddel in de scheikunde. Chemisch Weekblad **28:** 275–277.
4. Terpstra, P. 1938. Simple instructions for crystal measurement with a new model of the two-circle goniometer, especially adapted to the use in chemical laboratories. Rec. Trav. Chim. Pays-Bas **57:** 893–904.
5. Wolfe, C. W. 1941. Crystallographic procedures. Am. Mineral. **26:** 55–91.
6. Peacock, M. A. 1945. Determination of Crystal Form. Chapter XII, "Physical Methods of Organic Chemistry." Interscience. **1:** A. Weissberger, editor.
7. Wolfe, C. W. 1948. A new two-circle goniometer. Am. Mineral. **33:** 739–743.
8. Terpstra, P. Kristallometrie, p. 328. J. B. Wolters. Groningen, Batavia.
9. Buerger, M. J. 1942. X-ray Crystallography. Wiley. New York.
10. Donnay, J. D. H. & W. A. O'Brien. 1945. Microscope goniometry. Ind. Eng. Chem., Anal. Ed. **17:** 593–597.
11. Boldyrev, A. K. 1925. Principe de la nouvelle méthode de diagnose cristallographique de la matière. Mém. Soc. russe Min. **53:** 251–342. (Russian text, French summary).
12. Haan, J. H. 1932. Kristallometrische determineeringsmethoden, 178 pages. J. B. Wolters, Groningen. (Dutch text, German summary.)
13. Boldyrev, A. K. & W. W. Doliwo-Dobrowolsky. 1937. Bestimmungstabellen für Kristalle. Band I. Erste Hälfte. Einleitung. Tetragyrische Syngonie, 438 pp. Zentrales wissenschaftliches Institut der Geologie und Schürfung, Leningrad, Moscow. (Russian text, German translation of introduction.)
14. Fedorov, E. S. 1920. Das Krystallreich, Tabellen zur krystallochemischen Analyse, Mém. Acad. Sc. Russie (8), **36.** See also Zs. f. Kryst. **50:** 513. 1912.
15. Boldyrev, A. K. 1926. Kommentarii k rabote E. S. Fedorova, Das Krystallreich. Acad. Leningrad.
16. Barker, T. V. 1930. Systematic Crystallography. An essay on crystal description, classification and identification. xi + 115 pp., 76 figs. Thomas Murby and Co. London.
17. Donnay, J. D. H. 1945. Crystallo-chemical analysis, Chapter XIII, Physical Methods of Organic Chemistry. **1:** 561–583. A. Weissberger, editor. Interscience. New York; 1949. *Ibid.* 2nd Ed. **1:** 1017–1039. Chapter XVII.
    Porter, M. W. & R. C. Spiller. 1939. Crystallo-chemical analysis, the Barker Index at Oxford. Nature **144:** 298.
    Bannister, F. A. 1946. Physical methods for the identification of materials. Nature **157:** 234. Also Jour. Sci. Instruments **23:** (2), 1946.
18. Donnay, J. D. H. 1938. Le développement des zones cristallines. Ann. Soc. géol Belgique. **61** (B): 260–287.
19. Donnay, J. D. H. 1938. Crystal space-groups determined without X rays. Abtract, Am. Mineral. **23** (12, 2): 5; **24:** 184, 1939.
20. Donnay, J. D. H. 1946. La détermination du groupe spatial par les données morphologiques (avec bibliographie). Bull. Soc. fr. Min. **69:** 151–155, 1947.
21. Donnay, J. D. H. & D. Harker. 1937. Généralisation de la loi de Bravais. C. R. Ac. Sc. Paris **204:** 274–276.
22. Donnay, J. D. H. & D. Harker. 1937. A new law of crystal morphology extending the law of Bravais. Am. Mineral. **22:** (Palache volume) 446–467.
23. Donnay, J. D. H. 1943. Rules for the conventional orientation of crystals. Am. Mineral. **28:** 313–328 and 470.
24. Donnay, J. D. H. 1943. Resetting a triclinic unit-cell in the conventional orientation. Am. Mineral. **28:** 507–511.

QUANTITATIVE ANALYSIS BY MEANS OF CATALYTIC HYDROGENATION REACTIONS*

By E. C. Dunlop

Experimental Station, E. I. du Pont de Nemours and Company, Inc.,
Wilmington, Delaware

The analytical chemist of today makes use of many different properties of a material in order to characterize it as completely as possible. For example, some chemicals, such as unsaturated organic compounds, will react with gaseous hydrogen, under specified conditions, with a resulting loss in gas volume which can be measured. Such measurement permits quantitative analysis by means of catalytic hydrogenation reactions. Just as is the case with many of the techniques used by the analyst today, catalytic hydrogenation data require skillful interpretation and are sometimes useful only when interpreted along with other data obtained by separate techniques.

It has been known for a long time that unsaturated organic molecules could be hydrogenated in the presence of a catalyst and under certain specified conditions. This property, however, has been used only recently as an analytical tool. A number of papers have been published describing the apparatus and techniques used in carrying out the reaction. To mention some of these, articles by Prater and Haagen-Smit,[1] Johns and Seiferle,[2] Shriner,[3] Hallet,[4] Noller and Barusch,[5] and Joshel,[6] have appeared.

Apparatus

We have studied these various types of apparatus and have constructed similar but modified equipment. FIGURE 1 shows a diagram of our present equipment. This equipment is more closely related to that described by Lloyd M. Joshel[6] than to any of the others.

Interesting points about the equipment are listed below. The primary modifications which we have made are described in sections three and five.

1. The stopcocks are all oblique bore and Burrell's #2 heavy stopcock grease is used.

2. The reaction flask has a male grind and the buret system the female grind, thus helping to avoid contamination of the reaction flask with stopcock grease.

3. The reaction flask is immersed in a constant temperature bath and the burets are jacketed in order to circulate constant temperature liquids.

4. The connecting tubing is capillary tubing with dimensions of 8 mm. O. D., 3 mm. I. D.

5. The reaction flask has a number of sealed side arms for holding the sample or catalyst so that it can be added to the solvent as needed. The sample or catalyst is placed in a small glass boat which has a piece of iron sealed in one end. The boat is pushed into the flask when desired by means of a solenoid. Additional portions of the sample or catalyst can be added by having several boats in the different side arms.

---

* Contribution No. 265 from the Chemical Department, Experimental Station, E. I. du Pont de Nemours and Company, Inc., Wilmington, Del.

Procedure

We have standardized our procedure and technique, as have others, with the use of maleic acid. A pure sample of maleic acid having a melting point of 130.5°C. was used. This unsaturated dibasic carboxylic acid reacts with hydrogen to give succinic acid, one mole of H_2 per mole of maleic acid being absorbed. In confirmation of previous results reported in the literature, it was found that a sample size of approximately 100 milligrams and ten per cent that amount of catalyst gave the best operating quantities for our apparatus.

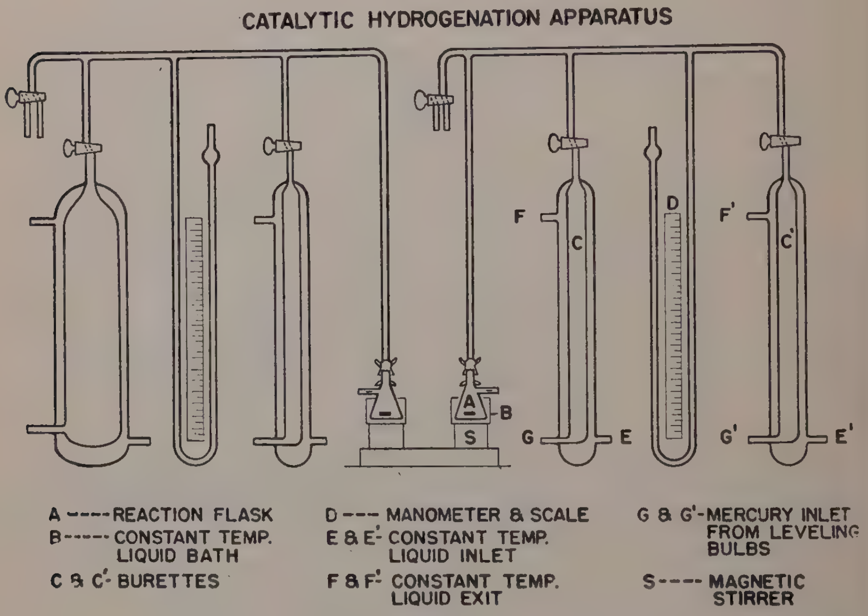
CATALYTIC HYDROGENATION APPARATUS
F
D
F'
C
C'
A
B
S
G
E
G'
E'
A ----REACTION FLASK
B-----CONSTANT TEMP. LIQUID BATH
C & C'- BURETTES
D --- MANOMETER & SCALE
E & E'- CONSTANT TEMP. LIQUID INLET
F & F'- CONSTANT TEMP. LIQUID EXIT
G & G'-MERCURY INLET FROM LEVELING BULBS
S---- MAGNETIC STIRRER

Figure 1.

The procedure adopted for carrying out analyses may be outlined as follows:

The apparatus should be clean and dry, and sufficient mercury should be in the burets and leveling bulbs.

The circulating pump should be turned on to circulate the constant temperature liquid through the buret jackets.

The reaction flask should be clean and dry and a small amount of grease applied to the male grind. Care should be taken to keep the grease from the top of the grind. Ten milligrams of catalyst and 15 milliliters of solvent are placed in the bottom of the flask and a glass enclosed magnet is also inserted. Approximately 100 milligrams of the sample is accurately weighed into the sample boat and placed in one side arm of the flask. The flask is then attached to the apparatus and the grind well seated and attached with spring clamps.

The constant temperature bath is then raised to surround the reaction flask and the magnetic stirrer is turned on. The system is then alternately evacuated and flushed with hydrogen four or five times and finally left filled with hydrogen. The leveling bulbs are adjusted so that the burets read 0.0 milliliter at atmospheric pressure. This is accomplished by venting or adding hydrogen. After taking the initial reading, the boat containing the sample is forced into the reaction flask by the solenoid and a positive pressure of 15–20 centimeters of mercury is applied by raising the leveling bulbs. The barometric pressure is recorded at the beginning and at the end of each determination. Hydrogenation is continued until no further decrease in pressure is noted on the manometer. This usually requires about 1 to 1½ hours. When hydrogenation is apparently complete, the leveling bulbs are adjusted to give atmospheric pressure in the apparatus and the buret reading is taken. The leveling bulbs are again raised to apply pressure of about 15–20 centimeters of mercury on the system for about 10 minutes. The system is then brought to atmospheric pressure and the burets read a second time. If this reading checks the previous one, the reaction is complete and the volume of hydrogen used is converted to standard conditions and the unsaturation value of the sample is calculated.

We have adopted the practice of reporting data in terms of grams of hydrogen per gram of sample. The data are used in several ways and this appears to be the most useful single form for all concerned. We have used the following catalysts: PtO_2, Pd-on-charcoal, nickel catalyst W-6 (Adkins-Billica, 1948), and Baker Colloid 46 (Palladium). We have used the following solvents: methanol, ethanol (95 per cent), ethanol (abs.), water, glacial acetic acid, ethyl acetate, and dioxane.

Results

We will now take up the results which we have obtained.

First, with maleic acid, the following table shows the results obtained with various sizes of samples, different catalysts and different solvents.

TABLE 1 indicates that 95 per cent ethanol, acetic acid, and dioxane solvents give the best results. Also, it may be seen from the table that either platinum oxide or palladium-on-charcoal catalyst can be used satisfactorily.

This has not been an exhaustive study, and it is not intended by these data to prove that the other solvents such as ethyl acetate and water are of no value. The purpose of this experiment has been to find the most satisfactory experimental conditions under which to carry out our analyses.

We have used this apparatus to determine the amount of unsaturation in high vapor pressure samples such as diisobutylene. In this experiment we used ice water in the circulation system, and the results, which check well with the theoretical value, are shown in TABLE 2.

Some work has been done with unsaturated ketones, and it is possible to determine the carbon-carbon unsaturation using platinum oxide or palladium on-charcoal catalyst in 95 per cent ethanol without reducing the carbonyl group. The carbonyl group can be reduced with nickel catalyst, prepared

TABLE 1

HYDROGENATION OF MALEIC ACID

Theory—Grams H_2/g. Sample = 0.017

Sample Wt.-mg.	*Catalyst-mg.*	*Solvent*	*Grams H_2/g. Sample*
100.8	10 PtO_2	Ethanol (95%)	0.017
96.6	10 PtO_2	Acetic acid	0.017
84.7	10 PtO_2	Dioxane	0.017
105.4	10 PtO_2	Methanol	0.016
90.8	10 PtO_2	Ethanol (abs.)	0.018
87.6	10 PtO_2	Ethyl acetate	0.015
85.6	10 PtO_2	Water	0.013
88.4	10 Pd on Charcoal	Acetic acid	0.017
85.0	10 Pd on Charcoal	Dioxane	0.017
85.3	10 Pd on Charcoal	Ethanol (95%)	0.017
	10 Baker Colloid 46	Ethanol (95%)	0.016

TABLE 2

HYDROGENATION OF DIISOBUTYLENE

Theory—Grams H_2/g. Sample = 0.0179

Sample wt.-mg.	*PtO_2 Catalyst wt.-mg.*	*Grams H_2/g. sample*
102.0	11.7	0.0170
86.0	10.0	0.0178
113.6	9.1	0.0168

TABLE 3

HYDROGENATION OF UNSATURATED KETONES

Sample	*Catalyst*	*Solvent*	*Grams H_2/g. sample*	
			Found	*Theory*
Methyl vinyl ketone (A)	Pd-on-charcoal	95% Ethanol	0.0320 0.0310	0.0288 (1C=C)
Acetone	Ni (W-6)	95% Ethanol	0.0338 0.0340	0.0348 (1C=O)
Methyl vinyl ketone (B)	PtO_2	95% Ethanol	0.0240 0.0232	0.0288 (1C=C)
Methy vinlyl ketone (B)	Ni (W-6)	95% Ethanol	0.0455 0.0454	0.0576 (1C=C) (1C=O)

TABLE 4

HYDROGENATION OF STYRENE

Sample	*Catalyst*	*Solvent*	*Grams H_2/g. sample*	
			Found	*Theory*
Styrene B.P. 61°C at 42 mm.	PtO_2	95% Ethanol	0.0186 0.0176	0.0194 1(C=C)
N_d^{25}—1.5439	PtO_2	95% Ethanol + ½ ml. HCl 95% Ethanol + 1 ml. HCl	0.0751 0.0694 0.0752	0.0775 4(C=C)

by the procedure described by H. Adkins and H. R. Billica,[7] in 95 per cent ethanol, which is made slightly alkaline.

TABLE 3 shows data for the reduction of the C═C bond in methyl vinyl ketone, the reduction of the carbonyl group in acetone, and the reduction of both the C═C bond and C═O bond in methyl vinyl ketone.

We obtained results that are close to the theoretical values for the first two samples above. The results for the methyl vinyl ketone sample (B) using PtO_2 catalyst and calculating on the basis of reduction of one C═C bond indicate 81 per cent MVK and using Ni catalyst (W-6) and calculating on the basis of reduction of both the C═C and C═O bonds indicate 78 per cent MVK.

The next experiment under discussion will be the analysis of a sample of cyclooctatetraene. This is an example of how more than one technique is involved in chemical analysis and also shows how intelligent interpretation is required from the analyst to both obtain and report the data. Ultraviolet absorption data were used in conjunction with the hydrogenation results.

The sample reacted with hydrogen in the presence of PtO_2 catalyst in 95 per cent ethanol to absorb 0.075 and 0.076 gram H_2/gram of sample. This corresponds to 97.5 per cent cyclooctatetraene calculated on the basis of four C═C bonds. Ultraviolet absorption data on the original sample indicated the presence of styrene. The absorption spectrum of the reduced sample was similar to that of ethylbenzene and, calculating the concentration of ethylbenzene, based on the absorption coefficient as given by the API (American Petroleum Institute) data for ethylbenzene, we got a value of approximately 5 per cent for the styrene in the original cyclooctatetraene sample.

A known sample of styrene was hydrogenated and the results in TABLE 4 show that the above experiment was correctly interpreted in that only the ethylenic bond was hydrogenated under the conditions used. Also included in TABLE 4 are data for the hydrogenation of the aromatic portion of the styrene. By the addition of acid, we were able to completely hydrogenate the sample of styrene.

Summary

A reaction flask has been described which has sealed side arms used for holding the sample until it is needed. This enables the operation to be carried out in a closed system, eliminating one leak hazard and simplifying the operation. Data have been shown for maleic acid in various solvent and catalyst combinations, and it is indicated that 95 per cent ethanol, acetic acid, and dioxane are excellent solvents with either PtO_2 or Pd-on-charcoal catalyst.

Unsaturated ketones (methyl vinyl ketone) have been analyzed by selectively hydrogenating the C═C and the C═O, using PtO_2 or Pd-on-charcoal catalyst for the C═C and Ni W-6 catalyst for the C═O.

The analysis of a sample of cyclooctatetraene containing some styrene has been made in conjunction with ultraviolet absorption spectrum analysis.

Cyclooctatetraene and the ethylenic group of styrene are hydrogenated in neutral solution with PtO_2 catalyst. The aromatic portion of the sample is hydrogenated along with the ethylenic bond when carried out in acidic alcoholic solution using PtO_2 catalyst.

Acknowledgment. The author wishes to acknowledge the assistance of Mr. R. K. Weaver, Mr. J. W. Robson, and Mr. S. F. Ford in carrying out the experiments and of Mr. Weaver in the development of the apparatus. I also wish to thank Dr. J. W. Stillman for his helpful suggestions.

Bibliography

1. PRATER, A. N. & A. J. HAAGEN-SMIT. 1940. Industrial and Engineering Chemistry. Analytical Edition **12:** 705.
2. JOHNS, I. B. & E. J. SEIFERLE. 1941. Industrial and Engineering Chemistry. Analytical Edition **13:** 841.
3. SHRINER, R. L. Quantitative Analysis of Organic Compounds. Edwards Brothers, Inc. Ann Arbor, Michigan.
4. HALLETT, L. T. 1942. Industrial and Engineering Chemistry. Analytical Edition **14:** 956.
5. NOLLER, C. R. & M. R. BARUSCH. 1942. Industrial and Engineering Chemistry. Analytical Edition **14:** 907.
6. JOSHEL, L. M. 1943. Industrial and Engineering Chemistry. Analytical Edition **15:** 590.
7. ADKINS, H. & H. R. BILLICA. 1948. J. Am. Chem. Soc. **70:** 695.

ANALYSIS OF MIXTURES BASED ON RATES OF REACTION

By T. S. Lee* and I. M. Kolthoff
School of Chemistry, University of Minnesota, Minneapolis, Minnesota

The analysis, by conventional means, of mixtures of two constituents that have similar chemical properties is often difficult or impossible. Mixtures of two organic compounds that contain the same functional group (*e.g.*, two esters or two aldehydes) are frequently encountered and present special difficulties to the analyst. For example, mixtures of homologous organic compounds or of certain ortho- and para-isomers usually cannot be analyzed by classical chemical methods. Methods that depend on physical properties of the compounds are usually not suitable either. In illustration of this point, ultraviolet spectrophotometry cannot be used to analyze a mixture of homologous ketones because the spectrum of each ketone is determined chiefly by the carbonyl group and is affected only slightly by the nature of the alkyl group substituents. Infrared spectrophotometry, which is capable of distinguishing between homologous organic compounds, requires expensive equipment and is frequently not applicable if the sample is available only as a dilute solution in water or in certain other common solvents. (On the other hand, infrared analysis is ideal if the apparatus is available and if the sample is available in a suitable form.)

It frequently happens that such mixtures of organic compounds can be analyzed by a method based on differences in rates of reactions of the components of the mixture with a given reagent. The effect of a substituent on the rate of reaction of a reactive group with a particular reagent is usually pronounced. Propylene, for example, reacts with perbenzoic acid at only one-thirtieth the rate at which 2-butylene reacts (see below). Methyl alcohol reacts with hydrobromic acid nearly six times as rapidly as ethyl alcohol does (solvent phenol, 80°).[1] It should be pointed out, however, that, if the substituents of the functional group are quite similar, as for example, *n*-butyl and *n*-amyl, the method of analysis based on reaction rate cannot be applied. Furthermore, the method is generally limited to mixtures of two components.

Highly specific methods for the analysis of mixtures based on rates of reaction have been described previously in the literature.[2–7] Most of these methods were developed for the investigation of specific physical chemical problems and are not convenient as general analytical procedures. They differ greatly from the proposed general method. In order to understand the principles underlying the proposed method of analysis, consider two compounds, A and B, that react with a reagent R at different rates. Suppose that the reaction of A with R is faster than the reaction of B with R, at a given constant temperature. Mixtures of A and B can be analyzed by the following procedure. A reaction solution is prepared in which the the total molar concentration of $A + B$ is specified and in which the concentration of R is also specified. The reaction is allowed to proceed for a specified time at a given constant temperature and then the amount of $A + B$ reacted is determined. It is apparent that, if the mixture is composed chiefly of A, the more reactive compound, a relatively large fraction of $A + B$ will have reacted after the specified reaction period. On the other hand, if the mixture is composed chiefly of B, the less reactive compound, a relatively small fraction of the mixture will have reacted. It should be noted that the method is an indirect one and possesses the disadvantages common to other indirect methods of analysis. The determination, therefore, of a small amount of one component in the presence of a large amount of the other is generally difficult.

---

* Present address: Department of Chemistry, University of Chicago, Chicago, Illinois.

A concrete illustration of the method is the procedure for the analysis of mixtures of ethyl and isopropyl acetates. (This procedure is based on the rates of reaction of the two esters with hydroxyl ion.) First, the total ester content of the sample is determined. Second, a reaction solution is prepared at 0°C in which the total concentration of ester is 0.0500 M and the initial concentration of alkali is also 0.0500 M. The mixture is allowed to stand for 33 minutes at 0°C and the concentration of hydroxyl ion remaining is then determined by acidimetric titration. Third, the concentration of hydroxyl ion remaining after the reaction period of 33 minutes is compared with a calibration curve that gives the initial composition of the mixture directly. Thus, two titrations (the determination of total ester content of the sample and the determination of the hydroxyl ion remaining at the end of the reaction period) are sufficient to establish the original composition of the mixture.

In general, the reactions of the two components of the mixture, A and B, with the reagent, R, may be called competitive reactions and be represented as follows:

$$A + R \rightarrow \text{products} \tag{1}$$

$$B + R \rightarrow \text{products} \tag{2}$$

So far as the analysis of mixtures is concerned, the most interesting and useful type of competitive reactions is that in which A and B are organic compounds that contain the same functional group. In such a case, the two reactions, (1) and (2), generally proceed by identical mechanisms and differ only in specific rates of reaction. Such a pair of reactions we propose to call homo-competitive reactions, the prefix homo- referring to the fact that both compound A and compound B contain the same functional group. The term homo-competitive reactions is extended to include first order reactions of the type:

$$A \rightarrow \text{products} \tag{3}$$

$$B \rightarrow \text{products} \tag{4}$$

in which A and B are organic compounds containing the same functional group. An example of first order homo-competitive reactions is the decomposition of formaldehyde bisulfite and acetaldehyde bisulfite.

In addition to the homo-competitive reactions mentioned above, there are many other types of competitive reactions. For example, the simultaneous reactions of bromine with an ethylenic bond (addition) and with a methylene group (substitution) might be called hetero-competitive reactions, since the reagent (bromine) is reacting with two *different* functional groups. Hetero-competitive reactions are not considered in this paper. They belong to the category in which one or more "side-reactions" occur, in addition to the main reaction with the reagent.

Mathematical Treatment

Although mathematical investigations of certain aspects of competitive reactions have been reported in the literature,[8, 9, 10] these investigations are of no use for the present purposes and will not be considered further.

It is possible to treat the kinetics of two homo-competitive reactions in an exact theoretical way. On the basis of this treatment, it is possible to calculate calibration curves for the analysis of mixtures from the values of the specific rate constants of the two homo-competitive reactions. (Alternatively, the calibration curve may be established empirically by analyzing mixtures of known composition.)

In order to calculate a calibration curve for the analysis of mixtures of A and B, it is necessary to use an equation relating the concentrations of A and B remaining to the reaction period. Equations will be derived for first order homo-competitive reactions and also for second order homo-competitive reactions.

First Order Reactions. The concentration of A remaining at any time, t, is given by the expression:

$$a = a_0\, e^{-k't} \tag{5}$$

In this equation, a is the concentration of A at any time, t; a_0 is the initial concentration of A; and k' is the specific rate constant for the reaction of A. A similar expression gives the concentration of B at any time, t. The sum of concentrations of A and B is, therefore, given by the expression:

$$a + b = a_0 e^{-k't} + b_0 e^{-k''t} \tag{6}$$

It is apparent from equation (6) that if the values of $a + b$, $a_0 + b_0$, t, k', and k'' are known, the individual values of a and b can be found (see below).

Second Order Reactions. If A and B react with a reagent by second order reactions (see reactions 1 and 2), the rates of disappearance of A and B will be given by the following expressions:

$$-\frac{da}{dt} = k'ar \tag{7}$$

$$-\frac{db}{dt} = k''br \tag{8}$$

In these equations, k' and k'' are the specific rate constants for the reactions of R with A and with B, respectively, and r is the concentration of the reagent R at any time, t. Equations (7) and (8) can be combined to give:

$$\frac{db}{da} = \frac{k''}{k'}\frac{b}{a} \tag{9}$$

Integration yields:

$$\log\frac{b}{b_0} = \frac{k''}{k'}\log\frac{a}{a_0} \tag{10}$$

or

$$\frac{b}{b_0} = \left(\frac{a}{a_0}\right)^{k''/k'} = \left(\frac{a}{a_0}\right)^{\alpha} \tag{11}$$

in which α represents the ratio of rate constants, k'':k'. (In the following derivations, it will be convenient to assume that k' is greater than k''; that is, the reaction of R with A is faster than the reaction of R with B. The value of α will therefore always be less than unity.) It is seen from equation (11) that the fraction of B remaining in the reaction mixture at any time is equal to the fraction of A remaining, raised to the power α. Calibration curves for the analysis of mixtures cannot be calculated directly from equation (11) because time, t, does not appear in it.

The derivation of an equation in which the concentration of A or B or R is expressed as a function of time is not simple. Equation (7) can be rewritten

$$-\frac{da}{dt} = k'\,a[(r_0 - a_0 - b_0) + a + b] \tag{12}$$

$$-\frac{da}{a[(r_0 - a_0 - b_0) + a + b]} = k'\,dt \tag{13}$$

The expression for b given in equation (11) is now substituted in (13).

$$-\frac{da}{a\left[(r_0 - a_0 - b_0) + a + \frac{b_0}{a_0^{\alpha}}\,a^{\alpha}\right]} = k't \tag{14}$$

It is necessary now to integrate equation (14). Because of the complexity of the integration, only the special case, $r_0 = a_0 + b_0$, will be considered. Equation (14) can also be integrated for the general case, $r_0 \neq a_0 + b_0$. The integrated equation for the general case is so complex, however, that it is of little practical value.

If $r_0 = a_0 + b_0$, equation (13) becomes:

$$\frac{da}{a(a + b)} = -k'\,dt \tag{15}$$

The left side of equation (15) is a function of a alone since:

$$b = \frac{b_0}{a_0^{\alpha}}\, a^{\alpha} \tag{16}$$

(See equation 11.) Integration of both sides of equation (16) yields:

$$-k't = \int_{a_0}^{a} \frac{da}{a^2\left(1 + \dfrac{b}{a}\right)} \tag{17}$$

The substitution, $y = \dfrac{b}{a}$, is made. In view of equation (16):

$$y = \frac{b_0}{a_0^{\alpha}}\, a^{\alpha-1}$$

Therefore:

$$da = \left(\frac{a_0^{\alpha}}{b_0}\right)^{1/(\alpha-1)} \frac{1}{(\alpha - 1)}\, y^{(2-\alpha)/(\alpha-1)}\, dy$$

$$a^2 = \left(\frac{a_0^{\alpha}}{b_0}\right)^{2/(\alpha-1)} y^{2/(\alpha-1)}$$

Substituting these values in equation (17) gives:

$$-k't = \int_{y_0}^{y} \left(\frac{b_0}{a_0^{\alpha}}\right)^{1/(\alpha-1)} \frac{1}{\alpha - 1}\, \frac{(y^{\alpha/(1-\alpha)})}{1 + y}\, dy \tag{18}$$

We let

$$C = \left(\frac{b_0}{a_0^{\alpha}}\right)^{1/(\alpha-1)} \left(\frac{1}{\alpha - 1}\right) \tag{19}$$

and

$$\beta = \frac{\alpha}{1 - \alpha}. \tag{20}$$

It has been assumed that α is always less than one (see above). The value of β is also less than one if the value of α is less than $\frac{1}{2}$. Equation (18) becomes

$$-k't = C \int_{y_0}^{y} \frac{y^{\beta}}{1 + y}\, dy \tag{21}$$

Another substitution, $x = 1 + y$, is made:

$$\begin{aligned} -k't &= C \int_{x_0}^{x} \frac{(x - 1)^{\beta}}{x}\, dx \\ -k't &= C \int_{x_0}^{x} \frac{x^{\beta}\left(1 - \dfrac{1}{x}\right)^{\beta} dx}{x} \\ -k't &= C \int_{x_0}^{x} x^{\beta-1}\left(1 - \frac{1}{x}\right)^{\beta} dx \end{aligned} \tag{22}$$

The term $\left(1 - \frac{1}{x}\right)^\beta$ can be expanded by the binomial expansion:

$$-k't = C\int_{x0}^{x}\left[x^{\beta-1} - \beta x^{\beta-2} + \frac{\beta(\beta-1)}{2!}x^{\beta-3}\cdots\right]dx$$

$$-k't = C\left[\frac{x^\beta}{\beta} - \frac{\beta}{(\beta-1)}x^{\beta-1} + \frac{\beta(\beta-1)}{2!(\beta-2)}x^{\beta-2}\cdots\right]_{x0}^{x} \tag{23}$$

in which $\beta = \frac{\alpha}{1-\alpha}$; $\alpha = k''/k'$ and $x = 1 + y = 1 + b/a = 1 + \left(\frac{b_0}{a_0^\alpha}\right)a^{\alpha-1}$ and C is defined by equation (19).

Equation (23) is of considerable practical importance in the analysis of mixtures. Calculations made from this equation are given below.

It should be mentioned that, if the initial concentration of R is much greater than the sum of the initial concentrations of A and B (*i.e.*, if $r_0 \gg a_0 + b_0$), the reactions of A and B will be pseudo-unimolecular. In this case, the concentrations of A and B remaining after a given reaction period are represented by the following equation:

$$a + b = a_0e^{-k'r_0t} + b_0e^{-k''r_0t} \tag{24}$$

The derivation of equation (24) is similar to that of equation (6).

Optimum Reaction Period. The calibration curve for the analysis of mixtures is a plot of the percentage of $A + B$ reacted after a given reaction period *versus* the initial composition of the mixture. The slope of the calibration curve, and therefore, the accuracy of the analysis, are dependent on the choice of the reaction period. For every pair of homo-competitive reactions, there exists an "optimum reaction period." The calibration curve corresponding to the optimum reaction period has a greater slope than the calibration curve corresponding to any other reaction period. Consequently, the maximum accuracy in the analysis of reaction mixtures is obtained by employing the optimum reaction period. For a pair of first order homo-competitive reactions, the optimum reaction period is calculated from the equation:

$$t_{\text{opt.}} = \frac{\ln (k'/k'')}{k' - k''} \tag{25}$$

For a pair of second order homo-competitive reactions, if $r_0 = a_0 + b_0$:

$$t_{\text{opt.}} = \frac{\sqrt{k''/k'}}{k''r_0} \tag{26}$$

For a pair of second order homo-competitive reactions, if $r_0 \gg a_0 + b_0$:

$$t_{\text{opt.}} = \frac{\ln (k'/k'')}{r_0(k' - k'')} \tag{27}$$

(The derivation of equations 25–27 will be given in a subsequent publication.)

Numerical Calculations

Calibration curves for the analysis of mixtures of A and B can be found empirically by analyzing mixtures of known composition. Alternatively, the calibration curve may be calculated from equations (6), (23), and (24), provided that the values of the specific rate constants of the two reactions are known. The calculations are sometimes tedious but can be greatly shortened if the following procedures of calculation are used.

First Order Reactions. The calibration curve for a pair of first order homo-competitive reactions is found by plotting values of $\frac{a+b}{a_0+b_0}$ (calculated from equation 6) versus values of $\frac{a_0}{a_0+b_0}$. Inasmuch as k', k'', t, r_0, and (a_0+b_0) are constant in the analysis of mixtures, it is apparent that the calibration curve for first order reactions is a straight line.

TABLE 1

CALCULATION OF CALIBRATION CURVES FOR FIRST ORDER HOMO-COMPETITIVE REACTIONS

α	$(\%\ (A+B)\ \mathit{Remaining})_{100\%\ A}$	$(\%\ (A+B)\ \mathit{Remaining})_{100\%\ B}$
$\frac{1}{3}$	19	57
$\frac{1}{5}$	13.5	67.5
$\frac{1}{10}$	8	78
$\frac{1}{25}$	3.5	87.5

If the optimum reaction period (see above) is employed, a simplified method of calculating the calibration curve can be used. Combination of equation (25) with equation (6) results in the following equations:

$$\frac{a}{a_0} = (\%\text{ of }(A+B)\text{ remaining})_{100\%\,A} = \alpha^{1/(1-\alpha)} \tag{28}$$

$$\frac{b}{b_0} = (\%\text{ of }(A+B)\text{ remaining})_{100\%\,B} = \alpha^{\alpha/(1-\alpha)} \tag{29}$$

in which the subscript $_{100\%A}$ refers to a "mixture" with composition 100% A, and α is the ratio of specific rate constants k''/k'. Thus, if the optimum reaction period is employed, the calibration curve for first order reactions can be found by joining with a straight line the points calculated for 100% A (equation 28) and for 100% B (equation 29). The results of the calculations of calibration curves for four typical pairs of first order homo-competitive reactions are given in TABLE 1 and in FIGURE 1. It should be noted from equations (28) and (29) that, if the optimum reaction period is employed, the calibration curve for first order reactions is determined solely by the value of α, the ratio of rate constants.

Second Order Reactions. Calibration curves for second order homo-competitive reactions are not, in general, straight lines, although usually they are nearly straight. The ease with which the calibration curves can be calculated is dependent on the ratio of the two second order rate constants. If this ratio is greater than 25, the calibration curves can be calculated in a simple manner, as will be described below. If the ratio is less than 25, however, the calculation is more difficult and can be performed only for two special cases: $r_0 \gg a_0 + b_0$ and $r_0 = a_0 + b_0$.

(a) $r_0 \gg a_0 + b_0$. For this case, the reactions of A and B with R are pseudo-unimolecular. Consequently, equation (24) or equations (28) and (29) may be used in calculating the calibration curves, as described above. It should be noted that the calibration curves of FIGURE 1 apply in this case.

(b) $r_0 = a_0 + b_0$. The equation representing the rate of reaction of A and B with the reagent is equation (23) above. Equation (23) can be represented in the following simple form:

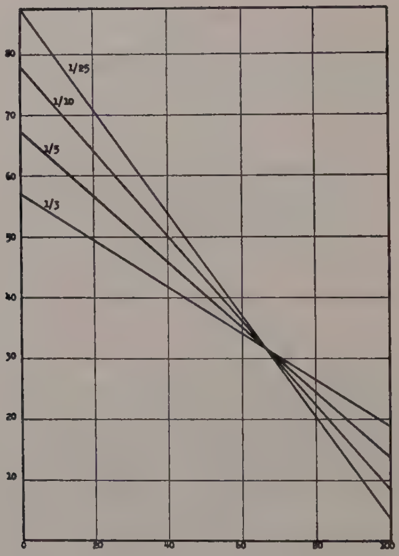

FIGURE 1. Calculated calibration curves for analysis of mixtures (first order reactions).

$$-k't = C(f - f_0) \tag{30}$$

In this equation, $C = \left(\frac{b_0}{\alpha_0^\alpha}\right)^{1/(\alpha-1)} \frac{1}{\alpha-1}$, f is the value of the expression in brackets in equation (23) at any time, t, and f_0 is the value of the same expression initially, at $t = 0$. The numerical computations involved in the calculation of the curves from equation (30) and the values of the two rate constants are tedious but may be shortened if the following procedure of calculation is adopted:

Step 1. The values of C (equation 30) are calculated for a series of hypothetical mixtures containing 0 per cent A, 10 per cent A, 20 per cent A, *etc.* The results of such calculations are given in TABLE 2. In this particular example, it is assumed that the value of α, the ratio of rate constants, is

0.254. (This is the ratio of rates of saponification of isopropyl and ethyl esters at 0°C. The theoretical calibration curve calculated below is compared with the experimental results of the analyses of mixtures of isopropyl and ethyl esters in FIGURE 3.)*

TABLE 2

CALCULATION OF VALUES OF C ($\alpha = 0.254$, $r_0 = a_0 + b_0 = 0.05$ M)

Initial composition of mixture (%A)	*Initial concentration*		C
	a_0 (M)	b_0 (M)	
0	0	0.050	0
10	0.005	.045	−14.10
20	.010	.040	−20.88
30	.015	.035	−28.70
40	.020	.030	−38.86
50	.025	.025	−53.62
60	.030	.020	−76.80
70	.035	.015	−119.3
80	.040	.010	−214.4
90	.045	.005	−566.5
100	.050	0	

TABLE 3

CALCULATION OF VALUES OF f, EQUATION 30 ($\alpha = 0.254$)

b/a	x	*1st term**	*2nd term*	*3rd term*	*4th term*	*5th term*	*f, Sum of terms*
0.20	1.20	3.125	0.458	0.050	0.014	0.006	3.653
0.25	1.25	3.169	0.446	0.047	0.013	0.005	3.679
0.30	1.30	3.211	0.434	0.044	0.012	0.004	3.706
0.35	1.35	3.253	.424	.041	.011	.004	3.732
0.40	1.40	3.294	.414	.039	.010	.003	3.759
0.50	1.50	3.372	.395	.035	.008	.003	3.812
0.60	1.60	3.447	.379	.031	.007	neg.	3.863
0.80	1.80	3.587	.350	.026	.005	"	3.968
1.0	2.0	3.718	.327	.021	.004	"	4.070
1.2	2.2	3.841	.307	.018	.003	"	4.170
1.5	2.5	4.012	.282	.015	.002	"	4.311
1.75	2.75	4.144	.265	.013	.002	"	4.423
2	3	4.270	.250	.011	.001	"	4.533
3	4	4.708	.207	.007	.001	"	4.922
4	5	5.084	.179	.005	neg.	"	5.267
5	6	5.404	.158	.003	"	"	5.566
6	7	5.698	.143	.003	"	"	5.843
7	8	5.962	.131	.002	"	"	6.095
8	9	6.206	.121	.002	"	"	6.329
10	11	6.646	.107	.001	"	"	6.754
15	16	7.548	.083	neg.	"	"	7.631
20	21	8.282	.069	"	"	"	8.351
25	26	8.925	.060	"	"	"	8.985
30	31	9.457	.054	"	"	"	9.511

* "1st Term" refers to the first term of the infinite series of equation (23); *i.e.*, $\frac{1}{\beta} x^{\beta}$.

---

* The specific rate constant for the reaction of isopropyl acetate with hydroxyl ion is 0.303 l. mole^{-1} min.$^{-1}$ at 0° and that of ethyl acetate with hydroxyl ion is 1.19 l. mole^{-1} min.$^{-1}$. Substitution of these values in equation (26) yields 33.3 minutes as the optimum reaction period at 0°. This reaction period is used in analyses of mixtures of the two esters (see FIGURE 3).

Step 2. The values of f (equation 30) are calculated for several different ratios of $b:a$. The results of such calculations are given in TABLE 3. It will be observed that, when b/a is less than about 0.5, five terms of the infinite series that appears in equation (23) must be calculated. For greater ratios of b/a, fewer terms are needed to yield a sufficiently accurate value of f.

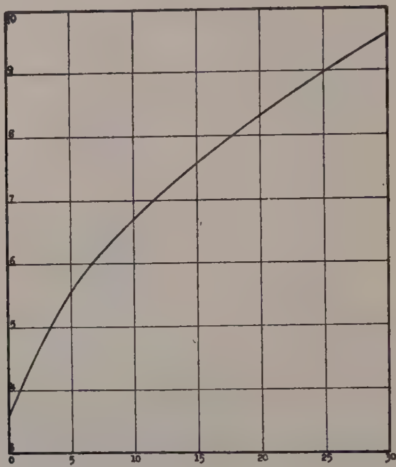

FIGURE 2. Relation between f of equation 30 and b/a. ($\alpha = 0.254$)

TABLE 4

CALCULATION OF b/a ($\alpha = 0.254$, $k' = 1.19\ \text{min}^{-1}\ \text{M}^{-1}$, $r_0 = a_0 + b_0 = 0.05$ M)

Composition of mixture (%A)	$\left(\frac{b}{a}\right)_0$	f_0[*]	$\frac{-k't}{C}$[†]	f[‡]	$\frac{b}{a}$[§]
0	—	—	—	—	—
10	9.000	6.542	2.811	9.353	28.4
20	4.000	5.267	1.898	7.165	12.15
30	2.333	4.675	1.381	6.056	6.81
40	1.500	4.311	1.020	5.331	4.22
50	1.000	4.070	0.739	4.809	2.665
60	0.6667	3.898	0.516	4.414	1.730
70	0.4296	3.774	0.332	4.106	1.073
80	0.2500	3.679	0.185	3.864	0.600
90	0.1111	—	—	—	—
100	—	—	—	—	—

[*] Obtained from plots similar to FIGURE 2, but larger scale.

[†] The value of t is taken to be 33.3 min., the optimum period of reaction for mixtures of ethyl and isopropyl acetates.

[‡] From equation (31).

[§] From plots similar to FIGURE 2.

Also, the smaller the value of α, the more rapidly the series converges, and, consequently, the fewer the terms needed. In other words, only a few terms need be calculated if the ratio of one of the reactions is very much greater than the rate of the other.

The values of f are plotted against b/a in FIGURE 2. In order to obtain the necessary accuracy in the steps that follow, it is necessary to plot the values of b/a of TABLE 3 on a very much larger scale than is shown in FIGURE 2.

TABLE 5

CALCULATION OF % OF ($A + B$) REMAINING ($\alpha = 0.254$, $k' = 1.19$ min^{-1} M^{-1}, $r_0 = a_0 + b_0 = 0.05$ M)

Initial composition of mixture (%A)	$\frac{b}{a}$	a	b	*% of (A + B) remaining*
0	—	—	—	66.5*
10	28.4	0.00107	0.0304	63.0
20	12.15	.00226	.0274	59.4
30	6.81	.00357	.0243	55.8
40	4.22	.00500	.0211	52.2
50	2.665	.00672	.01790	49.2
60	1.730	.00837	.01448	45.7
70	1.073	.01023	.01097	42.4
80	0.600	.01240	.00744	39.7
90	—	—	—	—
100	—	—	—	33.5*

* The *% of* ($A + B$) *remaining* in "mixtures" containing initially 0% A and 100% A was calculated simply by means of the ordinary second order rate law equation (33a).

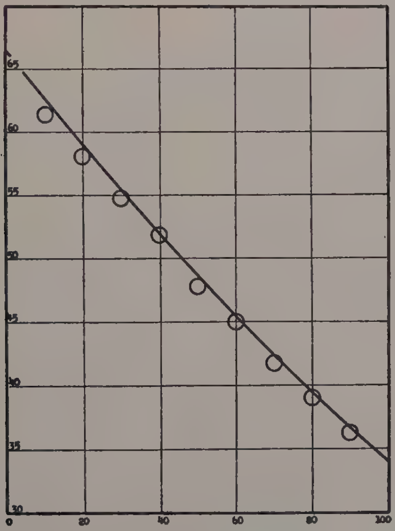

FIGURE 3. Analysis of mixtures of ethyl and isopropyl acetates at 0°C. (Curve is theoretical, points are experimental.)

Step 3. The value of f_0 is found from the plot of f *vs.* b/a. This is illustrated in TABLE 4, column 3. The value of f is then calculated from the known values of f_0, $k't$, and C:

$$f = f_0 - \frac{k't}{C} \tag{31}$$

(Cf. equation 30). The results are given in column 5 of TABLE 4. The value of b/a corresponding to the value of f is then obtained from the plot of f *vs.* b/a (FIGURE 2).

Step 4. The values of a and b are calculated from the value of b/a by means of the following equation:

$$a = \left(\frac{a_0^\alpha}{b_0}\right)^{1/(\alpha-1)} \left(\frac{b}{a}\right)^{1/(\alpha-1)} \qquad (32)$$

(Equation 32 is derived from equation 11). The results of such calculations are given in TABLE 5 and in FIGURE 3 (curve is theoretical, points are experimental, see below). It will be noted that the calibration curve is nearly a straight line. (This is also true if the difference in rate constants of the two reactions is large. See FIGURE 4.)

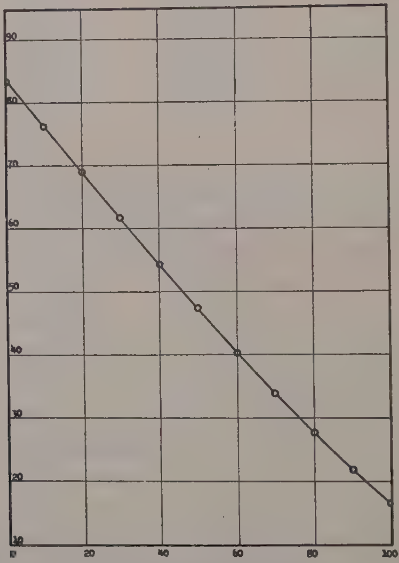

FIGURE 4. Calculated calibration curve for analysis of mixtures ($\alpha = 0.04$, $k' = 1$ min^{-1} M^{-1}, $r_0 = a_0 +$ $= 0.05$ M).

The methods described above are useful in calculating calibration curves for second order homo-competitive reactions if the ratio of rate constants is less than 25 and if $r_0 = a_0 + b_0$ or $r_0 \gg a_0 + b_0$. If the ratio of rate constants is greater than 25, however, a more convenient method of calculation can be employed. In the simplified method, it is assumed that the reaction of A (the faster reacting component of the mixture) with the reagent R is represented by the ordinary equation for a second order reaction:*

$$k't = \frac{1}{(r_0 - a_0)} \ln \frac{a_0}{r_0} \frac{(r_0 - a_0 + a)}{a} \qquad (33)$$

---

*If $r_0 = a_0$, equation (33) is indeterminate. In this special case, the equation:

$$k't = \frac{1}{a} - \frac{1}{a_0} \qquad (33a)$$

must be used instead of equation (33).

Thus, the reaction of A with R is assumed to proceed as though B were absent. In calculating the amount of B remaining after the specified reaction period, it is assumed that the effective initial concentration of reagent is $r_0 - a_0$ rather than r_0. That is, it is assumed that A reacts instantaneously with the reagent and so reduces the effective concentration of reagent from r_0 to $r_0 - a_0$. Consequently, the following equation, which is analogous to equation (33), can be written:

$$k''t = \frac{1}{(r_0 - a_0) - b_0} \ln \left[\frac{b_0}{(r_0 - a_0)} \; \frac{(r_0 - a_0) - b_0 + b}{b} \right] \qquad (34)$$

An illustration of the use of the simplified method of calculating calibration curves is given in TABLE 6. It is arbitrarily assumed that k' is 1.00 $\text{min}^{-1}\,\text{M}^{-1}$ and that k'' is 0.04 $\text{min}^{-1}\,\text{M}^{-1}$ (therefore, α is 1/25), and that $r_0 =$ $a_0 + b_0 = 0.05$ M. The optimum reaction period for the analysis is computed from equation (26), and found to be 100 min. In column 4 of TABLE 6 are given the results of the calculation of concentration of A remaining (equation 33) and in column 5 are given the results of calculation of the concentration of B remaining (equation 34). The results of calculation of the % of $(A + B)$ remaining (column 6) are accurate to at least a few tenths of a per cent. The calibration curve is shown in FIGURE 4.

TABLE 6

CALCULATION OF PER CENT OF $(A + B)$ REMAINING BY THE APPROXIMATE METHOD ($\alpha = 0.04$, $k' = 1\ \text{min}^{-1}\ \text{M}^{-1}$, $r_0 = a_0 + b_0 = 0.05$ M)

Initial composition of mixture (% A)	*Initial concentrations* (M)		*Concentrations of A and B remaining at end of reactn. period* (M)		*% of (A + B) remaining*
	a_0	b_0	a	b	
0	0	0.050	0	0.04167	83.3
10	0.005	.045	0.000050	.03814	76.4
20	.010	.040	.000145	.03448	69.3
30	.015	.035	.000315	.03070	62.0
40	.020	.030	.000610	.02679	54.8
50	.025	.025	.00107	.02273	47.0
60	.030	.020	.00177	.01852	40.6
70	.035	.015	.00278	.01415	33.9
80	.040	.010	.00416	.00962	27.6
90	.045	.005	.00601	.00490	21.8
100	.050	0	.00833	0	16.7

Results of Analyses of Mixtures

It has been found that the homo-competitive method of analysis is practical if the rates of the two homo-competitive reactions (either first order reactions or second order reactions) differ by a factor of four or more. The following applications of the method have been made:

Analysis of Mixtures of Esters. The reaction of esters with hydroxyl ion (saponification) is a second order reaction. The relative rates of saponification[11, 12, 13] of methyl, ethyl, isopropyl, and tertiary butyl acetates at

25° are in the ratio 119:72:17:1. The relative rates of saponification of methyl formate, acetate, monochloracetate, and dichloracetate at 25° are in the ratio 223:1:761:16,000. From these values, it is seen that the analysis of many pairs of esters is possible. As an example of analysis of compounds that do not react with the reagent at greatly different rates, mixtures of ethyl acetate and isopropyl acetate were analyzed and the results were compared with the calibration curve calculated from the two specific rate constants (FIGURE 3). The theoretical curve agreed with the experimental points within 1–3 per cent. The average deviation (error) in analysis of mixtures of the two esters was 2 per cent (absolute). The experimental details will be reported in detail in a subsequent publication.

Analysis of Mixtures of Olefins. The rates of reaction of perbenzoic acid with the following types of olefins, $RCH{=}CH_2$, $RC(CH_3){=}CH_2$, $RCH{=}CHR$, and $RC(CH_3){=}CHR$ (mixture of chloroform and benzene as solvent) to form epoxides was found to be 1:25:30:400 at 25°. It is thus possible to analyze mixtures containing two different types of olefins or other ethylenic compounds. As an example of the analysis of mixtures of ethylenic compounds, mixtures of oleic and undecylenic acid were analyzed.[14] These compounds contain double bonds of the types, $RCH{=}CHR$ and $RCH{=}CH_2$, respectively. The accuracy of the analyses was about 1 per cent (absolute).

The homo-competitive method of analysis was also applied to the analysis of synthetic rubbers for "internal" and "external" double bonds. The analysis presented several special difficulties but it was found possible to overcome these and to devise a practical and convenient procedure. The experimental work has been described and discussed in detail in papers published elsewhere.[14]

Analysis of Mixtures of Carbonyl Compounds. Analysis of mixtures of carbonyl compounds might be based on rates of formation of aldehyde and ketone bisulfite addition products. It was found, however, that it is generally preferable to base the analyses on rates of decomposition of the addition products. The rates of decomposition of formaldehyde, acetaldehyde, propionaldehyde, benzaldehyde, and acetone bisulfites were found to be in the ratio of 1:60:160:1600:400 (at 25° and pH 3.4). As an illustration of the analytical method, mixtures of acetone and formaldehyde were analyzed. A preliminary investigation of the effect of pH on the rates of decomposition disclosed that the ratio of rates of decomposition was very large in solutions of high acidity. Thus, in 1 N hydrochloric acid at 25°, the rates of decomposition of acetone bisulfite and formaldehyde bisulfite are in the ratio of more than 10,000:1. Analyses of mixtures of the two carbonyl compounds yielded results accurate to at least 1 per cent. This investigation will be described in detail elsewhere.

It is expected that analysis based on homo-competitive reactions will be used chiefly for the following types of mixtures: mixtures of homologous organic compounds, especially of methyl and ethyl compounds; mixtures of primary and secondary, or of secondary and tertiary organic compounds; mixtures of ortho- and para-isomers, *etc.*; mixtures of different types of ethylenic compounds; mixtures of monochloro- and dichloro-organic compounds, *etc.*

Summary

A method for the analysis of mixtures of compounds based on the difference in rates of reaction of the components of the mixture with a given reagent has been described. The method is useful chiefly for the analysis of mixtures of two organic compounds that contain the same functional group. In general, the procedure requires two titrations for the analysis of each mixture. One titration establishes the total molar amount of the two compounds, A and B, in the mixture. The second titration gives the percentage of $A + B$ reacted with the reagent under standard conditions (*i.e.*, with a given initial molar concentration of reagent and $A + B$, at a given temperature, and for a given optimum reaction period). The percentage of $A + B$ reacted (or unreacted) after the optimum reaction period is then compared with a calibration curve that gives the original composition of the mixture directly.

Mathematical expressions have been developed that represent the kinetics of the reaction of a reagent with a mixture of two compounds under various conditions. The computations involved in the theoretical calculation of calibration curves are illustrated. (Calibration curves can also be found from the experimental results of analyses of mixtures of known composition.)

Experimental results of the applications of the method to the analyses of several types of mixtures of organic compounds are discussed.

Acknowledgment

The authors are indebted to Dr. Robert G. Parr and Professor Bryce L. Crawford, Jr., for the derivation of equation (23).

1. BENNETT, G. M. & F. M. REYNOLDS. J. Chem. Soc. **1935:** 131.
2. CONNER, T. & G. F. WRIGHT. 1946. J. Am. Chem. Soc. **68:** 256.
3. DILLON, R. T., W. G. YOUNG, & H. J. LUCAS. 1930. J. Am. Chem. Soc. **52:** 1953.
4. STERN, G. 1940. Reischsamt. Wirtschaftsausbau, Pruf. -Nr. **43:** 15. C. A. **41:** 6490.
5. DVORNIKOFF, M. N. & H. L. MORRILL. 1938. Anal. Chem. **20:** 935.
6. CLARENS, J. 1921. Bull. soc. chim. **29:** 837.
7. SAFFER, A. & B. L. JOHNSON. 1948. Ind. Eng. Chem. **40:** 538; see also: SOLOMON, G., C. KONIGSBERGER, & A. J. ULTÉE. 1948. Rubber Foundation. Delft, Netherlands. Communication No. 82.
8. HUGHES, E. D., C. K. INGOLD, & U. G. SHAPIRO. J. Chem. Soc. **1936:** 231.
9. RAKOWSKI, A. 1907. Z. physik. Chem. **57:** 321.
10. GAPON, E. N. 1929. Ukrainskii Khem. Zhur., 4 Sci. Pt.: 333–339.
11. SKRABAL, A., *et al.* Monatsh. **45:** 148 (1924); **47:** 17, 30 (1926); **48:** 459 (1927); **50:** 369 (1928).
12. PALOMAA, M. H. 1938. Ber. **71B:** 480.
13. HAMMETT, L. P. 1940. Physical Organic Chemistry. p. 211. McGraw-Hill. New York.
14. KOLTHOFF, I. M., T. S. LEE, & M. A. MAIRS. 1947. J. Polymer Sci. **2:** 199, 206, 220.

AUTOMATIC PAPER CHROMATOGRAPHY

By Ralph H. Müller and Doris L. Clegg*
Department of Chemistry, New York University, New York, N. Y.

Introduction

Chromatography is a highly developed subject which provides techniques well-nigh indispensable in analysis, preparative organic chemistry, and biochemistry. The extensive literature is summarized in several monographs.[21, 22, 27, 28] A special branch of the subject involves the use of paper in the form of sheets, discs, strips, or fibres in which very effective separations of complex mixtures can be attained. The applications are primarily, though not exclusively, analytical, and their value lies mostly in the small quantities of material required for examination. The separation of the components of a mixture by permitting the mixture to diffuse through a paper matrix accomplishes two things. It permits complete separation by the simple expedient of cutting out a section of the paper and extracting with a suitable solvent, and it permits qualitative identification on the basis of the preferential rate of diffusion. Under carefully controlled and specified conditions, identification is established in terms of the R_f factor, which represents the ratio of the distance traversed by the substance to that traversed by the solvent. If the process is extended to the use of a second solvent, and in a direction perpendicular to the first, then a new and confirmatory set of R_f values may be used for identification, or to resolve a pair which may have exhibited inappreciable differences in their R_f values in the first separation. This is two-dimensional paper chromatography,[5] which, among other applications, has been extremely useful in the analysis of amino acid mixtures.

In view of the fact that the techniques of paper chromatography are so generally useful, and can be carried out with very simple and inexpensive equipment, one may well ask why it is profitable to employ instrumental aids in studying paper chromatograms. The use of instrumental aids, even fairly complicated ones, are justified for several reasons. For one thing, they are capable of refining the present techniques in quantitative estimations. What is perhaps more important is the ease with which extensive data can be accumulated on the kinetics of the process and on the influence of the many factors which affect the process. The simple matter of selecting appropriate solvent mixtures is highly empirical and there are no guiding generalizations. The busy analyst or biochemist is likely to let well enough alone when he has found a suitable solvent mixture for a given system, but in all likelihood the next problem will require another series of inspired hunches to find the optimum conditions.

Despite the efforts of several able investigators,[3, 4, 6-12, 17-20, 23-26] the theoretical foundations of chromatography are in a very elementary state and practice far outruns the few generalizations which can be used to predict the optimum conditions for a new problem. It is likely that ordered progress will result from kinetic studies made under carefully controlled conditions and that the constant interplay of theory and experiment will eventually yield a more logical and coherent description of those complex phenomena. This does not overlook the certainty that important and striking applications will continue to be made with very simple equipment.

---

* This paper was abstracted from a portion of the thesis presented by D. L. Clegg to the faculty of the Graduate School of New York University in partial fulfillment of the requirements for the degree of Doctor of Philosophy, June, 1950.

It is equally certain that the full resources of modern instrumentation can be applied to chromatography with profit and that they will be best employed if the information is automatically recorded. A series of investigations in this laboratory is concerned with the application of various physical techniques, optical, electrical, and dielectric, to this problem.

It is obvious that standard photometric techniques and instruments can be employed in the examination of finished paper chromatograms and that the results are likely to be more useful and precise as a consequence. A recording photometer would seem to offer more complete information and eliminate the tedium. Still more useful would be means for following the progress of a chromatographic separation. Some experimental approaches in this direction are described in this paper.

Photometry of Paper Chromatograms

The quantitative evaluation of paper chromatograms has been accomplished with filter photometers, using a special mounting frame and optical system for the paper strips.[1, 2] More useful and more readily interpretable results are obtained if the measurements involve a transmittancy determination rather than a reflectance measurement. This is substantiated more fully by the experience of Liebhafsky, reported elsewhere in this monograph.* Nevertheless, we have found that rapidly recorded reflectance measurements have their uses, particularly when it is desired to establish the spatial distribution of the material along a strip or disc of paper.

The difficulty resides in the fact that there is no known simple relationship between concentration and reflectivity, whereas, in transmittancy, the deviations from the Lambert-Beer law are not too serious to prevent a direct determination of concentration. In general, it may be said that transmittancy measurements require greater photometric sensitivity and elegance than the reflectance measurements, but are simpler to interpret. We have used both and the choice is dictated largely by the type of information which is desired.

A simple arrangement for the evaluation of paper chromatograms by reflectance is shown schematically in FIGURE 1. A small synchronous clock-motor (1 R.P.M.) is provided with a split mounting arbor on its shaft. The specimen holders in this case consisted of selected glass vials upon which the paper strips could be mounted by means of Scotch tape. The vials could be slipped over the split arbor, where they were held with sufficient rigidity. The scanning system consists of a 6V concentrated helical filament lamp operated from storage batteries, a bilateral horizontal slit, S, a suitable filter, F, and a stopped-down achromatic lens, L, which focuses a

---

* Pp. 997–1014.

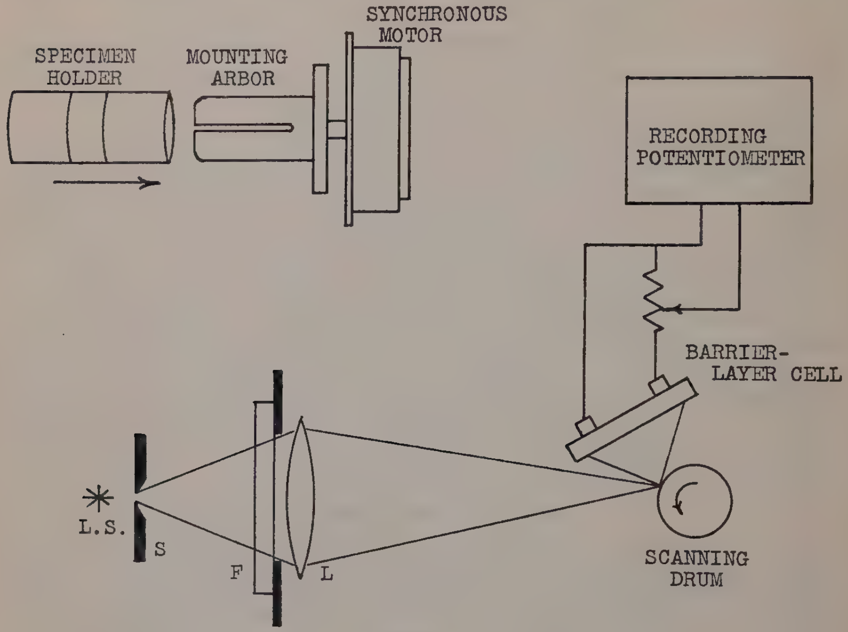

FIGURE 1.

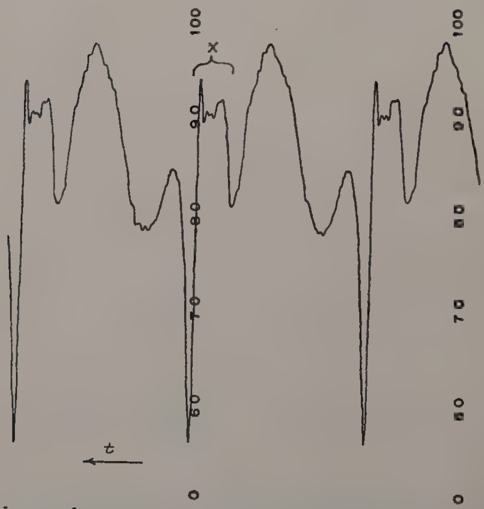

FIGURE 2. Recorded paper chromatogram of toluidine blue-brilliant green. Approximately two micrograms.

fine rectangular image of the slit on the scanning drum which holds the specimen. The light which is reflected from the specimen is received by a barrier layer photocell, the output of which is fed through a shunt to a 2.5 mv Brown Electronik recorder. Since the scanning drum and recorder chart are synchronously driven, the resulting record is accurately related to distance along the chromatogram. The scalar relationship is most readily established by scanning a piece of cross-section paper, in which every division is registered as it passes the scanning beam of light. Some degree of variation in the scale can be accomplished by changing the recorder chart speed, but, in this instrument, the scanning rate is fixed. The choice of filter F involves a compromise for multi-component colored systems. Obviously, it is impossible to choose a spectral region which is best suited to all components present. For a general survey of the specimen, a region is chosen for which all components exhibit some degree of absorption. Since the information is so rapidly recorded and without further attention, this limitation is minimized by repeating the scanning operation with a different filter. There are some instances in which the filter limitation becomes an asset. For example, if a specimen has been examined for the presence of a trace of impurity, it is possible to exaggerate or enhance its presence by scanning in a spectral region in which its absorption is much greater than the bulk constituents.

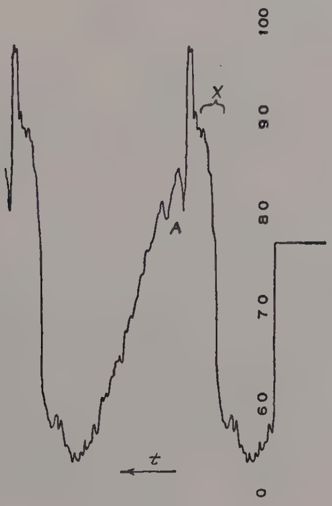

FIGURE 3. Recorded paper chromatogram of leaf pigments.

Typical examples of recordings made with this equipment are shown in FIGURES 2 and 3. In both illustrations, elapsed time reads from right to left, the top represents maximum reflectivity and the reflectivity decreases toward the bottom. Both illustrations reveal little of interest to the chromatographer, other than the degree of reproducibility, speed of recording, and certain obvious defects which were remedied in an improved design. In FIGURE 2, each sharp downward spike (56.1 per cent reflectivity) corresponds to the toluidine blue zone. The rise to the immediate left corresponds to a clear, more faintly colored zone, followed by the brilliant green zone. Beyond this, the rapid rise in reflectivity represents clear paper. The irregularities encompassed by the indicator X correspond to the overlapping edges of the paper strip and the Scotch tape binding. This nuisance has been eliminated in the improved design by a microswitch arrangement which short circuits the recorder for the duration of the overlap interval. The elapsed time for a complete scan is one minute and, to show the degree of reproducibility, is repeated approximately two and a half times in FIGURE 2.

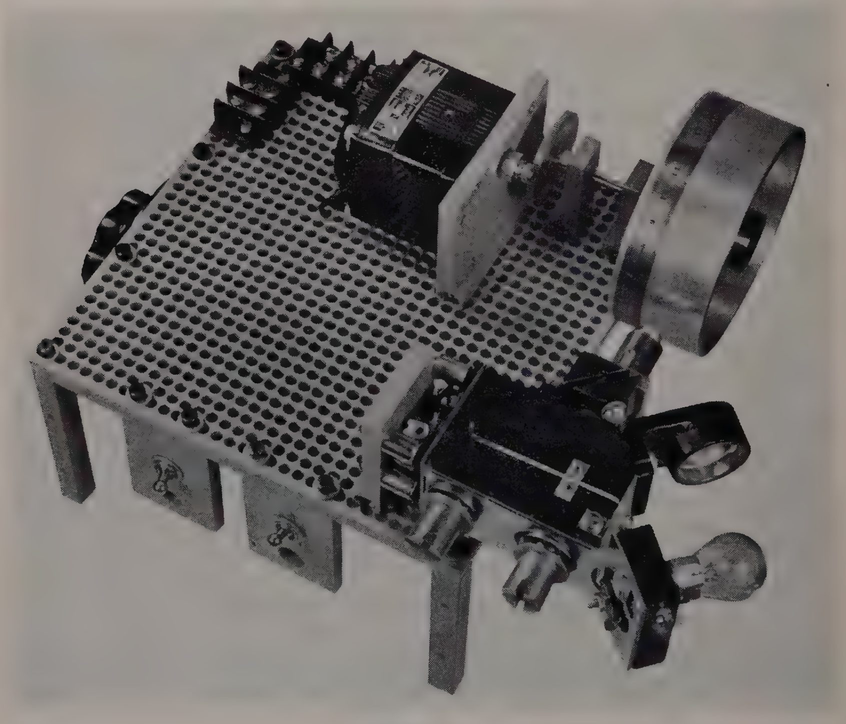

FIGURE 4.

In FIGURE 3, a recording is shown for a chromatogram of an autumn leaf extract. The peaks at A correspond to a pink zone of an anthocyanine. In duplicate samples, such zones were cut out, extracted, and measured at pH 3.6 in a Beckman spectrophotometer, from which the close resemblance of the absorption spectrum to reported values for typical anthocyanines was demonstrated. There was no interest at the time in further identification or in the stronger absorption shown in FIGURE 3 for three distinct and reproducible yellow and brown bands.

The advantage of scanning in this manner lies in the speed of operation, reproducibility, and the fact that the record is repeated over and over again without attention. With minor rearrangements in the optical system, the use of a glass or clear plastic drum permits the recording by transmittancy rather than reflection.

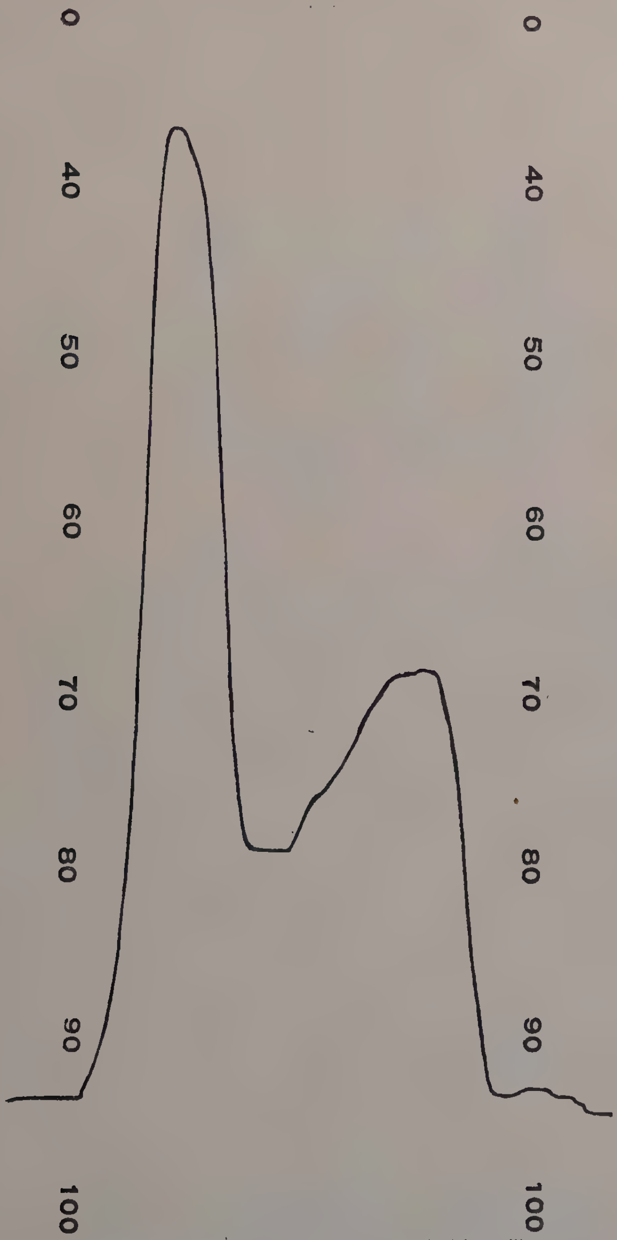

FIGURE 5. Recorded paper chromatogram of methyl violet-aniline orange.

An improved arrangement for reflectance scanning is shown in FIGURE 4. The mechanical elements shown have been assembled from the convenient components used by servo-mechanism engineers.* A Bodine synchronous motor provides the drive through suitable gear reduction and the sample holders consist of a series of stainless steel drums of varying diameters. Each of these is fitted with a steel millimeter tape flush with the periphery of the drum and against which the strip chromatogram can be aligned. The optical scanning unit shown in the right foreground is a commercial device widely employed in wire and radio transmission of pictures.† In this unit, an area of the sample is flood-lighted by the lamp and lens system. A microscope objective with a built-in stop picks up reflected light from an area of approximately 0.01 square inch and focuses it on a phototube within the case. Two varieties of phototube are available, the conventional kind and another adaptable to frequency modulation of the signal. We have modified this assembly so that it is possible to use a small barrier layer cell as well. In addition, provision has been made to incorporate filters in the illumination system. This system and the micro-switch cut-out are not shown in FIGURE 4. The improvements in this instrument permit a wide choice in sample size and a speed of scanning which can be selected quickly by a change in drum size or of gear reduction ratio. A typical photometric recording obtained with this instrument is shown in FIGURE 5.

Dynamic Scanning

The devices which have been described so far have distinct limitations and are used primarily to evaluate finished and developed chromatograms. It has been found far more useful to provide means for studying the behavior of a system while the separations are in progress. The first of these, which was set up in the summer of 1948, established the design factors from which a simpler and less expensive instrument can be designed. Since this system has been described,[13, 14] a very brief mention here will suffice. Advantage was taken of the well-known use of confined barriers in restricting the flow through the paper to a narrow channel. As shown in FIGURE 6, paraffin barriers were embossed on filter paper and the sample was deposited at the lower portion of the rectangular channel. An eluting liquid could be added in the circular area below it, and, as it ascended, the components could be selectively driven upward. At a suitably chosen point, the advancing column was scanned by a monochromatic beam of light. The general arrangement of scanning and recording equipment is shown in FIGURE 7, and FIGURE 8 shows typical results for the preferential rate of movement of solvent and components as they passed the scanning spot of light.

Although our interest and concern has been primarily with dyes and pigments, or with specimens from which a colored compound can be developed, it is recognized that the recording of colorless substances is of much more general interest. These techniques can be adapted to the ultraviolet, but in our experience it is not essential, as one might imagine, to use expensive quartz optics and phototubes for this region. Some very encouraging results have been obtained with the use of fluorescent targets and these may be either in the form of receiving screens or fluorescent patches incorporated in a portion of the paper. These investigations are not sufficiently advanced to report on at this point.

---

* Available from Servomechanisms, Inc., Mineola, L. I., N. Y.
† Times Facsimile Corp., Times Bldg., N. Y., N. Y.

Means are available for the continuous examination of chromatograms during their development. It is conceivable that one can move a beam of light rapidly over the sample and present the resultant transmittance or reflectance continuously on the screen of a cathode ray tube. Elaborate mechanical means for moving the beam are unnecessary, because one can better employ a cathode ray tube as a scanning light source. This technique has been described by one of us.[15, 16] The principle of cathode ray scanning as applied to paper chromatograms is shown in FIGURE 9. The cathode ray

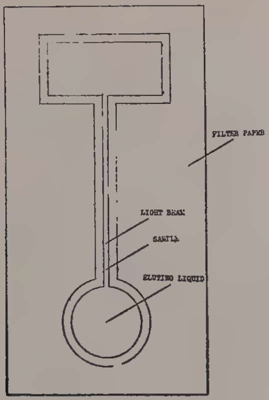

FIGURE 6.

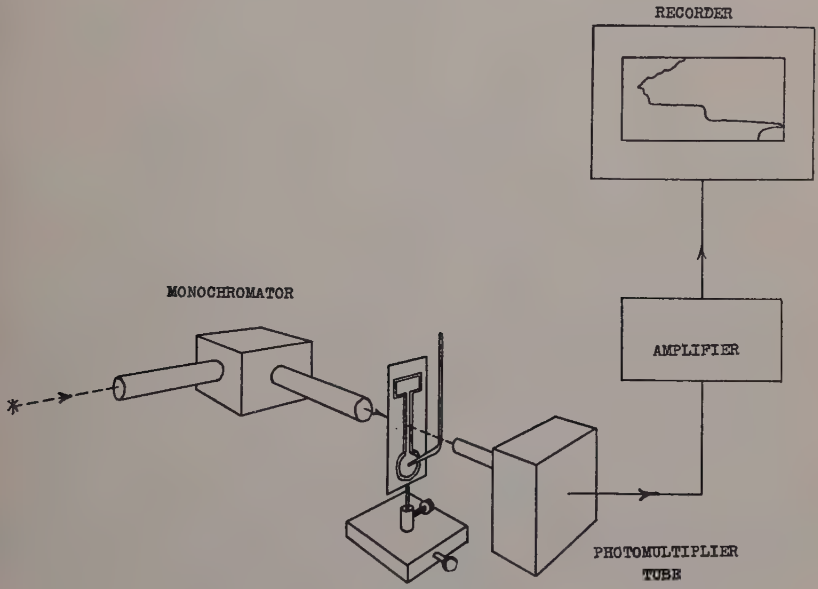

FIGURE 7.

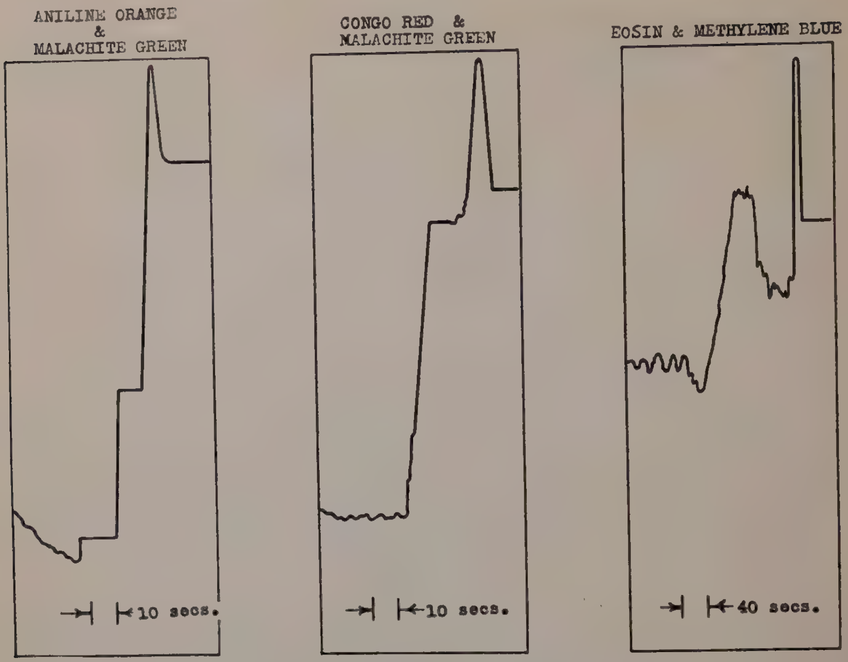
ANILINE ORANGE & MALACHITE GREEN

CONGO RED & MALACHITE GREEN

EOSIN & METHYLENE BLUE

Figure 8.

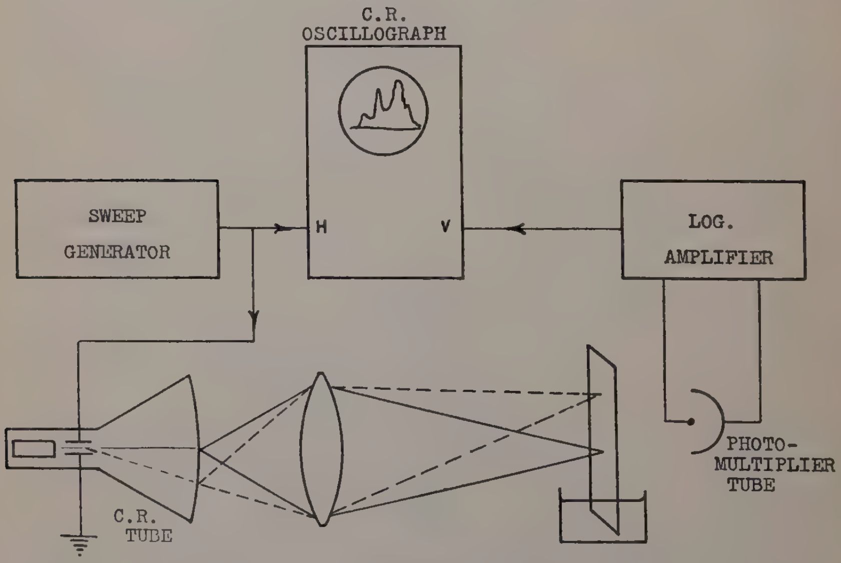

Figure 9.

tube at the lower left has its beam deflected in a vertical direction by the usual saw-tooth sweep generator. The flying spot of light is focussed on the paper by a lens. The light which is transmitted through the specimen is received by a photomultiplier tube and drives the vertical deflection plates of a cathode ray oscillograph. An intermediate logarithmic amplifier is useful, though not essential, because the presentation will then be in terms of extinction values. The horizontal deflector plates of the oscillograph are driven by the same sweep generator. As a result, the horizontal axis represents distance along the paper strip, and the vertical excursions of the pattern are a measure of the opacity. The advantages of this technique are not immediately apparent. It might be assumed that the cathode ray picture should be photographed from time to time if anything other than an enlarged view of the process is desired. Actually, the instantaneous values of the photo current may be used in several ways. For example, suppose it is desired to establish the time at which solvent and two or three components reach one or several reference points on the paper. In this case, suitable triggers would be synchronized with the sweep generator and their presence would be ignored until the scanned pattern produced fluctuations at the same instant (distance). Their simultaneous occurrence would then be recorded. No ambiguity would result, because solvent increases the transmittancy and colored zones decrease it, and the pulse directions would be reversed as a consequence. The electronic means for such temporal discrimination are well established and are discussed briefly in reference 16.

The principal advantage of rapid scanning as described above is the ease with which the resultant photocurrent may be modified electronically for indication or control purposes. Thus, if the presence of an absorbing zone gives rise to a gently rising current, then, at high speeds of scanning, this is readily amplified, differentiated, and made to generate an abrupt pulse. If the zone becomes more translucent, as it will when pure solvent appears, a pulse of the opposite polarity can be generated. Despite these advantages, there is some merit and particular use for intermittent scanning. Consider the case in which the rise of eluting liquid will occur over a useful range and effect measurable separation of several components in a period of three hours. If provision is made to scan the strip with a spot of light from bottom to top at a uniform rate and within 30 seconds, the high speed recorder can trace the photometric record with adequate fidelity. If this process is repeated automatically at 2- or 3-minute intervals, one will have a set of 90 or 60 tracings for the entire process. From these data, rather complete information can be deduced, such as eluent diffusion rate, relative R_f values, concentration distribution in the various zones, *etc.* Since high chart speeds are required, it is useful to stop the chart for one or two minute intervals and initiate its motion automatically some 5 or 10 seconds before each scan. Appropriate markers to indicate the exact beginning of a scan are most easily incorporated on the record by means of pencil reference lines on the sample. When these are scanned, very sharp index lines appear on the chart.

These arrangements, with minor modifications, are all useful in the study of paper chromatography. By their use, interesting regularities and degrees of predictability can be evolved in what is otherwise a highly empirical, but extremely useful, technique of modern analysis.

Bibliography

1. Block, R. J. 1948. Science. **108:** 608.
2. Bull, H. B., J. W. Hahn, & V. H. Baptist. 1949. J. Am. Chem. Soc. **71:** 550.
3. Cassidy, H. G. 1946. J. Chem. Education. **23:** 427.
4. Claeson, S. 1948. Ann. N. Y. Acad. Sci. **49:** 183.
5. Consden, R., A. H. Gordon, & A. J. P. Martin. 1947. Biochem. J. **41:** 590.
6. Craig, L. C. 1944. J. Biol. Chem. **155:** 519.
7. Craig, L. C., H. Mighton, E. Titus, & C. Golumbic. 1948. Anal. Chem. **20:** 134.
8. Dole, M. 1947. J. Chem. Phys. **15:** 447.
9. Martin, A. J. P. 1948. Ann. N. Y. Acad. Sci. **49:** 249.
10. Martin, A. J. P. & R. L. M. Synge. 1941. Biochem. J. **35:** 1358.
11. Mayer, S. W. & E. R. Tompkins. J. Am. Chem. Soc. **69:** 2866.
12. Müller, P. B. 1944. Helv. Chim. Acta. **27:** 404.
13. Müller, R. H. & D. L. Clegg. 1949. Anal. Chem. **21:** 192.
14. Müller, R. H. & D. L. Clegg. 1949. Anal. Chem. **21:** 1123.
15. Müller, R. H. 1947. In Radar Aids to Navigation. Vol. II, M.I.T. Radiation Lab. Series. McGraw-Hill. N. Y.
16. Müller, R. H. 1947. Anal. Chem. **19:** 74.
17. Offord, A. C. & J. Weiss. 1945. Nature **155:** 725.
18. Spedding, F. H., A. F. Voigt, E. M. Gladrow, & N. R. Sleight. 1948. J. Am. Chem. Soc. **70:** 1671.
19. Steward, F. C., W. Stepka, & J. F. Thompson. 1948. Science **107:** 451.
20. Strain, H. H. 1942. J. Phys. Chem. **46:** 1151.
21. Strain, H. H. 1945. Chromatographic Adsorption Analysis. Interscience Publishers, Inc. N. Y.
22. Strain, H. H. 1949. Anal. Chem. **21:** 75.
23. Thomas, H. C. 1948. Ann. N. Y. Acad. Sci. **49:** 161.
24. Tiselius, A. 1947. Advances in Protein Chemistry. Vol. III. Academic Press. N. Y.
25. Tompkins, E. R., J. X. Khym, & W. E. Cohn. 1947. J. Am. Chem. Soc. **69:** 2769–77.
26. Weil-Malherbe, H. J. Chem. Soc. **1943:** 303.
27. Williams, T. I. 1947. An Introduction to Chromatography. Chemical Publishing Co. N. Y.
28. Zechmeister, L. & L. Cholnoky. 1937. Die Chromatographische Adsorptionsmethode. Julius Springer. Germany.

MONOGRAPHIC PUBLICATIONS
OF
THE NEW YORK ACADEMY OF SCIENCES
(Lyceum of Natural History, 1817–1876)

(1) The Annals (octavo series), established in 1823, contain the scientific contributions and reports of researches, together with the records of meetings of the Academy. The articles which comprise each volume are printed separately, each in its own cover, and are distributed immediately upon publication. The price of the separate articles depends upon their length and the number of illustrations, and may be ascertained upon application to the Executive Director of the Academy.

Current numbers of the Annals are sent free to all Members of the Academy desiring them.

(2) The Special Publications, established in 1939, are issued at irregular intervals as cloth-bound volumes. The price of each volume will be advertised at time of issue.

(3) The Memoirs (quarto series), established in 1895, are issued at irregular intervals. It is intended that each volume shall be devoted to monographs relating to some particular department of Science. Volume I, Part 1, is devoted to Astronomical Memoirs, Volume II to Zoological Memoirs. No more parts of the Memoirs have been published to date. The price is one dollar per part.

(4) The Scientific Survey of Puerto Rico and the Virgin Islands (octavo series), established in 1919, gives the detailed reports of the anthropological, botanical, geological, paleontological, zoological, and meteorological surveys of these islands.

Subscriptions and inquiries concerning current and back numbers of any of the publications of the Academy should be addressed to

EXECUTIVE DIRECTOR
The New York Academy of Sciences
2 East Sixty-third Street
New York 21, N. Y.

DATE DUE

DEMCO 38-297